Focal Adhesion Kinase in Cardiac Development and Disease

Laura Antonietta DiMichele

A dissertation submitted to the faculty of the University of North Carolina at Chapel Hill in partial fulfillment of the requirements for the degree of Doctor of Philosophy in the Department of Pathology and Laboratory Medicine.

Chapel Hill
2007

Approved by:

Advisor: Joan M. Taylor

Reader: Christopher P. Mack

Reader: Susan Lord

Reader: Virginia Godfrey

Reader: Cam Patterson

ABSTRACT

LAURA ANTONIETTA DIMICHELE: Focal Adhesion Kinase in Cardiac Development and Disease
(Under the direction of Joan M. Taylor)

In the United States, nearly 80 million adults are affected by cardiovascular disease. The spectrum of disease range from congenital structural defects to acquired structural changes in response to an increased hemodynamic load on the heart, myocardial infarction, or hormonal imbalance. Cardiovascular disease accounts for significant amounts of morbidity and mortality and is currently the number one cause of death in the U.S.

Congenital heart disease is the most common cause of infant death from birth defects. Genetic studies in lower vertebrates have been critical to the understanding of the specific factors required for heart development. These studies suggest that cardiac abnormalities may be mediated by abnormal regulation of transcription factors. Although several transcription factors involved in cardiac development have been elucidated, much regarding specific signaling pathways implicated in abnormal cardiogenesis is still unknown.

Acquired cardiac disease can occur in response to various stimuli. For example, an increased hemodynamic load can result in compensatory hypertrophic remodeling and may progress to pathologic hypertrophy. A common manifestation of this pathologic process is a constellation of symptoms known as congestive heart failure.

Focal Adhesion Kinase (FAK) is responsible for a variety of biological functions including cell adhesion, migration, proliferation, and survival. Several studies demonstrated a role for FAK binding partners and/or for upstream activators of FAK throughout cardiac development and disease. However, since germline deletion of FAK results in early embryonic lethality, it is difficult to study the specific role for FAK in cardiac development and disease. Therefore, we addressed this issue by creating several mouse models which express tissue specific expression of FAK, or its dominant negative FAK-related non-kinase (FRNK). We used these mice to investigate the role of FAK in cardiogenesis, anabolic growth, and cardiac disease. Collectively, these conditional mouse models demonstrated that FAK activity and/or its expression is required for cardiomyocyte proliferation throughout development, is dispensable for anabolic growth of the heart, and is necessary and sufficient for the induction of cardiac hypertrophy. Further characterization of the precise signaling pathways downstream of FAK may lead to targets for future therapeutic intervention to treat congenital and acquired heart disease.

To my nieces Annabella Donna Pizzi and Giovanna Laura Pizzi, may they follow their heart in everything they do

ACKNOWLEDGEMENTS

I am grateful for the knowledge and support of my dissertation committee: Christopher Mack, Susan Lord, Virginia Godfrey, Cam Patterson and my advisor Joan Taylor. They've consistently demonstrated remarkable passion for their work and I have been privileged to work with them throughout this process.

It is with deepest gratitude and appreciation that I acknowledge the support of my fellow graduate students and co-workers. I have been very fortunate to work with a wonderful group of extremely intelligent, considerate, and generous people. Their friendship has remained invaluable to me throughout this process.

I owe a special thanks to my husband whose patience and understanding throughout graduate school and especially the dissertation writing was incredible. Finding him will remain as my best discovery in graduate school.

Lastly, I would not have made it without the love and support of my family, especially my parents. They continue to serve as a great source of inspiration and have seen me through this difficult process, constantly believing in me. I love you all very much.

TABLE OF CONTENTS

Page

LIST OF TABLES..... xi

LISTOF FIGURES..... xii

LIST OF ABBREVIATIONS..... xv

Chapter

1. GENERAL INTRODUCTION..... 1

A. Congenital and Acquired Cardiac Defects..... 2

B. Integrin Signaling..... 3

1. FAK A Coordinator of Integrin Signaling..... 4
2. Models of Conditional FAK Deletion..... 7
3. Proline Rich Tyrosine Kinase 2 (PYK2)..... 9
4. FAK-Related Non-Kinase (FRNK)..... 10

C. Cardiac Development..... 11

1. Genetics of Cardiac Development..... 12
2. FAK and FAK-Related Proteins in Cardiac Development..... 14

D. Cardiac Disease..... 16

1. Gene Mutations in Human Cardiomyopathies..... 17
2. Signaling Mechanisms Involved in Cardiac Disease..... 20
3. Downstream Effectors of FAK Involved in Hypertrophy..... 23

4. FAK's Role in Cardiac Hypertrophy…… 26

E. Goal of Thesis…….... 26

II. MYOCYTE-RESTICTED FAK DELETION ATTENUATES PRESSURE-OVERLOAD INDUCED HYPERTROPHY……..... 38

A. Introduction…….. 38

B. Materials and Methods…….…….…… 41

1. Generation of MFKO mice……..…… 41

2. Antibodies and Reagents……..... 41

3. Biomechanical Stress……..…….. 41

4. Transthoracic Echocardiography…… 42

5. Histological Analysis and Immunohistochemistry…… 43

6. Electron Microscopy…… 44

7. Quantitative RT-PCR……..... 44

8. Western Blotting…….. 45

9. Cardiac Catheterization…….. 45

10. Statistics…… 47

C. Results…… 48

1. Myocyte-Restricted Deletion of FAK in Adult Mice……..... 48

2. FAK is Not Required for Basal Cardiac Function……... 48

3. Pressure-Overload-Induced Structural Remodeling and Hypertrophic Gene Expression are Attenuated in MFKO mice…… 50

4. Persistent Pressure-Overload in MFKO Mice Leads to Cardiac Dysfunction…… 54

5. Absence of FAK Impairs MapKinase Activation Following Hypertrophic Stimuli…… 55

D. Discussion…….. 57

III. FAK ACTIVITY IS NECESSARY AND SUFFICIENT TO INDUCE CARDIAC HYPERTROPHY..... 94

A. Introduction…….. 94

B. Material and Methods…… 98

1. Generation of MycFRNK Mice…….…… 98
2. Generation of SuperFAK Mice…… 98
3. Western Blotting…… 99
4. Histological Analysis and Immunohistochemistry…… 99
5. Antibodies and Reagents……... 100
6. Transthoracic Echocardiography…….. 100
7. Quantitative RT-PCR…….. 101
8. Statistics……..... 102

C. Results……..…… 103

1. Generation of $CX1^{frnk}$ Mice…… 103
2. Ventricle Targeted Expression of FRNK…… 104
3. Histological and Functional Analysis of $CX1^{frnk}Mlc2v^{Cre}$ Hearts.. 105
4. $CX1^{frnk}Mlc2v^{Cre}$ Mice Exhibit A delayed Hypertrophic Response..... 105
5. Generation of SuperFAK Mouse……..…… 107
6. Characterization of the Two βMHCSuperFAK Transgenic Mouse Lines …… 107
7. Characterization of the SuperFAK 2 Mouse Line…….. 108
8. Characterization of the SuperFAK 1 Mouse Line…….. 109

D. Discussion..... 111

IV. FAK ACTIVITY IS REQUIRED FOR PROPER CARDIAC DEVELOPMENT..... 140

A. Introduction..... 140

B. Materials and Methods..... 144

1. Generation of the MycFRNK Mouse..... 144

2. Generation of SuperFAK Mouse..... 144

3. Western Blotting..... 145

4. Histological Analysis and Immunohistochemistry..... 146

5. Antibodies and Reagents..... 146

6. Quantitative RT-PCR..... 146

7. Apoptosis and Cell Proliferation Assays..... 147

8. Statistics..... 148

C. Results..... 149

1. FRNK Protein is Not Detectible in Developing or Postnatal Hearts..... 149

2. Nkx2.5 Targeted Expression of FRNK..... 149

3. Histological and Morphological Analysis of the CX1^{frnk}Nxk2.5^{cre} Mouse..... 150

4. MycFRNK Expression Results in Decreased Cell Proliferation but Does Not Affect Apoptosis..... 152

5. Embryonic Lethality is Due to A Cardiomyocyte Specific Growth Defect..... 153

D. Discussion..... 155

V. GENERAL DISCUSSION..... 178

REFERENCES……..……..... 184

LIST OF TABLES

Table		Page
2.1	Echocardiograph Analysis in Baseline, Banded and Aged Mice……..	64
2.2	Baseline Contractility in Control and MFKO Mice……...	68
2.3	Fibrosis in Control and MFKO Mice……..	71
2.4	Echocardiograph Analysis in Baseline and Banded Mice……..	80
3.1	Baseline Echocardiography in CX1^{frnk}Mlc2v^{Cre} and Control Mice…….	122

LIST OF FIGURES

Figure		Page
1.1	Schematic of Focal Adhesion Kinase (FAK) and Focal Adhesion Kinase Related Non-Kinase (FRNK)……..	28-29
1.2	Sarcomeric and Cytoskeletal Proteins Involved in Human Cardiomyopathies……..	30-31
1.3	FAK is Central for the Correct Function of Z-disk Proteins……..	32-33
1.4	Maladaptive and Physiological Signaling Pathways…….....	34-35
1.5	Pathways Involved in Cardiac Hypertrophy…….	36-37
2.1	Targeted Myocyte Specific Disruption of Mouse Focal Adhesion Kinase…….	62-63
2.2	FAK is Required for Myocyte Growth……...	65-67
2.3	FAK is Not Required for Maintenance of Myocyte Cyto-Architecture.....	69-70
2.4	FAK is Essential fro Pressure-Overload-Induced Hypertrophy……	72-73
2.5	FAK is Required for Increased Posterior Wall Thickness…….....	74-75
2.6	MFKO Hearts Have Reduced Myocyte Area……..	76-77
2.7	Functional and Morphological Changes Induced by TAC in Control and MFKO mice……...	78-79
2.8	Post TAC MFKO Hearts Have Increased Fibrosis but MFKO Myocytes Display Normal Cyto-Architecture…….....	81-82
2.9	MFKO Hearts Have Similar Ultra-Structure as Controls……..	83-84
2.10	FAK Deletion Does Not Alter Expression of Apoptotic Markers…..	85-86
2.11	FAK Modulates ANF Expression following TAC…….	87-88

2.12	Chronic Banding Leads to Systolic Dysfunction in MFKO Mice…..	89-90
2.13	FAK is Required for Maximal ERK Activation Induced by Banding and Adrenergic Stress…….……....	91-93
3.1	Characterization of the MycFRNK Transgenic Mouse……..	116-117
3.2	Targeted Myocyte Specific Inhibition of Focal Adhesion Kinase….	118-119
3.3	Inhibition of FAK in the Postnatal Heart Does Not Alter Anabolic Growth……...	120-121
3.4	Cardiac Expression of MycFRNK Attenuates the Hypertrophic Response Following Aortic Banding……..	123-124
3.5	Construction of the SuperFAK Transgene……..	125-126
3.6	Identification of the Two SuperFAK Transgenic Mouse Lines…….	127-128
3.7	Characterization of the SuperFAK Mouse……...	129-130
3.8	Histological Analysis of SuperFAK Hearts……..	131-132
3.9	Increased FAK Activity Results in Increased Cardiomyocyte Cell Area……...	133-134
3.10	FAK Activity Modulates Hypertrophic Gene Expression……..	135-136
3.11	Prolonged Exposure to SuperFAK Increases Cardiac Size and Function……..….	137-138
4.1	Expression of FAK and FRNK During Heart Development…….	160-161
4.2	Generation of CX1^{frnk}Nxk2.5^{Cre} Mice……...	162-163
4.3	Histological Analysis of CX1^{frnk}Nxk2.5^{Cre} Mice……..	164-165
4.4	Decreased FAK Activity in CX1^{frnk}Nxk2.5^{Cre} Hearts result in a Cardiomyocyte Proliferation Defect……...	166-167
4.5	4.1 Comparable Histology in Other Tissues with Nxk2.5 Expressing Cells……..	168-169

4.6 Inhibition of FAK Activity Does Not Increase Apoptosis……..…… 170-171

4.7 Decreased FAK Activity Inhibits Cellular Proliferation……... 172-173

4.8 Generation of SuperFAK Rescue Mice…… 174-175

4.9 4.2 SuperFAK Alleviates Proliferation and Ventricular Septation Defect……..…….. 176-177

ABBREVIATIONS

Ab	Antibody
ANF	Atrial Natruretic Protein
AngII	Angiotensin II
ATP	Adenosine Triphosphate
βMHC	β Myosin Heavy Chain
BrdU	Bromodeoxyuridine
CHF	Congestive Heart Failure
d	Diastole
DCM	Dilated Cardiomyopathy
ECM	Extracellular Matrix
EF	Ejection Fraction
EGF	Epidermal Growth Factor
ERK	Extracellular Signal-Related Kinase
FAK	Focal Adhesion Kinase
FN	Fibronectin
FRNK	FAK-related non-kinase
FS	Fractional Shortening
GPCR	G-Protein Coupled Receptor
Grb2	Growth Factor Receptor Bound Protein 2
HCM	Hypertrophic Cardiomyopathy
HR	Heart Rate
IGF	Insulin Growth Factor

IVS	Interventricular Septum
JNK	c-Jun N-Terminal Kinase
LVED	Left Ventricular End Diameter
LVPWT	Left Ventricle Posterior Wall Thickness
MAPK	Mitogen Activated Protein Kinase
p130Cas	p130 Crk-Associated Substrate
PBS	Phosphate Buffered Saline
PDGF	Platelet Derived Growth Factor
PE	Phenylephrine
PI3K	Phosphatidylinositol 3 Kinase
PLC	Phospholipase C
Pyk2	Proline Rich Kinase 2
s	Systole
SMC	Smooth Muscle Cell

Chapter I

GENERAL INTRODUCTION

In this thesis, I describe my work highlighting the importance of focal adhesion kinase (FAK) in cardiac development and disease. Specifically Chapter II investigates the role of FAK in the progression of cardiac hypertrophy. In this chapter I demonstrated that deletion of FAK protein attenuates the hypertrophic response following aortic constriction. Chapter III explores the possibility that FAK activity is both required and sufficient for the induction of cardiac hypertrophy. In this chapter I utilized two distinct mouse models, one which expresses FRNK specifically in the myocardium which we have used to examine whether inhibition of FAK activity will block the pressure-overload induced hypertrophic response, and a second novel mouse model which expresses constitutively active FAK in the heart. Lastly, Chapter IV describes a mouse model in which cardiac restricted overexpression of the dominant negative of FAK, FAK-related non-kinase (FRNK) is induced in the heart field in mid-gestation and leads to embryonic lethality between day 14-15 secondary to a significant proliferation defect. I begin with a general introduction on congenital and acquired cardiac diseases, then discuss integrin signaling and the importance of FAK signaling in a variety of biological processes, followed by general introductions regarding development and cardiac disease then finally respectively discuss the specific involvement of FAK in these processes.

A. Congenital and Acquired Cardiac Defects

Human heart development initiates at 20 days post-conception with the formation of the cardiogenic plate and continues until a four-chambered heart is formed, thirty days later. In mice, the equivalent process is completed in 6 days. During this period of organogenesis, there are ample occasions for defects to occur. In fact, congenital heart disease affects close to 1% of human newborns and is the most frequent form of major birth defect [1]. These birth defects can manifest in many variants. The most common congenital defect is the ventricular septal defect which acts as a left to right shunt, allowing oxygen rich blood to flow into the right ventricle instead of moving into the aorta. Others defects include atrial septal defects, pulmonary and aortic stenosis, and transposition of the great arteries in addition to patent ductus arteriosus, which misdirects blood into the lungs due to the failure of this temporary vessel to close. Combinations of these defects are observed in both DiGeorge Syndrome and Tetralogy of Fallot which consists of the combination of four defects, ventricular septal defect, pulmonary valve stenosis, misplaced aorta, and ventricular hypertrophy. These disorders represent a proportion of commonly recognized congenital cardiac developmental defects that commonly affect cardiac function.

Cardiac morphogenesis is complete upon birth and normal heart growth occurs by an anabolic mechanism that involves increased cardiac cell size. However, the adult heart can remodel in response to a number of factors that can eventually lead to cardiac diseases. Many stimuli such as an increased

hemodynamic load on the heart, myocardial infarction, or hormonal imbalance will place strain on the heart and cause it to develop compensatory hypertrophy. Over time, the initial response leads to chronic pathological hypertrophy characterized by increased left ventricle thickness, amplified myofibrillar protein content, and an altered pattern of cardiac gene expression. The resultant clinical outcome is congestive heart failure, a syndrome with significant morbidity and mortality that afflicts nearly 5 million Americans today.

On a cellular level, the interaction of cardiomyocytes with their extracellular environment is essential for normal physiological formation of the heart. In addition, these interactions provide the structural, chemical, and mechanical substrate necessary to sustain adequate function of the adult heart [2]. Understanding the specific signaling pathways involved between the extracellular environment and intracellular proteins is integral in the discoveries of targeted therapies for both congenital heart defects and acquired cardiac diseases.

B. Integrin Signaling

The extracellular matrix interacts with a family of cell surface receptors referred to as integrins. This interaction activates a number of downstream cellular signaling pathways important in a variety biological processes [3]. Integrins were discovered as proteins that were involved in transmembrane linkage between fibronectin and actin and eventually described as an “integrin” because it was both an integral membrane protein and involved in cellular and extracellular matrix (ECM) integrity [4, 5]. Integrins are heterodimeric transmembrane receptors composed of an α and β subunit [6]. In mammals, integrins comprise a family of 18α and 8β

subunits which can form into 24 known combinations of α/β heterodimers. The combination of the specific α and β subunits direct the ligand specificity of the integrin complex [7].

Within this large family of integrins, a smaller number of α and β chains are specific to the heart. In cardiomyocytes, six distinct α subunits (α_1,α_3,α_5,α_6,α_7, and α_{10}) are expressed only with the $\beta 1$ subunit, including a splice variant of β1,termed β_{1D}, which is the isoform primarily expressed in the postnatal heart [8, 9]. Some integrins, including α_1 and α_5, are temporally regulated, being expressed in the embryonic heart then downregulated postnatally and upregulated following aortic constriction, an experimental model of pressure-overload [2]. Upon ligand binding, integrins cluster into focal contacts which also contain specific cytoskeleton proteins such as talin, vinculin, α-actinin, and actin [10]. In addition to their function as structural links between the ECM and cytoskeleton, integrins regulate a variety of downstream biological pathways [11].

1. FAK, a Coordinator of Integrin Signaling

FAK is a key protein involved in integrin signaling. Upon integrin clustering, FAK is recruited to sites of cellular contact to the ECM called focal adhesions[7]. Although integrin ligation is the main activator of FAK, FAK is also activated by growth factors, neuropeptides, G-protein coupled receptor agonists, and mechanical stimuli [12]. FAK contains an N-terminal domain, a C-terminal focal adhesion targeting domain, and a central kinase domain (Figure 1.1). The N-terminus of FAK resembles a protein domain termed a FERM domain named for its presence of four

proteins; (erythrocyte band four 1-ezrin-radixin-moesin) which interacts with transmembrane receptors and with plasma membrane lipids [13]. The amino terminus of FAK interacts with several proteins including the tail of β1-containing integrins, activated platelet derived growth factor (PDGF) and epidermal growth factor (EGF) receptors, the tyrosine kinase Etk, and FERM domain-containing protein ezrin; each of which could be involved in regulating FAK's activity [13]. The C-terminus of FAK is rich in protein-protein interaction sites and contains a focal adhesion targeting site (FAT) that directs FAK to sites of focal adhesions which is essential for its function [14]. The FAT domain contains binding sites for two focal adhesion-associated proteins, paxillin and talin. FAK binds to paxillin's leucine rich sequences referred to as LD motifs. These motifs function in protein-protein interactions. Paxillin also binds directly to the cytoplasmic domain of integrin α subunits as well as vinculin, a focal adhesion protein. Therefore, it has been postulated that paxillin may act as a docking partner for FAK at focal adhesions, although FAK recruitment to focal adhesions is not completely dependent on binding to paxillin [15].

As described briefly above, integrin clustering is a major activator of FAK, resulting in rapid auto-phosphorylation. The major site of tyrosine auto-phosphorylation is tyrosine 397 which correlates with increased catalytic activity. This phospho-tyrosine acts as a docking site for the SH2 domain for the Src family of tyrosine kinases as well as other SH2 containing proteins, which include phosphotidylinositol 3 kinase (PI3K), phospholipase Cγ (PLCγ), and the adapter protein Grb7 [16]. In addition, this Y397-dependent activation of FAK leads to the

tyrosine phosphorylation of FAK-binding proteins p130Cas and paxillin [17]. FAK contains five other sites of tyrosine phosphorylation that are likely phosphorylated by bound Src kinases [18]. Phosphorylation of Y576 and Y577 are important for maximal catalytic activity and signaling to downstream effectors [18]. Phosphorylation of tyrosine 925 creates a binding site for the SH2 domain of Grb2 [19]. Grb2 is an adaptor molecule that connects FAK to the MAP kinase signaling pathway by binding to Sos, a GEF (guanine nucleotide exchange factor) for Ras. In addition, FAK catalyzed phosphorylation of p130Cas (p130 Crk-associated substrate) and/or paxillin can lead to Ras activation by the adaptor molecule Crk.

The activation of FAK and subsequent activation of downstream effectors are responsible for a variety of biological functions. Through signaling pathways involving PI3K, PLCγ, MAP kinase, paxillin and p130Cas, FAK has a role in cell adhesion, migration, proliferation, and survival. In addition, FAK regulates the turnover of focal adhesions by modulating Rho activity. This process may involve the FAK binding partner GRAF, a negative inhibitor of Rho [20]. As noted earlier, autophosphorylation of FAK leads to activation of the p130Cas pathway as well as PI3K. Experiments using a FAK mutant defective for p130Cas binding failed to induce p130Cas phosphorylation and attenuated cell migration [21]. Additional studies also showed that a FAK mutant that did not to associate with PI3K also failed to stimulate motility *in vitro* [22]. There is also evidence that suggests that FAK may function to regulate cell proliferation by controlling the levels of cyclinD through increased transcription of the cyclin D gene by enhancing the binding of an Ets transcription factor to the cyclin D promoter [23]. Lastly, in some cell types, FAK has

been implicated to increase cell survival. Studies have shown that in response to a variety of stimuli, inhibition of FAK can induce apoptosis while overexpression can prevent apoptosis [12]. The mechanism for FAK-dependent cell survival is not completely understood, but it may involve the association of FAK with PI3K and activation of AKT, as well as through Grb2 interaction with the Ras/MAPK pathway [24, 25].

In wildtype embryos, FAK expression gradually increases from E8.0 onward and is ubiquitously expressed, though expression is most predominant in the mesoderm at midgestation (E8.5) [26]. Consistent with FAK's critical biological functions *in vitro*, the germline deletion of FAK results in embryonic lethality around E8.5. The FAK deficient embryos exhibit a general mesodermal deficiency similar to that of the fibronectin (FN) null mouse. Closer examination revealed an absent notochord, defects in the fusion of the cardiac plates, and poor vascularization of the embryo and yolk sac [26]. Overall, in the absence of FAK, the embryos display defects in cell proliferation and/or differentiation, as well as cell migration.

2. Models of conditional FAK deletion

Initially experiments performed on cultured fibroblasts derived from the *fak*$^{-/-}$ embryos revealed that depletion of FAK led to reduced motility and increased apoptosis [27, 28]. However, recent data using Cre/loxP technology has elucidated cell type specific functions of FAK. Studies from the Reichart lab explored the role of FAK in the nervous system. They developed a floxed FAK mouse which was crossed with the *emx*1 promoter which is active in neuroepithelial precursors of neurons and glia in the developing cortex and hippocampus beginning at embryonic

day 9 [29]. Interestingly, FAK deletion in either radial glia or meningeal fibroblasts resulted in aberrant neuronal migration, but the FAK deletion in neurons alone did not result in a migration defect [29]. However, FAK depletion led to disrupted laminin organization and overall basement membrane assembly and/or remodeling, indicating that FAK was likely activating in a non-cell autonomous effect to modify neuronal migration.

Using a similar floxed FAK mouse with an endothelial cell specific Tie2-Cre, Jun-Lin Guan's group discovered that endothelial cell specific deletion of FAK leads to embryonic lethality. The embryos were able to develop normally through early embryogenesis. However, in late embryogenesis (E13.5) the FAK depleted endothelial cells exhibited proliferation and migration abnormalities manifesting in defective angiogenesis that was evident in the embryos, yolk sac, and placenta. The embryos also exhibited vascular defects and associated edema [30]. There was conflicting data published shortly after Jun-Lin Guan's group which showed embryonic lethality at an earlier stage, between E10.5 and 11.5, using the Tie2-cre crossed to a different floxed FAK mouse**.** These endothelial cells (EC) derived from the mutant embryos revealed no apparent decrease in proliferation or migration, but instead the ECs had aberrant lamellipodial extensions, altered actin cytoskeleton, and nonpolarized cell movement [31]. Additionally this work demonstrated that FAK played a cell-autonomous function in ECs and that it is crucial for vascular development [31]. The different phenotypes in these two models may be due to the specific timing of FAK deletion using the two different floxed mice and highlight the

possibility that FAK can have different functions throughout the various stages of development.

Recently we published data using the floxed FAK mice developed by the Reichart lab, showing that FAK deletion from Nkx2.5-Cre expressing cells in the primary and secondary heart field resulted in lethality shortly after birth. These mice had a profound sub-aortic ventricular septal defect and associated mal-alignment of the outflow tract due to a specific cardiomyocyte migration defect in the absence of any noted proliferation or cell survival defects [32].

My work described in Chapter II utilized the Mlc2v-Cre line to induce a cardiomyocyte-specific deletion in the adult myocardium. In this model, conditional deletion of FAK from the myocardium of adult mice did not affect basal cardiac performance, myocyte viability, or myofibrillar architecture. However, deletion of FAK attenuated the increase in left ventricular posterior wall thickness, myocyte cross-sectional area and hypertrophy-associated atrial natriuretic factor induction following pressure overload in the absence of apoptosis [33]. These data highlight a necessary role for FAK in pathological remodeling and suggests a role for FAK as the mechanotransducer for biomechanical stress in the heart.

3. Proline Rich Tyrosine Kinase 2 (Pyk2)

A protein that shares approximately 48% amino acid identity (65% similarity) with FAK is Pyk2 (proline rich tyrosine kinase 2). Both proteins share similar domains and both have been identified in human, mouse, chicken, and frog[34]. Unlike FAK's ubiquitous expression, Pyk2 is highly expressed in the central nervous system and in cells from hematopoietic origin. A number of FAK's binding partners

also bind Pyk2, including Src family kinases and paxillin. Unlike FAK, Pyk2 is localized to the cytoplasm and concentrated in perinuclear regions and is regulated by stimuli that elevate cytoplasmic levels of calcium [12]. Studies in FAK-deficient fibroblasts showed Pyk2 localization at sites of focal adhesions and integrin induced phosphorylation of Pyk2, suggesting that Pyk2 may compensate for loss of FAK in some circumstances to mediate signal transduction [35]. Although these two molecules are very similar in structure, studies have shown that over-expression of Pyk2, but not FAK, in rat and mouse fibroblasts leads to apoptotic cell death [35]. Lastly, the Pyk2 null mice, unlike FAK null mice, are viable and fertile without any overt developmental phenotype with the exception of a macrophage migration and function defect [36]. Throughout our studies we have taken measures to determine whether Pyk2 may function to compensate or even exacerbate the phenotypes observed in our conditional FAK knock-out mice.

4. FAK-Related Non-Kinase (FRNK)

FAK-related non-kinase or FRNK is a 43 kDa version of FAK comprised of the C-terminus of FAK, but lacking the kinase domain (Figure 1.1). Since FRNK is comprised of the C-terminus of FAK, it is targeted to focal adhesions and binds to critical FAK binding partners (p130Cas, paxillin, talin, GRAF). FRNK is transcribed from an alternative promoter located in the intron of the FAK gene. Unlike FAK, FRNK is expressed primarily in the vasculature smooth muscle and is upregulated following vascular injury [37]. Interestingly, studies have shown that FRNK can act as an inhibitor of integrin dependent FAK activity and downstream signaling. Since FAK is activated by homodimer formation and trans-phosphorylation FRNK likely

inhibits FAK activity by forming inactive FAK:FRNK heterodimers [12]. FRNK has been used as a tool to study the role of FAK in many systems including the cardiovascular system. For example, infection of cultured cardiomyocytes with an adenovirus containing GFP-FRNK attenuated phenylepherine (PE)-stimulated hypertrophy, determined by cell size, sarcomeric organization, and induction of atrial natriuretic factor [37, 38]. Further studies used FRNK to determine its ability to inhibit endothelin-1 and stretch mediated hypertrophy [39]. My studies described in Chapter III of this thesis describe a mouse model we generated that overexpresses FRNK in myocytes shortly after birth. This model has enabled us to examine a role for FAK in anabolic growth of the heart and will allow us to determine the different roles of FAK as a signaling molecule versus a scaffold for focal adhesion proteins.

C. Cardiac Development

The heart is the first organ to form in the embryo and is crucial for embryonic viability. Defects in the carefully orchestrated steps that govern cardiac development contribute significantly to fetal and childhood mortality [40]. Congential heart abnormalities are the most common birth defect and account for most of the deaths from birth defects during the first year of life and their frequency in miscarried pregnancies is estimated to be tenfold higher [41, 42]. Although in the past decade, much has been elucidated regarding the molecular blueprint underlying cardiac morphogenesis, there are many details that remain to be revealed. Such questions are directed at describing how diverse cell fates are specified, the mechanisms that connect mutations in specific proteins to cardiac phenotypes, as well as the details of the cell-autonomous and non-cell autonomous signaling mechanisms controlling

myocyte growth and function [43]. Understanding these mechanisms will hopefully provide new therapies targeted at restoring cardiac function in patients afflicted with congenital heart disease.

1. Genetics of Cardiac Development

Congenital heart defects can occur during the multiple steps involved in cardiac development. The first step involves specification of the cardiac precursors followed by the migration of these cells and fusion of the heart tube. The second step is the formation of cardiac chambers due to a rightward looping of the heart tube. Following chamber formation, a series of events leads to the development of the myocardial protrusions into the lumen called trabeculations, the construction of heart valves, and septation of the chambers. Finally, the development of the multilayered spiral system of the ventricles completes the myocardial architecture [44].

The heart forms from two separate progenitor cell populations or heart fields referred to as the primary and secondary heart fields. These fields divide from a common progenitor at gastrulation [45-47]. The primary heart field arises from the anterior splanchnic mesoderm and is responsible for the formation of the cardiac crescent and ultimately the left ventricle and atria [48]. The secondary heart field arising from the pharyngeal mesoderm contributes to the right ventricle and outflow tract [45, 46, 49]. The primary heart field is distinguished by expression of specific transcription factors Tbx5, bhHLH and Hand2 whereas the secondary heart field is mediated by the transcription factor Isl1 and Fgf10 [45, 46]. The homeobox gene Nxk2.5 is expressed in both heart fields [50].

Following gastrulation, the mesoderm migrates to form the cardiac crescents. At this time, the specification of cardiomyocytes occurs from the anterior lateral mesoderm in response to factors excreted from the adjacent ectoderm, including bone morphogenic proteins. In vertebrates, the expression of the homeobox gene Nkx2.5 is the earliest marker of the cardiac lineage [51]. Soon after specification, the cardiac precursor cells migrate anteriorly towards the midline and fuse into a single heart tube. This migration is directed by FN within the ECM. The cardiac tube contains a distinct myocardial layer of one to two cell layers and an endocardial layer separated by an acellular cardiac jelly composed of ECM. Studies have highlighted the importance of GATA transcription factors in the formation of the heart tube [52]. GATA4 null mice arrested in development between E7.0 and E9.5 due to severe abnormalities including an absent primitive heart tube and foregut [52]. At this stage the heart tube is divided along the anterior-posterior axis into precursors for the fully formed heart and there is the addition of cells from the secondary heart field. This heart tube next undergoes a rightward looping to change the anterior/posterior polarity of the heart to left/right polarity. This change is necessary to align the ventricles with the vasculature and for proper orientation of the pulmonary artery on the right and the systemic artery (aorta) on the left [53]. Left-right symmetry is guided by the transcription factor Pxt2 which is expressed on the left side of developing organs. Solidification of the basal portions of the trabeculae via proliferation of the ventricular myocytes involves neuregulin growth factors secreted from the endocarduim to their myocardial receptors Erb2 and Erb4 [54]. Other endocardial factors such as vascular endothelial growth factor (VEGF) and

angiopoetin-1 are involved in ventricular trabeculation [55, 56]. This compaction correlates with the invasion of coronary vasculature from the epicardium and also occurs around the same time as the formation of cardiac valves. Signaling between the endocardial and myocardial cells in the endocardial cushions involves TGFβ and induces the transformation of endocardial cells into mesenchymal cells which then migrate into the cushions to form the fibrous tissue of the valves [57]. In addition, studies have revealed the transcription factors, NF-ATc and Smad6 are important in the formation of cardiac valves [58, 59]. Although these genes represent a basic plan for development, further discovery of the genetic complexity involved in cardiac development is critical not only for the understanding of congenital defects but also for treatment of adult acquired cardiac diseases.

2. FAK and FAK-Related Proteins in Cardiac Development

As noted above, the germline deletion of FAK is embryonic lethal between E8.5 and E10. The mesodermal defect resulting from the loss of FAK indicates that FAK may be important in cardiac development. In support of this hypothesis, the major activator of FAK (FN), as well as several FAK binding partners of have been implicated in heart development.

The major extrinsic activator of FAK signaling is the ECM protein, FN. A study involving a model that inactivates both FN alleles causes embryonic lethality at E8.5, highlights the importance of FN in development [60]. Development of *FN*$^{-/-}$ embryos proceeds normally through implantation and gastrulation, however as the embryo progresses it displays fundamental defects in mesodermal migration, adhesion, proliferation, or differentiation. Specifically, these mouse embryos display

abnormal vasculature and a structurally deformed heart. In the more severe phenotypes, the loss of FN resulted in a lack of fusion of the heart primordia. In less severe models, the heart contained thickened myocardial tissue, a defect in cardiac jelly, and abnormal endothelium [61]. Overall, FN is critical for embryonic development of the embryo as well as for cardiac development.

Mice that have been engineered to delete p130Cas, an adaptor molecule that is phosphorylated by FAK and is important in cell migration and proliferation, result in an embryonic lethal phenotype at embryonic day 12.5. These embryos exhibit marked growth retardation and overall systemic congestion compared to controls. The p130Cas null hearts were poorly formed and contained myofibrillar disorganization and disruption of the Z-disks [62]. This data provides evidence that alterations in the FAK signaling cascade can lead to defective sarcomeric organization and impaired cardiac development.

Another FAK binding protein essential for heart development is paxillin. Paxillin is phosphorylated following integrin activation and serves as a scaffold to mediate downstream integrin signals. Germline deletion of paxillin results in a similar phenotype as the deletion of FN [63]. In both models, there are defects in the development of mesoderm derived structures including the heart. In *ex vivo* experiments, *paxillin*$^{-/-}$ cells show deficient focal adhesion formation, migration, and localization of FAK to focal adhesions. Because of this similarity with the *FN*$^{-/-}$ mouse, paxillin is thought to be a critical transducer of FN signals in development [63].

Given that the FAK germline deletion leads to profound mesodermal defect and due to the variety of FAK binding proteins that are involved in cardiac development, it seems to follow that FAK regulates critical pathways that are necessary for normal cardiac development and function. Elucidating these pathways may provide insight into the signaling mechanisms underlying several congenital heart abnormalities and may ultimately result in new targeted small-molecule therapeutics.

D. Cardiac Disease

Currently, approximately 5 million Americans are afflicted with congestive heart failure (CHF), with 550,000 cases diagnosed in the United States each year [64]. This emerging epidemic is caused by a complex combination of structural, functional, and biological alterations [65]. The induction of CHF associated with cardiac hypertrophy is an initial compensatory response to an increased hemodynamic load on the heart. These adaptive mechanisms include local and systemic release of cytokines, peptides, and neurohormones, that result in increased cardiomyocyte size and increased myofibrillar content [66]. However, chronic stimulation by pressure or volume overload, myocardial infarction, or hormonal imbalance can lead to pathological hypertrophy and eventually congestive heart failure, characterized by an altered pattern of cardiac gene expression, fibrosis, re-expression of fetal gene transcripts and cardiac dysfunction [67, 68]. Despite the recent advances in the study of heart disease and the understanding of cardiac function at genetic and molecular levels, cardiovascular disease is still the number one cause of death in the western world [1]. It therefore stands that continued

investigation into the signaling pathways governing normal and abnormal cardiac growth, apoptosis and survival is key to the process of developing novel therapies for treatment of CHF [43].

1. Gene Mutations in Human Cardiomyopathies

In response to constant pathological stress the heart undergoes ventricular remodeling. This remodeling can manifest as one of two distinct pathologies, hypertrophic cardiomyopathy (HCM) involving increased wall thickness without chamber expansion or dilated cardiomyopathy (DCM) associated with normal or increased wall thickness and enlarged chamber size [69]. Physiologically, these phenotypic changes result in impaired diastolic relaxation in HCM and impaired systolic function in DCM [70]. Histologically, HCM is characterized by enlarged, disorganized myocytes that die prematurely and subsequently result in increased fibrosis. While DCM also demonstrates degenerating myocytes and increased fibrosis, it is notably characterized by lack of myocyte disarray [69]. The incidence of sudden cardiac death in HCM is 2-4% in adults and current treatment involving β-blockers, calcium channel antagonists, and antiarrhythmic drugs appear to be promising treatments [71]. However, despite advancements in therapy, the average five year survival rate for DCM patients who do not undergo cardiac transplant is less than 50% [71].

Studies detailing cases of familial hypertrophic cardiomyopathy reveal that mutations in genes encoding structural sarcomeric proteins are implicated in the disease [72, 73]. Heart cells generate contractile force by the sarcomere and transmit this force to the ECM [69]. The proteins located at the Z disks of

sarcomeres sense the stretch on the cell and transduce signals that are necessary for cardiomyocyte contraction. Genetic studies of familial hypertrophic cardiomyopathy have identified several genetic mutations in sarcomeric proteins that include the β myosin heavy chain (βMHC), myosin binding protein C (MyBP-C), cardiac troponin T (TnT) and cardiac troponin I (TnI), tropomyosin(Tm), myosin light chain, actin, and titin (Figure 1.2) [74, 75]. Actin is the major component of the thin filament and forms a complex with Tm and troponins, contributing to the contractile unit of heart muscle. Part of the thick filament is made of βMHC. βMHC contains a head region that binds actin and ATP and is essential for generation of movement needed for contraction [76]. The S2 subfragment of βMHC binds to the head region of βMHC and connects to MyBP-C and titin, assembling the thick fragment and stabilizing the protein [76]. Mutations in actin, Tm, βMHC, TnT, TnI, MyBP-C, and titin, can lead to DCM however the sites mutated in these proteins differ than the mutations linked to HCM [69]. Mutations in sarcomeric proteins observed in patients with HCM characteristically result in increased actin-activated ATPase activity as well as greater force production and faster actin-filament sliding whereas mutations observed in DCM result in impaired force transmission.

Although some mutations in sarcomeric genes are linked to DCM, the majority of DCM patients have mutations in cytoskeletal proteins [72, 73]. Alterations in desmin, dystrophin, metavinculin, muscle LIM protein (MLP), α-actinin, and ZASP have all been linked to DCM [77]. Desmin is a cytoskeletal protein that is involved in intermediate filament organization and is responsible for connecting the nuclear and plasma membranes, thereby stabilizing the sarcomere [78]. Dystrophin, a large

cytoskeletal protein, interacts with actin and is thought to play a role in force transduction [79]. Located in the intercalated disks, metavinculin, an isoform of vinculin, anchors thin filaments and is involved in force transmission [80]. Interacting with both titin and α-actinin, a protein involved in anchoring myofibrillar actin filaments, MLP is implicated in muscle differentiation and sarcomere assembly [78]. Lastly, ZASP plays an important role bridging the sarcomere to the cytoskeletal network. Despite their varied functions, mutations in these genes result in a DCM phenotype.

It follows that the above discussed proteins provide structural functions and therefore must work in concert with a signaling molecule that is able to sense the stretch applied to the cell. FAK, although yet to be implicated in human cardiomyopathies, connects the sarcomeric proteins to the ECM and may be responsible for transmitting signals activated in myocyte stretch and contraction. As stated above, FAK is activated following integrin ligation and FAK drives the formation of a focal adhesion complex that involves many of the aforementioned proteins that may play a role in human cardiomyopathies. Therefore it is possible that FAK is acting as an effector for the mechanosensors in the cell (the integrins), and impaired FAK signaling could affect the subsequent downstream proteins involved in both HCM and DCM (Figure 1.3). Studies discussed in Chapter II of this thesis suggest that if FAK is absent from the focal adhesion complex, which is known to link Z disk proteins to the ECM and for force transmission, a DCM phenotype occurs following aortic constriction. In addition, I discuss a novel mouse model in Chapter III which ectopically expresses FRNK in the myocardium. In this

model the absence of FAK activity is dispensable for anabolic growth but abrogates the hypertrophic progression following aortic constriction. These data indicate that FAK activity is essential for this process. Furthermore, I also introduce a novel, cardiac specific FAK overexpression model that results in hypertrophic remodeling of the myocardium (Figure 1.3). In summary, our findings support a model whereby FAK activity is central to the signaling complex between the ECM and Z-disk proteins.

2. Signaling Mechanisms Involved in Cardiac Hypertrophy

Varieties of cellular receptors are stimulated during cardiac hypertrophy and lead to different responses. Generally, the activation of receptor tyrosine kinases (IGF-1) initiates a physiological hypertrophy phenotype where as activation of the G protein coupled receptors (GPCR) stimulates a pathological hypertrophy response. Both physiological hypertrophy and pathological hypertrophy have the same initial compensatory response. In physiological hypertrophy, increased exercise leads to compensatory cell growth, which is beneficial to the heart over time. However, in pathological hypertrophy, the initial compensatory growth is followed by detrimental reversion to the fetal gene profile, and increased fibrosis, culminating in heart failure and an eventual increase in morbidity and mortality. Although many molecules have been defined to have a specific role in either pathological or physiological hypertrophy, the further delineation of the distinct signaling pathways is critical for the treatment of heart disease (Figure 1.4). From here on, unless specified, cardiac hypertrophy refers to the pathological response.

Normal anabolic cardiac growth and physiological hypertrophy are largely mediated through insulin growth factor-1 (IGF-1) and growth hormone (GH). GH is activated via increased production of IGF-1. IGF-1 signals through its membrane tyrosine kinase receptor (orange in Figure 1.4), activating the PI3K subunit α (p110α). This event activates downstream effectors such as the Ser/Thr kinase AKT and its activator 3-phosphoinositide-dependent protein kinase-1 (PDK-1) [81-83].

The major signaling pathway implicated in physiological hypertrophy involves PI3K, a protein implicated in various cellular processes including proliferation, survival, and cytoskeleton organization [84-87]. PI3K is part of a group of lipid kinases which are activated by receptor tyrosine kinases such as IGF-1 and GPCRs to regulate various cellular functions, including cell growth and survival [83]. *In vivo* data have shown that mice expressing a constitutively active form of PI3K in myocytes develop increased myocyte cell size and increased cardiac contractility with no evidence of pathological hypertrophy, implicating a crucial role for PI3K in the regulation of cardiac cell growth [85, 87]. In addition, loss of kinase activity of the α- and γ- subunits of PI3K leads to different effects. Mice expressing a cardiac specific dominant negative of p110α show that p110α is required for the induction of physiological hypertrophy but is not necessary for the hypertrophic response to pressure overload. In addition, data from mice carrying a targeted mutation in the PI3Kγ gene show that the p110γ is required for stress induced hypertrophy but not normal growth [87-89]. The downstream effector, AKT, is required for normal heart growth as suggested by data from AKT null mice [90]. In fact, AKT null mice have

defects in both fetal and postnatal growth. There defects continue into adulthood [90]. Downstream targets of AKT include the mammalian target of rapamycin (mTOR), and glycogen synthase kinase 3β (GSK3β). The serine/threonine protein kinase mTOR mediates protein synthesis and transcription necessary for hypertrophy [91-93]. GSK3β is a serine/threonine protein kinase that is catalytically active even under unstimulated conditions [94]. When stimulated by IGF-1 signaling through the PI3K-AKT pathway, GSK3β is phosphorylated and becomes a negative regulator of cardiac pathological hypertrophy by inhibiting increases in the rate of protein synthesis and hypertrophic gene expression [95, 96].

In addition to IGF signaling, PKCε, a molecule thought to be specific to physiological hypertrophy, is activated by mechanical stress, GPCR, and physiological hypertrophic stimuli [97, 98].

GPCRs (green in Figure 1.4) are activated by hormones or neurotransmitters [99]. The G protein G_q is thought to be important in the induction of cardiac hypertrophy because ligands such as phenylepherine, angiotensin II (AngII) and endothelin I activate G_q-coupled receptors and trigger *in vitro* induction of cardiomyocyte hypertrophy [100-102]. *In vivo* studies have also implicated a role for GPCR in pressure overload ventricular hypertrophy [103]. These studies utilize transgenic mice that display an overexpression of either $G\alpha_q$, α1-adrenergic receptors (ARs) or AngII receptors and all develop cardiac hypertrophy [104-106]. Progression of hypertrophy is accompanied by an increased accumulation of ECM proteins, such as FN [107]. Many studies have noted an intimate relationship between cardiac hypertrophy and modifications in the ECM as reviewed by Bendall

et. al. [108]. As noted above, integrins (red in Figure 1.4) mediate interactions between the cell membrane and the ECM, which results in the formation of transient signaling complexes termed focal adhesions. Interestingly, the $\alpha_5\beta_1$ integrin (which is the major FN receptor) has been shown to be upregulated during the progression of cardiac hypertrophy [109]. Studies have shown that blocking β-1 integrin effectively blocks hypertrophy and that overexpression of activated α5 integrin stimulates hypertrophy [110, 111]. Therefore, signaling via integrins (red) and GPCR (green) are both associated with hypertrophy (Figure 1.4). Downstream signals from each of these receptor groups have also been shown to be upregulated or activated following the induction of cardiac hypertrophy such as mitogen-activated protein kinase (MAPK) family members, (specifically extracellular–regulated kinases (ERK1/2) [112] and p38 MAPK [113]) as well as protein kinase C [114], Rho [115] and FAK [116]. Therefore, these data indicate that signaling through GPCR mainly activates a pathological response whereas signaling through the tyrosine kinases is able to induce a physiological hypertrophic response.

3. Downstream Effectors of FAK Involved in Hypertrophy

The aggregation of integrins on the cell membrane is the major activator of FAK and results in the assembly of a multicomponent signaling complex [117]. In addition to integrin clustering, growth factor stimulation by PDGF, [118] and EGF, [55]), as well as signaling through some GPCRs by ligands such as PE and lysophophatidic acid, also activate FAK [119]. Therefore, FAK is activated by a variety of stimuli, including integrin clustering, growth factors, and GPCR, indicating

that FAK may be a key molecule in coordinating the downstream signals that regulate cell growth (Figure 1.5).

FAK is known to mediate downstream biological signals involved in hypertrophy through FYN, CSK, PI3K, PLC-γ, and MAPK pathways [12, 120]. In fact, transgenic models altering these downstream effectors of FAK including PI3K, the small GTPases Rac and Rho, ERK, and PKC, induce or attenuate the hypertrophy.

As stated earlier, PI3K is activated by IGF-1 and plays a crucial role in the regulation of cardiac cell growth throughout development and in the progression of physiological hypertrophy [85, 87]. Several transgenic mouse models altering the PI3K subunits as well as the downstream effector of PI3K, AKT, demonstrate the importance of this signaling pathway in the progression of physiological hypertrophy.

The small GTPases are a critical signaling link between cell membrane receptors and intracellular pathways. The GTPases are small proteins that bind guanosine triphosphate (GTP) and regulate a wide variety of functions in the cell including growth, differentiation and migration. The Rho family of small G proteins (Rho, Ras, Cdc42), are involved in cytoskeletal organization of cardiomyocytes [121]. RhoA activates RhoKinase (ROCK) which, in turn, activates myosin light chain kinase (MLCK). MLCK, which can also be activated by calmodulin is involved in sarcomeric organization in vitro [122]. In addition, dominant negative RhoA can inhibit PE, ET-1, or Gq stimulated hypertrophy in vitro, while in vivo overexpression of RhoA led to cardiac abnormalities that resulted in heart failure [123]. Mice containing a constitutively active form of Ras were able to induce cardiac hypertrophy and in vitro Ras expression resulted in hypertrophic gene expression.

Accordingly, the dominant negative Ras mutant prevented PE-induced hypertrophy [124].

There are several MAP kinases that likely have a role in cardiac hypertrophy. In response to acute pressure overload, ERK1/2 is activated and stimulates expression of immediate early genes known to be activated in initial stages of hypertrophic growth [125]. Direct evidence implicating ERK1/2 signaling comes from studies in which a transgenic mouse containing activated MEK1 (immediate upstream activator of ERK1/2) downstream of the cardiac specific αMHC promoter was generated. This mouse demonstrated mild concentric hypertrophy and an increase in heart weight to body weight ratio, along with increased contractile performance. Overall, these studies highlighted that the MEK1/ERK1/2 pathway was sufficient to induce a hypertrophic response *in vivo*[126]. Interestingly, following mechanical stress, the adaptor molecule Grb2 is recruited to FAK. Grb2 can activate MAPK via interactions with Ras. Mice haploinsufficient for Grb2 inhibit p38MAPK and JNK activation following pressure overload and attenuate the hypertrophic response[127]. Thus each of these MAP Kinases may play a role in the development of cardiac hypertrophy.

Isoforms of PKC, a ubiquitously expressed serine/threonine kinase, are also involved in the progression of cardiac hypertrophy. Multiple studies have shown that transgenic expression of PKCβ and ε are likely involved in the progression of cardiac hypertrophy. However, only PKCα has been shown to be necessary and sufficient to induce hypertrophy *in vitro*[128].

4. FAK's Role in Cardiac Hypertrophy

Although FAK protein levels are low in the adult heart relative to the fetal heart, studies have demonstrated that FAK activity is increased in hypertrophic hearts [107]. As stated above, past *in vitro* experiments conducted by our lab indicate that ectopic expression of FRNK (inhibition of FAK activity) attenuated PE induced cardiomyocyte hypertrophy. Subsequent reports have shown that overexpression of FRNK also attenuated endothelin-I and stretch/angiotensin II-stimulated cardiomyocyte hypertrophy [129, 130]. Knowing that FAK plays a role *in vitro* in the induction of cardiomyocyte hypertrophy, and that many signals both downstream and upstream of FAK signaling are involved in the promotion of hypertrophy in humans and mice, we hypothesized that FAK is likely an important transducer of the hypertrophic signals in the adult heart.

E. Goals of Thesis

In this thesis I explore the role of FAK throughout cardiac development, anabolic growth, and in the progression of cardiac disease. To study FAK, we have created novel mouse models that allow us to study the effect of decreased FAK activity in the developing heart fields as well as the postnatal heart. In addition, we have conditionally deleted FAK from the adult myocardium allowing us to study its role in the progression of pressure-overload induced hypertrophy. We have also generated a mouse model with conditional overexpression of constitutively active FAK in the myocardium to see if in the absence of stimuli, increased FAK activity will induce cardiac hypertrophy. In Chapter II of this thesis I show that following aortic constriction, mice with FAK deleted from the myocardium, fail to undergo

compensatory hypertrophy following pressure overload. Knowing that FAK deletion was able to attenuate the hypertrophic response, Chapter III asks whether FAK activity is necessary and sufficient for the induction of hypertrophy. In this chapter, I show that adult mice that exhibit cardiac specific inhibition of FAK activity from one day postnatal onward are phenotypically and physiologically similar to littermate controls, but have attenuated hypertrophic response. This chapter also describes a novel transgenic mouse model which expresses a constitutively active form of FAK from at least E12.5 onward under the control of a modified βMHC promoter. Thus far, my data suggests that the continual activation of FAK is sufficient to induce cardiac hypertrophy. Chapter IV of this thesis describes the investigation of the overexpression of FRNK in the heart fields of the developing heart and shows that decreased FAK activity at mid-gestation is critical for embryonic viability. Conditional overexpression of FRNK resulted in a significant decrease in myocyte proliferation, and malformations of the endocardial cushion collectively resulting in ventricular and atrial septal defects, as well as defects in valulogenesis. These studies suggest that FAK activity is crucial for cardiac morphogenesis.

Figure 1.1 Schematic of Focal Adhesion Kinase (FAK) and Focal Adhesion Kinase-Related Non-Kinase (FRNK). FAK contains three major domains, an N-terminal integrin binding domain, a central kinase domain and a C-terminal focal adhesion targeting domain (FAT). The major auto-phosphorylation site on FAK is at tyrosine 397 which acts as a docking site for the SH2 domain of Src. FRNK is transcribed from an alternative promoter located in the intron of the FAK gene and is identical to the C-terminus of FAK, but lacks the kinase domain.

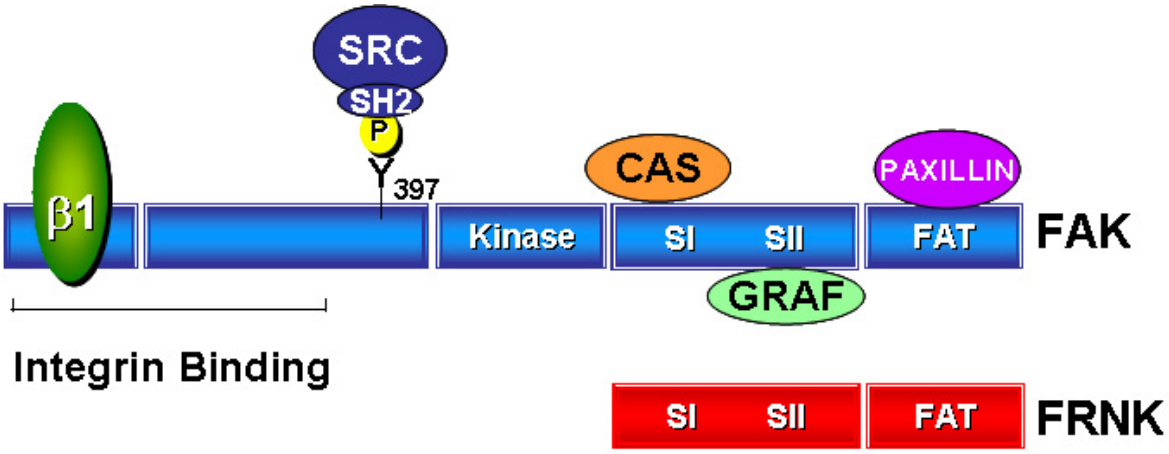
SRC
SH2
P
397
β1
CAS
PAXILLIN
Kinase
SI
SII
FAT
FAK
GRAF
Integrin Binding
SI
SII
FAT
FRNK

Figure 1.2 Sarcomeric and Cytoskeletal Proteins Involved in Human Cardiomyopathies. Familial hypertrophic cardiomyopathy (HCM) is linked to mutations in genes encoding structural sarcomeric proteins. However, dilated cardiomyopathy (DCM) is linked to mutations in genes encoding cytoskeletal proteins. Both the sarcomeric and cytoskeletal proteins are located at the Z-disk of the myofibrills.

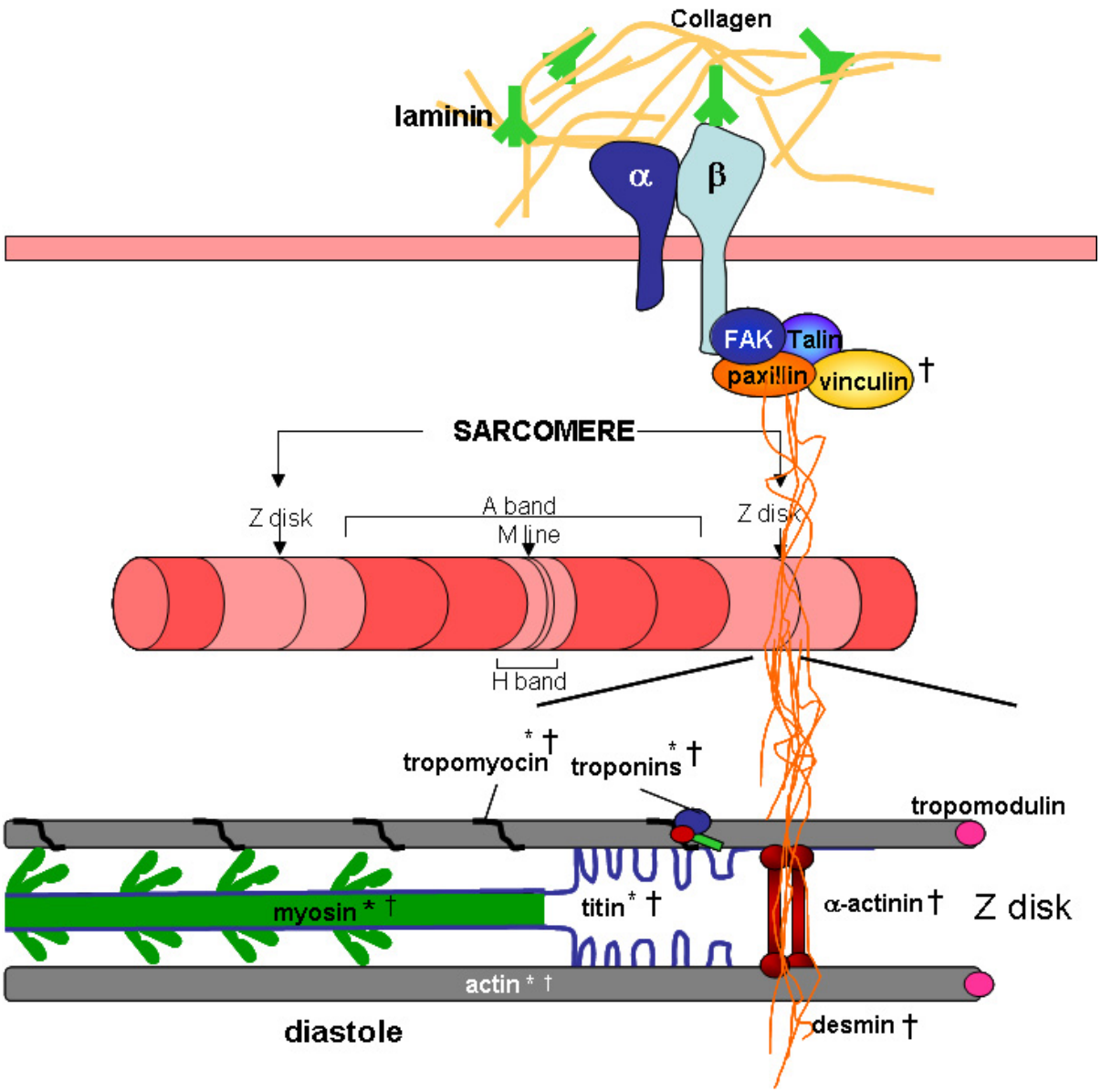

HCM *	DCM †	
βMHC	Metavinculin	βMHC
TnTs	Zasp	TnTs
Tm	Desmin	Tm
Actin	Dystrophin	Actin
MyBP-C	MLP	MyBP-C
Titin	α-actinin	Titin

Figure 1.3 FAK is Central for the Correct Function of Z-disk Proteins. Disruptions in sarcomeric proteins lead to HCM. This process is likely mediated by malformations in contractility sensed by receptors. Receptors initiate signaling cascade to induce hypertrophy which involved the addition of sarcomeric units. FAK may be central to these mechano-induced signals.

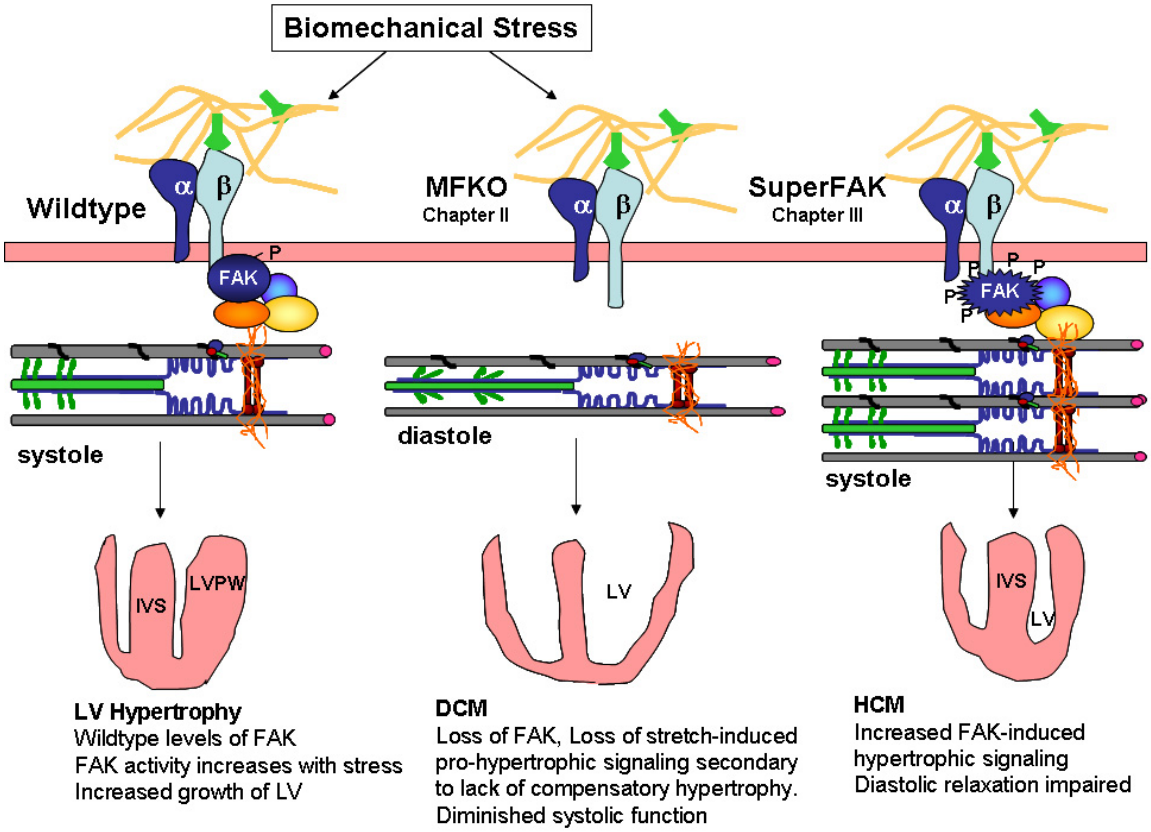
Biomechanical Stress
Wildtype
MFKO
Chapter II
SuperFAK
Chapter III
α
β
P
FAK
systole
diastole
systole
IVS
LVPW
LV
IVS
LV
LV Hypertrophy
Wildtype levels of FAK
FAK activity increases with stress
Increased growth of LV
DCM
Loss of FAK, Loss of stretch-induced pro-hypertrophic signaling secondary to lack of compensatory hypertrophy.
Diminished systolic function
HCM
Increased FAK-induced hypertrophic signaling
Diastolic relaxation impaired

Figure 1.4. Maladaptive and Physiological Signaling Pathways. FAK is activated following a variety of stimuli which act through receptors including GPCRs, integrins, and growth factor receptors. Signaling through GPCRs and integrins activated downstream effectors involved in maladaptive hypertrophic remodeling, whereas signaling through the growth factor receptor IGF-1 stimulates the physiological hypertrophic pathway.

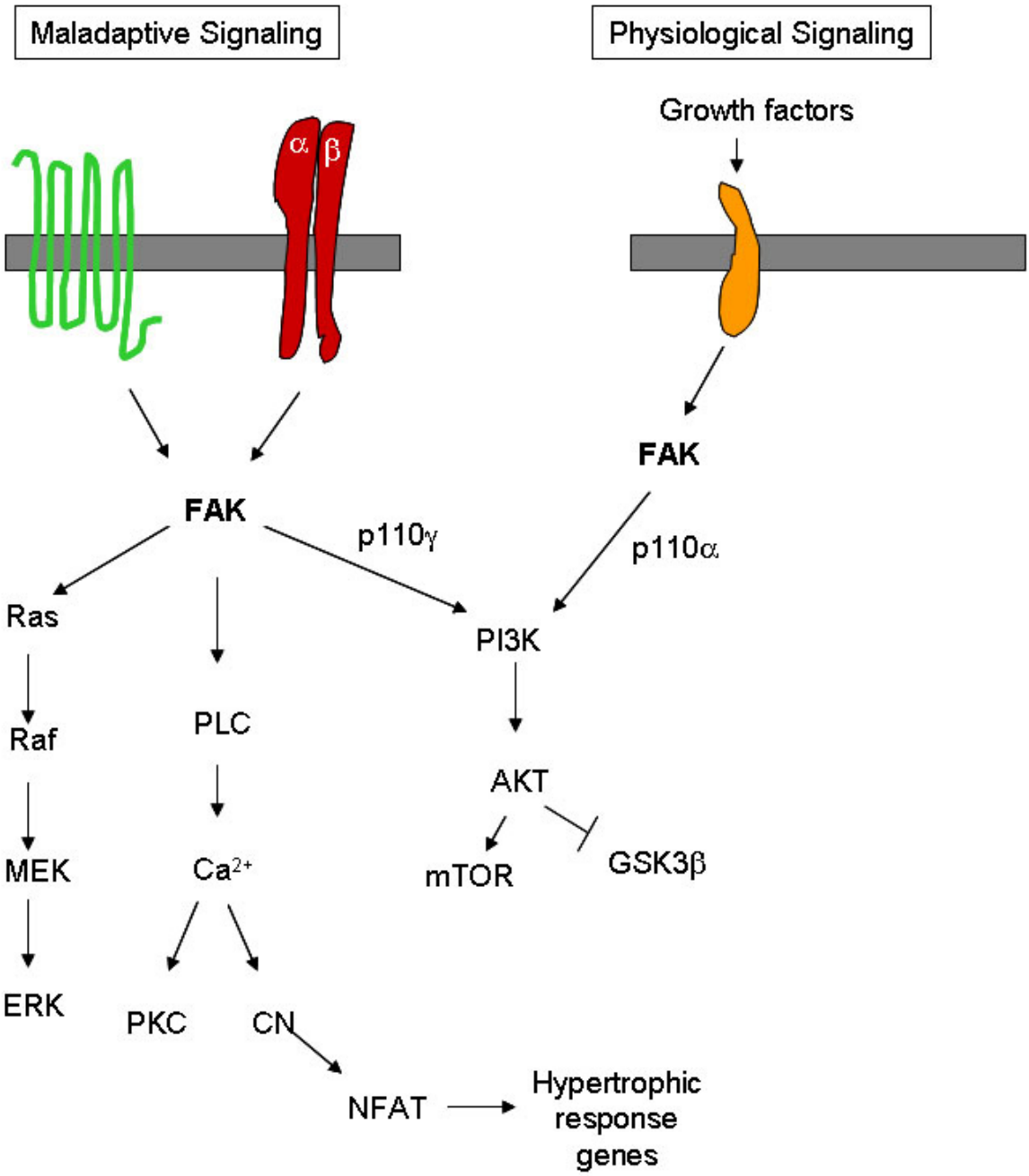
Maladaptive Signaling
Physiological Signaling
Growth factors
α
β
FAK
FAK
p110γ
p110α
Ras
PI3K
Raf
PLC
AKT
MEK
Ca2+
mTOR
GSK3β
ERK
PKC
CN
NFAT
Hypertrophic response genes

Figure 1.5 Pathways Involved in Cardiac Hypertrophy. Cardiac hypertrophy can be stimulated through various pathways including those stimulated by integrins, GPCR, calcium channels ad receptor tyrosine kinases. Interestingly, the pathways that induce cardiac hypertrophy also stimulate FAK activity.

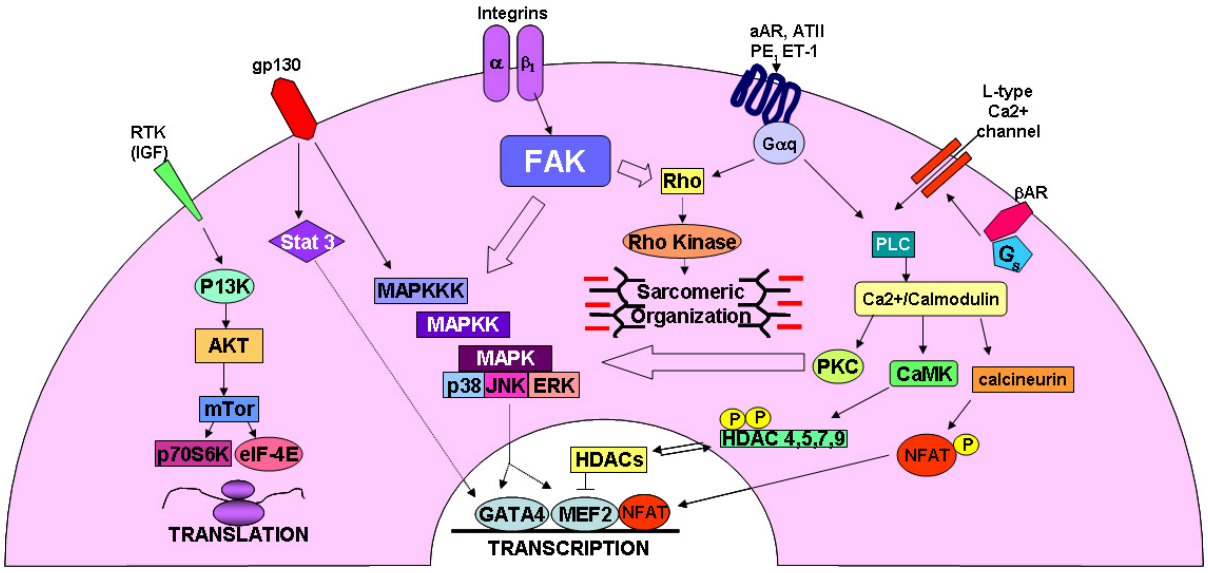
Integrins
α β1
gp130
aAR, ATII
PE, ET-1
L-type
Ca2+
channel
RTK
(IGF)
FAK
Rho
Gαq
βAR
Gs
Stat 3
Rho Kinase
PLC
P13K
MAPKKK
Sarcomeric
Organization
Ca2+/Calmodulin
AKT
MAPKK
MAPK
p38 JNK ERK
PKC
CaMK
calcineurin
mTor
P P
HDAC 4,5,7,9
p70S6K
eIF-4E
HDACs
NFAT
P
GATA4
MEF2
NFAT
TRANSLATION
TRANSCRIPTION

CHAPTER II

MYOCYTE-RESTRICTED FAK DELETION ATTENUATES PRESSURE-OVERLOAD INDUCED HYPERTROPHY

A. Introduction

In the face of chronic pressure or volume overload, the adult heart undergoes pathological hypertrophic growth. This response is characterized by an increase in cardiomyocyte size and myofibrillar content as well as an altered pattern of cardiac gene expression including induction of immediate early genes and re-expression of several fetal gene transcripts. Initially these changes are compensatory, but may eventually lead to decreases in cardiac performance and heart failure [128]. The precise molecular mechanisms that regulate anabolic or pathologic myocardial hypertrophy are not completely known, but studies have implicated a variety of neuroendocrine and autocrine factors, many of which act through G-protein coupled receptors (in particular those coupled to $G\alpha_q$) [131].

Extensive evidence indicates that extracellular matrix (ECM)/integrin receptor signaling is also an important regulator of myocardial hypertrophy. Upregulation of collagen III, fibronectin (FN), osteopontin, or their cognate integrin receptors, β_1, α_3 and α_5, correlates with the advancement of cardiac hypertrophy in animal models [132]. Also transgenic mice that express a myocyte-restricted activated α_5 integrin develop profound cardiac hypertrophy [133], whereas myocyte-restricted deletion of

the β_1 integrin in adult mouse hearts leads to a dilated cardiomyopathy and concomitant heart failure [60, 134]. In addition, mutations in the structural focal adhesion proteins muscle LIM protein and metavinculin are associated with dilated cardiomyopathy in patients [80, 135]. Collectively, these studies underscore the possibility that defects in integrin signaling may play a direct role in regulating cardiomyocyte sarcomere formation and function during cardiac development and disease.

One of the major proteins involved in the integrin intracellular signaling cascade is the non-receptor protein tyrosine kinase, focal adhesion kinase (FAK), which is strongly and rapidly activated by various growth factors and by ligation of all β_1, β_3 or β_5 containing integrins [136]. Through multiple protein-protein interactions, activation of FAK results in the subsequent activation of the ERK and JNK growth promoting MAP kinases and the cytoskeletal regulating small molecular weight GTPases Rac and Rho, some of the same molecules implicated in myocyte hypertrophy [131, 136].

Although a direct role for FAK in cardiac growth and development has yet to be examined, germline deletion of FAK results in general mesodermal defects and embryonic lethality between E7.5-10 (similar to both $FN^{-/-}$, and $\alpha_5^{-/-}$ mice) and $fak^{-/-}$ hearts lack separate mesocardial and endocardial layers, indicative of a defect in cardiomyocyte maturation [137-139]. Interestingly, recent work by our group and by others clearly indicate that FAK is activated in cultured cardiomyocytes by a variety of hypertrophic stimuli [140-143] and that increased cardiac FAK activity is induced following pressure-overload *in vivo* [144-147]. The idea that FAK activation may

play a direct role in the development of cardiomyocyte hypertrophy is evident from our initial findings that the activation of FAK is required for phenylephrine (PE)-stimulated hypertrophy of cultured cells and similar findings from others that FAK is required for maximal endothelin-1 and stretch-induced hypertrophy *in vitro* [141, 148, 149].

To test the possibility that FAK inactivation could prevent cardiac hypertrophy *in vivo*, we generated a mouse model that produces conditional myocyte-specific inhibition of FAK activity as well as a model that produces a conditional myocyte-specific deletion of FAK in the adult heart. In support of recent findings from Peng *et. al.*, we show that inactivation of FAK in the adult myocardium does not affect basal cardiac function [150]. However, we show that hearts with myocyte-specific FAK depletion or inhibition do not develop concentric hypertrophy upon induction of biomechanical stress by transverse aortic constriction (TAC). These studies show that FAK plays a significant role in the development of compensatory hypertrophy in the intact myocardium and highlight the possibility that FAK serves to integrate growth signals from various hypertrophic stimuli.

B. Materials and Methods

Generation of MFKO Mice. Drs. Louis Reichardt and Hilary Beggs (UCSF) graciously provided the *fak*^{flox} mice and Dr. Kenneth Chien (Harvard) graciously provided the *mlc2v*^{Cre} knock-in mice[29, 151]. All mice were backcrossed to the C57black6 background at least 8 generations prior to subsequent breeding. DNA isolated from tail snips or tissues was subjected to PCR analysis using primers specific for Cre and the presence of the targeted or recombined FAK allele as described previously [29, 151]. Mice were housed in an AAALAC accredited University Animal Care Facility.

Antibodies and Reagents. The anti-rabbit FAK antibody, the anti-mouse ERK2 antibody (1B3B9), the anti-mouse Bcl-2 antibody, and the anti-rabbit Bax antibody were purchased from Upstate Biotechnology, Inc. The phosphospecific ERK1/2 (p42/p44) antibody was purchased from Cell Signaling. The poly ADP-ribose polymerase-1 (PARP) antibody was purchased from Roche. The cardiac troponin T monoclonal antibody (13-11) was a gift from Nadia Malouf (UNC, Chapel Hill). Unless specified, antibodies were used at 1/1000 dilution.

Biomechanical stress. Mechanical stress was imposed on the left ventricle using the minimally invasive aortic banding as previously described [29]. Briefly, 20-30 g mice were anesthetized (sodium pentobarbital 0.06mg/gr IP), a small incision was made at the suprasternal notch and through the proximal portion of the sternum. Once the aortic arch was visualized, a 6.0 silk suture was placed under the aorta and tied tightly around the vessel using a blunt 27-gauge needle to establish the diameter of the ligature. Sham-operated animals underwent an identical procedure

except for lack of ligature placement. The skin was closed and the anesthetized animals were monitored on a heating pad until they recovered. The entire banding procedure lasted approximately 20 min per mouse. Effectiveness of the procedure was monitored by measuring the pulsatility indices before and after banding by Doppler imaging. An average 30-40 cm/sec rise in peak velocity (from a 65-75 cm/sec baseline) in the right carotid with a concomitant decrease in the peak velocity of the left carotid was observed with no significant difference in the gradient between MFKO mice and genetic controls. At end stage, the mice were euthanized by CO_2 inhalation and body weight was measured. Following perfusion of the heart with phosphate buffered saline, the hearts and lungs were excised, weighed, and tissues were processed for RNA, protein, or histological analysis as described in detail below. Although it has been reported that β-estrogen receptor signaling can lead to a depressed response to pressure overload induced-hypertrophy[152], we included both male and female mice in this study and found no gender difference in the propensity or extent of control or MFKO mice to undergo cardiac remodeling after TAC (data not shown). All animal use procedures have been reviewed and approved by the University of North Carolina's Animal Use and Care Committee.

Transthoracic echocardiography. Echocardiograph measurements were taken pre-operatively as well as the indicated time points after surgery using previously described methods [153]. Briefly, following light sedation with isoflurane, hair was removed from the chest and abdomen, and the mice are placed on a water-jacketed, warmed table in the left lateral decubitus position for imaging. A Visualsonic Ultrasound System (Vevo 660) ultrasound machine containing a 30 Mhz variable

frequency pediatric probe with a 1 cm offset was used to capture the echocardiogram. Standard long axis and short axis M-mode views were recorded when the mouse possessed a target heart rate between 450 and 650 beats per minute. End-diastolic and end-systolic interventricular septum (IVSd, IVSs), posterior wall thickness (PWTd, PWTs) and left ventricular internal diameters (LVEDD, LVESD) were calculated and averaged from three consecutive contractions using Visual Sonics software. Percent fractional shortening was calculated using: %FS={(LVEDD-LVESD)/LVEDD} x 100. Relative wall thickness was calculated using: RWT={(IVSd + PWd)/2}/(LVEDD/2). An additional group of mice represented in supplemental data underwent echocardiograph measurements under heavier sedation with isoflurane to decrease the stress imposed in the animal and to aid in acquiring more accurate measurements. Although similar structural measurements were found, a dampened fractional shortening measurement was calculated likely due to decreased heart rates.

Histological Analysis and Immunohistochemistry. Paraffin-embedded hearts were sectioned into 8 μm slices and stained with Masson's Trichrome stain (Sigma-Aldrich) to assess overall morphology and presence of fibrosis. Following the block of endogenous peroxidases with 0.3% H_2O_2 in methanol, sections were permeabilized with phosphate buffered saline containing 3% BSA w/ 0.2% Trition-X and then incubated with cardiac troponin T antibody in 1%BSA/PBS overnight at 4 degrees C. The sections were then washed with TBST (TBS plus 0.05% Triton-X), incubated with FITC- or Texas Red- conjugated donkey anti-mouse antibody for 90 min. at RT, rinsed, and mounted with Vectamount (Vector Labs). Cell area

measurements were conducted on TRITC-Lectin (Sigma-Aldrich) stained cross sections of the compact zone of the heart muscle using Image J software (NIH).

***Electron Microscopy*.** LVPW sections 1-2 mm^3 in size were placed in a fixative overnight containing 2% paraformaldehyde and 2.5% glutaraldehyde in 0.15 M sodium phosphate buffer, pH 7.4 and postfixed for in 1% osmium tetroxide/1.25% potassium ferrocyanide in sodium phosphate buffer. The tissues were rinsed in deionized water, dehydrated, and put through two changes of propylene oxide before embedding in epoxy resin. Representative longitudinal cells from the central LVPW were selected by light microscopy and 70 nm ultra thin sections were cut and collected on 200 mesh copper grids and stained with 4% aqueous uranyl acetate, followed by Reynolds' lead citrate. Random fields from the left ventricular mid wall were scanned and 10-20 separate myocytes/condition were observed using a LEO EM910 transmission electron microscope at 80kV (LEO Electron Microscopy, Thornwood, NY) and photographed using a Gatan Bioscan Digital Camera (Gatan, Inc., Pleasanton, CA) [154].

***Quantitative RT-PCR*.** Ventricles were harvested from end stage banded or sham-treated mice and placed in RNA later (Ambion). Samples were homogenized and RNA was extracted using Trizol reagent (Invitrogen) and quantified using Ribogreen spectrometry (Molecular Probes) according to the manufacturer's protocol. Each sample of RNA was diluted to 50 ng/μl in DEPC treated H_20. Each 30 μl RNA reaction mixture contained 0.5 μl of 0.1 μg/μl of primer, 1 μl of 20 μmol of probe 15μl of AB Gene one step master mix, and 0.1μl of RT enzyme. The primers and probes used were as follows: ANF forward GAGAAGATGCCGGTAGAAGA, ANF reverse

AAGCACTGCCGTCTCTCAGA, ANF probe FAM-ATGCCCCCGCAGGCCCTG-TAMARA, βMHC forward AGCTCAGCCATGCCAACCGT, βMHC reverse TGAGTGTCCTTCAGCAGACT, βMHC probe FAM-AGGCTCTTCACTTGTTTCTGGGCCTCA-TAMARA, αMHC forward AGCTCAGCCAGGCCAATAGA, αMHC reverse TGGGTGTCCTTCAAGTGAGC, αMHC probe FAM-AGAATTCTTCAGGTGTTTCTGTGCCTCAG-TAMARA, skeletal α-actin forward TCCTCACTGAGCGTGGCTAT, skeletal α-actin reverse AGCTTCTCTTTGATGTCGCG, skeletal α-actin probe FAM-CTTCGTGACCACAGCTGAACGTGAG-TAMARA, βactin forward CTGCCTGACGGCCAAGTC, βactin reverse CAAGAAGGAAGGCTGGAAAAGA, βactin probe FAM-CACTATTGGCAACGAGCGGTTCCG-TAMARA. c-Fos forward CAGTCAGAGAAGGCAAGGCA, c-fos reverse TCCTCTCTGTAATGCACCAG, c-Fos probe FAM-CATCCAGACGTGCCACTGCCCGA-TAMARA.

The real time-RT-PCR was performed using the ABI prism 7500 Sequence Detection System (PE Applied Biosystems) in 96-well plates under the following conditions: 30 minutes at 48 ˚C, 10 minutes at 95 ˚C, 40 cycles of 95 ˚C for 15 seconds, then 60 ˚C for one min. For semi-quantitative RT-PCR analysis, each 20□l reaction contained 250ng of ventricular RNA from end stage banded or sham-treated mice, 4μl reaction mix and 1μl reverse transcriptase using the iScript cDNA synthesis kit (BioRad). Each reaction was performed under the following conditions: 5 minutes at 25 ºC, 30 minutes at 42 ºC, then 5 minutes at 85 ºC. Each 50 μl PCR reaction mixture contained 2.5 μl of 10μM of primer, 4μl of dNTP mixture, 5μl of reaction buffer and 0.5 μl of TaKaRa Ex Taq enzyme. The reaction was performed

under the following conditions: 5 minutes at 94 ºC, 29 cycles of one minute at 94 ºC, one minute at 61 ºC, 2 minutes at 72 ºC, and then 10 minutes at 72 ºC. The primers used were as follows: Bax forward GCGTCCACCAAGAAGCTGAG, Bax reverse ACCACC CTGGTCTTGGATCC, Bcl-2 forward TGTGGCCTTCTTTGAGTTCG, Bcl-2 reverse TCACTTGTGGCCCAGGTATG.

Western Blotting. Tissues were lysed in modified radioimmune precipitation assay buffer (50 mM Hepes, 0.15 M NaCl, 2 mM EDTA, 0.1% Nonidet -40, 0.05% sodium deoxycholate, pH7.2) containing 1 mM 4-(2-amnionethyl)benzenesulfonyl fluoride hydroxychloride, 0.02 mg/ml aprotonin containing 5% Triton-X. Proteins were boiled in a sample buffer and resolved using SDS-PAGE and transferred to nitrocellulose. Western blots were preformed using a 1/1000 dilution of the appropriate primary antibody. Blots were washed in Tris-buffered saline, pH 7.4 plus 0.05% Triton-X, followed by incubation with either horseradish peroxide-conjugated protein A-Sepharose (Amersham Bioscience) or horseradish peroxide-conjugated rabbit anti-mouse antibody (Amersham Biosciences) at a 1/2000 dilution. Blots were visualized after incubation with chemiluminesence reagents (ECL, Amersham Biosciences). [155]. For quantitative measurements, blots were scanned and density was normalized to the density of a control protein for each sample.

Cardiac Catheterization. Mice were placed in a supine position, secured on the operating table, and anesthetized with inhaled isoflurane (3% for induction and 1-2% for maintenance). An approximately 1 cm midline incision from the lower mandible to the sternum was made, and the right common carotid artery was exposed and isolated by blunt dissection of the thin muscle layer around the trachea. A secure

suture was placed around the distal end of the artery and a loose suture was placed around the proximal end of the artery. A small vascular clip was then placed on the proximal end of the artery to minimize bleeding during catheter insertion. A 1 - 2 mm incision was cut near the distal end of the artery and the tip of a 1.4 French catheter (Millar Instruments) was inserted in to the artery. Following removal of the vascular clip from the proximal end of the artery, the catheter was advanced beyond the proximal suture and the suture was tightened around the catheter shaft. The catheter was then advanced retrograde down the ascending aorta through the aortic valve in to the left ventricle. The catheter shaft was gently rotated to achieve optimal placement of the tips along the axis of the left ventricle. Measurements of steady state pressure volume loops were taken ten minutes following catheter placement.

Statistics. Data are presented as mean ± SEM. Means were compared by 2-tailed Student's *t* test. $p<0.05$ was considered statistically significant.

C. Results

Myocyte-Restricted Deletion of FAK in Adult Mice

We used Cre/loxP technology to test the possibility that FAK inactivation could prevent cardiac hypertrophy in the intact myocardium. To inactivate the *fak* gene in a myocyte-restricted fashion in mice, we bred fak^{flox} mice to those that express Cre recombinase under the control of the ventricle specific *mlc2v* promoter ($mlc2v^{Cre/wt}$) [151] to obtain $fak^{flox/flox}mlc2v^{Cre/wt}$ mice; hereafter referred to as myocyte specific *fak* knockout mice (MFKO) (Figure 2.1a).

MFKO mice were born with the expected Mendelian frequency (Figure 2.1a), and we observed the selective appearance of the excised, recombined *fak* gene in the MFKO ventricles at 4-weeks postnatal (not shown), while maximal recombination occurred by 3-months (Figure 2.1b). Western analysis confirmed that FAK protein was dramatically reduced in MFKO ventricular lysate by 3-months postnatal, whereas FAK protein levels remained constant in other tissues including skeletal muscle, stomach and brain (Figure 2.1c,d). The low level of FAK protein remaining in the ventricular lysates from 3-months onward was likely due to its continuing expression in resident non-myocyte cells (i.e. cardiac fibroblasts, smooth muscle, and endothelial cells) that do not express Mlc2v.

FAK is Not Required for Basal Cardiac Function

Disruption of FAK expression in the adult heart did not lead to any overt abnormalities. Both sexes of MFKO mice lived a normal lifespan, were fertile, and females did not exhibit any complications during pregnancy, indicating that FAK is not required for the maintenance of normal heart function. In confirmation of this, we

found no evidence of left ventricular dysfunction as assessed by fractional shortening (FS) and ejection fraction (EF) derived from M-mode echocardiographs of the left ventricle (LV) of young (4-months) or old (14-months) hearts from MFKO mice in comparison to aged matched genetic controls (Figure 2.2, Table 2.1). At 14-months of age both lines of mice had a significant reduction in FS and MFKO mice had a significant reduction in EF when compared to the 4-month-old controls, but no significant differences in these parameters were observed between age matched controls (Figure 2.2, Table 2.1). Importantly, no significant difference was observed in posterior or interventricular septal wall thickness (PW, IVS) or LV chamber size, between the 4-month-old MFKO and genetic controls {*fak*$^{flox/flox}$mlc2v^{wt} (Table 2.1) or *fak*$^{wt/wt}$mlc2v^{Cre} (data not shown)}. Hemodynamic analysis by cardiac catheterization also revealed no significant differences in intrinsic contractility, diastolic function, and cardiac output between control and MFKO mice at 4-months of age, consistent with a previous report (Table 2.2; [150]). In addition 4-5-month-old MFKO mice had similar LVW:BW ratios (Figure 2.6a), cardiomyocyte cross-sectional area, myofibrillar organization, and levels of fibrosis compared to littermate controls (Figure 2.6b, 2.3a,b), indicating that the young MFKO mice are phenotypically indistinguishable from genetic controls.

Myocyte-restricted FAK deletion did have a slight but significant effect on heart growth during aging. Left ventricular weight versus body weight was significantly decreased in 14-month MFKO mice relative to aged matched controls (Figure 2.2a). Additionally, myocyte cross-sectional area was reduced slightly (by 5%; p=0.04 Fig 2b). Consistent with these findings, serial echocardiograph measurements revealed

a significant increase in thickness of LV posterior wall from 4 to 14-months in control mice but not in MFKO mice (Table 2.1, Figure 2.2d). Histological analysis of hearts from aged MFKO mice (14-months) revealed an increase in interstitial fibrosis in comparison to age matched controls (Figure 2.3a, Table 2.3), but no noticeable differences were found in sarcomeric integrity or myocyte alignment in comparison to hearts from age-matched control mice (Figure 2.3a, b). Thus, the absence of FAK in cardiac muscle is functionally tolerated, but FAK may regulate anabolic myocyte growth as the heart ages.

We next asked whether the depletion of FAK from myocytes was tolerated because of a compensatory increase in the FAK-related protein PYK2/CADTK which is known to have increased expression in *fak*$^{-/-}$ embryos and cells [156, 157]. However, we found comparable PYK2 protein levels (and activity) in control and MFKO hearts (Figure 2.3c, data not shown), indicating that PYK2 does not compensate for loss of FAK in this model.

Pressure-Overload-Induced Structural Remodeling and Hypertrophic Gene Expression is Attenuated in MFKO Mice

The absence of underlying developmental defects in the conditional MFKO mice at 4-5-months of age renders this model advantageous for determining whether FAK is important for the progression of pathological cardiac hypertrophy. 4-month-old control and MFKO mice were therefore subjected to a minimally invasive aortic banding procedure that provided an approximate 50% reduction in the lumen of the ascending aorta. Blinded echocardiograph measurements revealed several striking differences between the aged matched genetic controls and MFKO hearts following

4-weeks of transverse aortic constriction (TAC; Figure 2.4a,b, Table 2.I). Notably, the control TAC mice developed significant thickening of LVPW and IVS (approximately 50% and 30% increases in systole respectively), a significant reduction in LVED (approximate 40% decrease in end diastolic chamber dimension), and a 40% increase in FS compared to non-banded control mice. In contrast, the MFKO mice did not exhibit significant increases in LVPWT or FS comparison to the pre-banded MFKO mice (Table 2.1). Indeed, the percent change of each parameter from pre to post TAC was significantly decreased in MFKO hearts in comparison to control hearts (Figure 2.4a). Measurements from serial cross sections though banded control and MFKO hearts confirmed a significant reduction in relative LVPWT in 15/19 of the 4-week post TAC MFKO hearts in comparison to the control hearts (Figure 2.4b, Figure 2.5). Importantly, morphometric analysis revealed a significant decrease in myocyte cross-sectional area in the post-TAC MFKO hearts compared to post-TAC controls (Figure 2.6b). Although a significant increase in LVW/BW was observed following 4-weeks of TAC in MFKO hearts (possibly due to increased fibrosis, see below) the increase in MFKO hearts was reduced relative to control hearts (Figure 2.6a). Notably, no significant difference in the surgically-induced intensity of pressure-overload was observed between MFKO and the genetic controls as assessed by Doppler imaging (Figure 2.7a). A comparable concentric hypertrophic response was observed in our two groups of control mice {$fak^{flox/flox}$mlc2v^{wt} (shown) and $fak^{wt/wt}$mlc2v^{Cre} (data not shown)}, indicating that the lack of concentric hypertrophy observed in the MFKO mice was not due to adverse

effects of either the LoxP-targeted *fak* allele, expression of Cre, or haplo-insufficiency of Mlc2v.

Recently, a separate report was published in which the authors suggested that cardiac-restricted inactivation of FAK leads to cardiac dilation due to an eccentric hypertrophic response [150]. Therein, Peng *et. al.* examined mice at only one time point following TAC (10 days) which was not sufficient to induce concentric hypertrophy in their control animals, but they observed a significant increase LV chamber dimension in their CFKO mice when compared to banded controls [150]. To determine whether the change in chamber size was a primary or secondary response in our model, we banded a second group of mice (n=7 Control and MFKO) and examined their hypertrophic response by blinded echocardiography at 10-days and 4-weeks following TAC. As shown in Figure 2.7b, no significant differences were observed between either LVPW or LVED between MFKO and control hearts at 10-days following banding. However, similar to our previous large study of mice (Table 2.I), this separate study revealed a significant decrease in LVPW in 4-week banded MFKO hearts in comparison to 4-week banded control hearts. This change in LVPWT was accompanied by an increase in LVED in MFKO hearts relative to banded genetic controls, but like in our previous study MFKO LVED was not significantly increased from baseline MFKO hearts. Since the echocardiograph measurements for this new data set were taken while mice were under heavier sedation the data were analyzed separately and are presented in full in Table 2.4. These studies confirm our contention that FAK inactivation inhibits the compensatory concentric hypertrophic response following TAC.

Enhanced peri-vascular fibrosis as assessed by Masson's Trichrome staining was observed following TAC in both control and MFKO TAC hearts with more interstitial fibrosis found in MFKO TAC hearts (blue staining, Figure 2.8a top, Table 2.3). However, there was no significant difference in sarcomeric structure or integrity between control and MFKO hearts following TAC as visualized by troponin T staining (Figure 2.8a, 2.9).

There is some evidence indicating that the switch from hypertrophy to cardiac failure may involve activation of apoptotic pathways. For instance, aortic banding of mice with heart-restricted deletion of the $G\alpha_q$, *MEKK1* and *gp130* genes result in dilated cardiomyopathy accompanied by cellular apoptosis, an event presumably due to lack of activation of a critical survival signaling pathway during the hypertrophic process [109, 158, 159]. In some, but not all cell types, activation of FAK has been shown to be important for cell survival, and attenuating FAK signaling can lead to apoptosis [29, 31, 160, 161]. Although we did observe a greater extent of interstitial fibrosis in banded and aged MFKO hearts (likely due to increased myocyte drop-out), we did not observe an increase in apoptosis or apoptotic markers in control or MFKO hearts at baseline or following banding (Figure 2.9, 2.10). In addition, we found little if any evidence of apoptosis following TAC in either group as assessed by detection of DNA strand breaks by TUNEL (less than 0.03% TUNEL positive cells/condition, data not shown), PARP cleavage, or Bax/Bcl-2 expression levels (Figure 2.10b). Accordingly, ultra-structural analysis by transmission EM showed no evidence of apoptosis or necrosis following 4 weeks of TAC (Figure 2.9). Both control and MFKO myocytes within the central posterior wall (most affected by

pressure overload) revealed intact myofibrils, well-organized sarcomeres and intercalated disks and no evidence of mitochondrial blebbing. Thus, deletion of FAK does not appear to induce programmed cell death in mature cardiomyocytes.

Although PYK2 expression did increase following TAC, we found no significant difference in PYK2 levels (or activity) in MFKO TAC hearts relative to control TAC hearts (Figure 2.8, data not shown). Collectively, these data indicate that FAK is not required for the maintenance of proper myocyte architecture but is required for the promotion of biomechanical stress-induced myocyte hypertrophy.

Hearts from control and MFKO non-banded and 4-week TAC-induced mice were also analyzed for hypertrophic marker gene expression by quantitative RT-PCR. We examined the expression of atrial naturetic factor (ANF) because increased levels of this gene correlate highly with the degree of hypertrophy observed in several animal models [162]. As shown in Figure 2.11, ANF expression was, as expected, dramatically increased in the control mice after TAC. This increase was virtually abolished in the MFKO hearts (Figure 2.11a). Interestingly, banded MFKO hearts displayed a significant increase in α-MHC compared to banded controls whereas no significant difference in βMHC or skeletal α–actin was observed between the two groups post-banding (Figure 2.11b, data not shown). Collectively our data indicate that loss of FAK alters the structural and a subset of the molecular changes induced by pressure-overload.

Persistent Pressure-Overload in MFKO Mice Leads to Cardiac Dysfunction

Since the MFKO TAC hearts exhibited a reduced compensatory response following 4-weeks of pressure-overload, we asked whether the MFKO mice would

progress to heart failure after a more persistent challenge. Although greater than 90% survival was observed in control and MFKO mice banded for 8-12 weeks, the wet lung weights from the MFKO 8-week TAC group were significantly higher than non-banded mice, indicating substantial congestion, and the likelihood that the MFKO hearts were failing (Figure 12a). Accordingly, significant depression of cardiac output, a measure of contractile performance, was apparent in MFKO mice 12-weeks after TAC (Figure 2.12b). The decreased contractility in the MFKO mice was associated with an increase in interstitial fibrosis relative to control-banded hearts at 8 and 12-weeks (Table 2.3). However, sarcomeric integrity was maintained in these hearts as assessed by Troponin T staining (data not shown). These data indicate that the MFKO mice develop heart failure in response to chronic pressure-overload, and suggest the possibility that the blunted compensatory hypertrophic response in these mice was not sufficient to meet the increased hemodynamic demand.

Absence of FAK Impairs MapKinase Activation Following Hypertrophic Stimuli

It is possible that the requirement for functional signaling through FAK in pressure-overload-induced hypertrophy may be due to the ability of FAK to co-activate an essential growth pathway. Since ERK activation by hypertrophic stimuli precedes the characteristic changes in gene expression and inhibition of this signaling pathway can lessen maladaptive hypertrophic growth [163, 164], we evaluated ERK activity in control and MFKO hearts subjected to aortic banding for 1 and 4 days. Immunoblot analysis revealed reduced levels of ERK phosphorylation in MFKO hearts in comparison to control hearts after acute aortic constriction

although no change was observed at baseline (Figure 2.13a). Since cardiac hypertrophy induced by pressure-overload and neuro-humoral signals share some common mechanisms, we also examined ERK activation induced by adrenergic agonists in control and MFKO hearts. We injected an adrenergic cocktail previously shown to induce a strong hypertrophic response in mice [165]. As shown in Figure 2.13b, ERK was strongly activated in control hearts following acute adrenergic agonist injection, but was significantly lower in the MFKO hearts. We also examined activation of the immediate early gene cFos following acute banding. We found that cFos expression was significantly up-regulated in control hearts 4 days after TAC, but returned to baseline by the 7 day time point (Figure 2.13c). However, no significant increase in cFos expression was observed in MFKO hearts following banding, in accordance with data indicating that activation of cFos is dependent on ERK signaling (Figure 2.13c). These data indicate that ERK activation is uncoupled in the absence of FAK, and highlight the possibility that FAK activity is required for the initial wave of signaling induced by both pressure-overload and adrenergic stress.

D. Discussion

Previous work by our group and others indicate that FAK is important in the hypertrophic response. Herein, we have used a mouse model in which myocyte-restricted FAK deletion in early adulthood results in mice whose hearts are functionally and morphologically similar to those of control mice, confirming recent work from Peng et. al. [150]. However, we found that myocyte-restricted deletion of FAK depressed heart growth during aging and markedly reduced the hypertrophic response to transverse aortic constriction as assessed by examination of several conserved features of pathological hypertrophy. Our data indicate that inhibition of FAK signaling alone is sufficient to suppress the diverse signaling inputs within the complex myocyte microenvironment *in vivo* that can modulate cardiac growth induced by stress and aging.

Our findings that FAK inactivation attenuates concentric hypertrophic remodeling differ with the conclusions drawn in the aforementioned manuscript by Peng *et. al.* who observed chamber dilation (or eccentric growth) in FAK null hearts following 10 days of TAC [150]. This discrepancy could be due to differences in the timing of FAK deletion, the extent of aortic constriction imposed in the two models and/or the genetic background of the mice used in these studies. Our findings that FAK inactivation attenuates concentric hypertrophic remodeling differ with the conclusions drawn in the aforementioned manuscript by Peng *et. al.* who observed chamber dilation (or eccentric growth) in FAK null hearts following 10 days of TAC [150]. As mentioned above, this discrepancy could be due to differences in the timing of FAK deletion, the extent of aortic constriction imposed in the two models

and/or the genetic background of the mice used in these studies. Notably, phenotypic diversity in cardiac morphology and response to cardiac pressure overload have been found between the most commonly used inbred mouse strains C57BL/6J (B6) and 129S1/SvImJ (129) [166, 167]. Although original engineering of our mice occurred on a 129 background, all mice used for our studies were backcrossed against B6 at least 8 generations. Thus, if the mice used in the Peng *et. al.* study were on a 129 or mixed background, this could explain our disparate findings. In addition, different Lox P-targeted *fak* mice were used for these studies, and temporal differences in FAK depletion were observed. Notably, the Peng *et. al.* study observed significant FAK protein depletion by 2 weeks postnatal, while in our study FAK protein levels were not significantly altered until 12 weeks postnatal. Thus, it is possible that the earlier onset of FAK inactivation in their study could have led to an underlying cardiac defect prior to banding that was exacerbated upon pressure-overload. In support of this contention, the FAK null hearts from the Peng *et. al.* study were reportedly failing by 9 months of age, while systolic function is maintained in our mice for at least 14 months of age and we have not observed any spontaneous or pregnancy-related mortality.

The late onset of recombination in our model system (3 months post-natal) was somewhat surprising since the *mlc2v*-promoter has been reported to drive Cre expression as early as embryonic day 8.5, however our results are consistent with several studies showing that maximal recombination of targeted genes is not observed until at least 6 weeks after birth (and some even later) using the same line [134, 168]. A distinct advantage of using our MFKO line is that it enables

examination of a direct role for FAK in the progression of adult onset cardiac diseases in mice that do not have any underlying developmental defects.

It is interesting that FAK is dispensable for basal myocyte function, while depletion of integrin receptors or various cytoskeletal components including vinculin, muscle LIM protein, desmin, plakoglobin, or N-cadherin all lead to rapid defects in sarcomeric integrity accompanied by considerable interstitial fibrosis [132]. These data indicate that although FAK co-resides with these cytoskeletal proteins in Z-disks, it is not an integral component of the contractile apparatus in myocytes. However, we did find that following persistent challenge MFKO hearts exhibited systolic dysfunction relative to control-banded hearts. This was likely a secondary effect due to insufficient compensation in response to TAC, since this model induces a rapid and severe remodeling response in control animals. There is some evidence indicating that the switch from hypertrophy to cardiac failure may involve activation of apoptotic pathways. Although we did observe a greater extent of interstitial fibrosis in banded and aged MFKO hearts (likely due to increased myocyte drop-out), we did not observe an increase in apoptosis or apoptotic markers at the time points examined. These data corroborate our previous studies showing that FAK inhibition in cultured cardiomyocytes did not induce programmed cell death and studies from others indicating that targeted deletion of FAK in keratinocytes or neurons did not induce apoptosis [29, 141, 161]. Taken together, these data indicate that the ensuing dysfunction in MFKO hearts is likely due to a passive necrotic process.

As a multi-functional adapter protein that associates with the integrin cytoplasmic tail, with actin, and with several adapter proteins that regulate various

catalytic signaling molecules, FAK is an ideal candidate to sense and respond to hormonal imbalances and/or alterations in the force-generating actin cytoskeleton by inducing coordinate activation of downstream hypertrophic growth signaling pathways. Our study revealed that myocyte-specific depletion of FAK dramatically reduces biomechanical stress or hypertrophic agonist–stimulated ERK activation. Given that activation of the MEK1-ERK1/2 signaling pathway *in vivo* precedes the induction of hypertrophic gene expression and that inhibition of these signaling pathways can lessen hypertrophic growth, it is reasonable to assume that reduced ERK activation may be the primary mechanism responsible for the blunted hypertrophic response in MFKO hearts [131, 163, 164].

In conclusion, our analysis of MFKO mice reveals that FAK is essential for the heart to sense and transduce a biomechanical insult into a compensatory hypertrophic response. This effect is likely due to the ability of FAK to modify the initial wave of ERK-dependent signaling induced by hypertrophic stimuli. Since cardiac hypertrophy induced by pressure-overload and neuro-humoral signals share common mechanisms, and since signaling from adrenergic receptors is depressed in MFKO hearts, it is possible that activation of FAK may be a common requirement for the initiation of the pathological hypertrophic response. Interestingly, recent studies have shown that while disruption of MEKK1 (like FAK) eventually leads to cardiac de-compensation following pressure-overload, inactivation of MEKK1 actually prevents systolic dysfunction induced by $G\alpha_q$ [169, 170]. Thus, further studies coupling various hypertrophic model systems with cardiac-targeted FAK disruption should lead to important new information with regard to the transition from

compensatory to de-compensated stages of cardiac hypertrophy and aid in determining under which circumstances FAK-dependent signaling pathways may be protective or detrimental. Whether targeted inhibition of FAK would be beneficial for the treatment of heart disease will likely depend on the contributing factors for disease.

Figure 2.1. Targeted Myocyte Specific Disruption of Mouse Focal Adhesion Kinase. ***a***, Diagrammatic representation of the *fak*$^{flox/flox}$ and *mlc2v*$^{Cre/wt}$ breeding strategy (n=725). ***b,*** PCR analyses of heart DNA from wild type mice (wt, 1.4 kb band), Flox (1.6kb band), and MFKO mice (recombined allele generates 327 bp band). ***c***, Protein extracts from 3-month-old control (C) and MFKO ventricles were processed by SDS-PAGE and probed with anti-FAK or anti-ERK antibodies. Densitometry quantification of FAK expression compared to an ERK loading control (right, n=3). ***d***, Protein extracts from skeletal muscle, stomach, and brain from 3-month-old control (C) and MFKO mice processed as described above using an anti-FAK antibody.

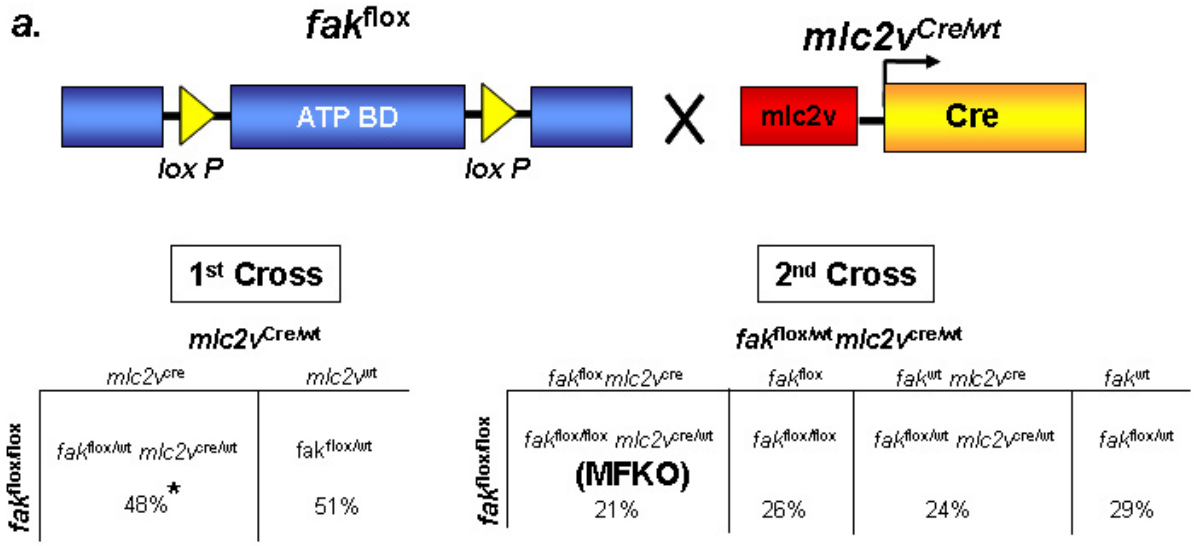
a.
fak^flox
ATP BD
lox P
lox P
mlc2v^Cre/wt
mlc2v
Cre
1st Cross
mlc2v^Cre/wt
mlc2v^cre
mlc2v^wt
fak^flox/flox
fak^flox/wt mlc2v^cre/wt
48%*
fak^flox/wt
51%
2nd Cross
fak^flox/wt mlc2v^cre/wt
fak^flox mlc2v^cre
fak^flox
fak^wt mlc2v^cre
fak^wt
fak^flox/flox
fak^flox/flox mlc2v^cre/wt
(MFKO)
21%
fak^flox/flox
26%
fak^flox/wt mlc2v^cre/wt
24%
fak^flox/wt
29%

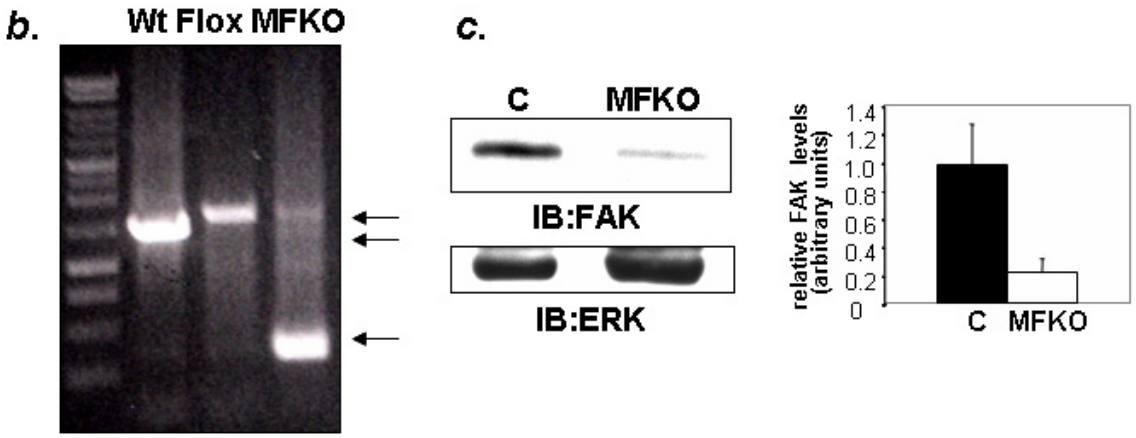
b.
Wt Flox MFKO
c.
C
MFKO
IB:FAK
IB:ERK
relative FAK levels (arbitrary units)
1.4
1.2
1.0
0.8
0.6
0.4
0.2
0
C
MFKO

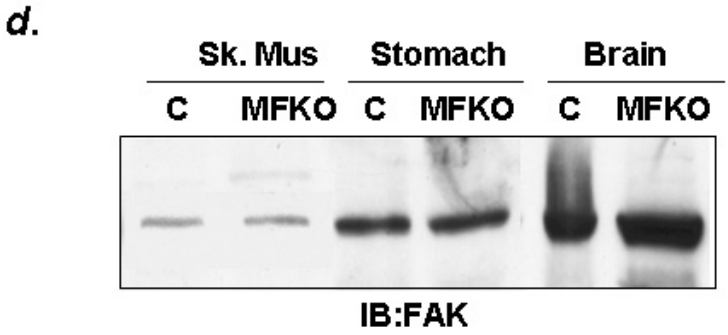
d.
Sk. Mus
Stomach
Brain
C
MFKO
C
MFKO
C
MFKO
IB:FAK

Table 2.1 Echocardiographic analysis in baseline, banded, and aged mice

	CONTROL			MFKO		
	4 month (baseline)	5 month (banded)	14 month (aged)	4 month (baseline)	5 month (banded)	14 month (aged)
LVEdD(mm)	3.1 + 0.1	2.6 + 0.1 †	3.9 + 0.3 †	3.2 + 0.1	3.1 + 0.1 §	4.2 + 0.2 ‡
LVEsD (mm)	2.1 + 0.1	1.3 + 0.1 †	2.8 + 0.4 †	2.0 + 0.1	1.8 + 0.2 §	3.0 + 0.2 ‡
LVPWTd (mm)	0.8 ± 0.06	1.3 ± 0.1 †	1.3 ± 0.2 †	1.0 ± 0.1	1.2 ± 0.1	1.1 ± 0.2
LVPWTs(mm)	1.1 ± 0.1	1.6 ± 0.1 †	1.6 ± 0.2 †	1.2 ± 0.1	1.5 ± 0.1 ^	1.5 ± 0.3
IVSd (mm)	1.1 ± 0.04	1.3 ± 0.1 †	1.3 ± 0.2 †	1.1 ± 0.04	1.2 ± 0.06 ^	1.3 ± 0.3 ^
IVSs(mm)	1.5 ± 0.1	1.9 ± 0.1 †	1.7 ± 0.2 *	1.6 ± 0.1	1.7 ± 0.1 ^	1.6 ± 0.3
%FS	35.1 ± 2.1	50.3 ± 3.0 †	28.5 ± 5.6 *	38.5 ± 2.4	43.4 ± 3.1	23.9 ± 3.7 ^
%EF	63.3 + 2.9	81.7 + 2.6 †	54.5 + 4.0	68.2 + 0.03	72.7 + 0.04	47.0 + 3.3 ^
HR	501 ± 31	640 ± 25	492 ± 32	567 ± 24	611 ± 25	479 ± 27

†, P<0.001; *, P< 0.05 versus baseline Control. ‡, P<0.01; ^, P<0.05 versus baseline MFKO. §, P<0.01 versus banded control. %FS, percent fractional shortening; HR, heart rate; d, diastole; s, systole. 4 month (baseline) Control n=22, 14 month Control n=10, 4-month (baseline) MFKO n=33, 14-month MFKO n=6, 4wk banded Control n=15, 4wk banded MFKO n=25.

Figure 2.2. FAK is Required for Myocyte Growth. ***a,*** Baseline function of 4-month and 14-month-old control (C) and MFKO hearts as determined by M-mode echocardiography (*, $p<0.05$ when compared to baseline genetic control; see Table I for measured values and number of mice/condition). ***b,*** LV weight (LVW) to body weight (BW) ratio for 14-month-old control (n=10) and MFKO (n=6) mice. *, $p<0.05$. (bottom panel) ***c,*** Cross sectional myocyte area of control and MFKO myocytes from 14 month old hearts, n=at least 285 per condition. *p, <0.05 compared to control. ***d,*** Left ventricular posterior wall thickness measured in control and MFKO 14 month old hearts. *p,<0.05 compared to control (bottom).

a.

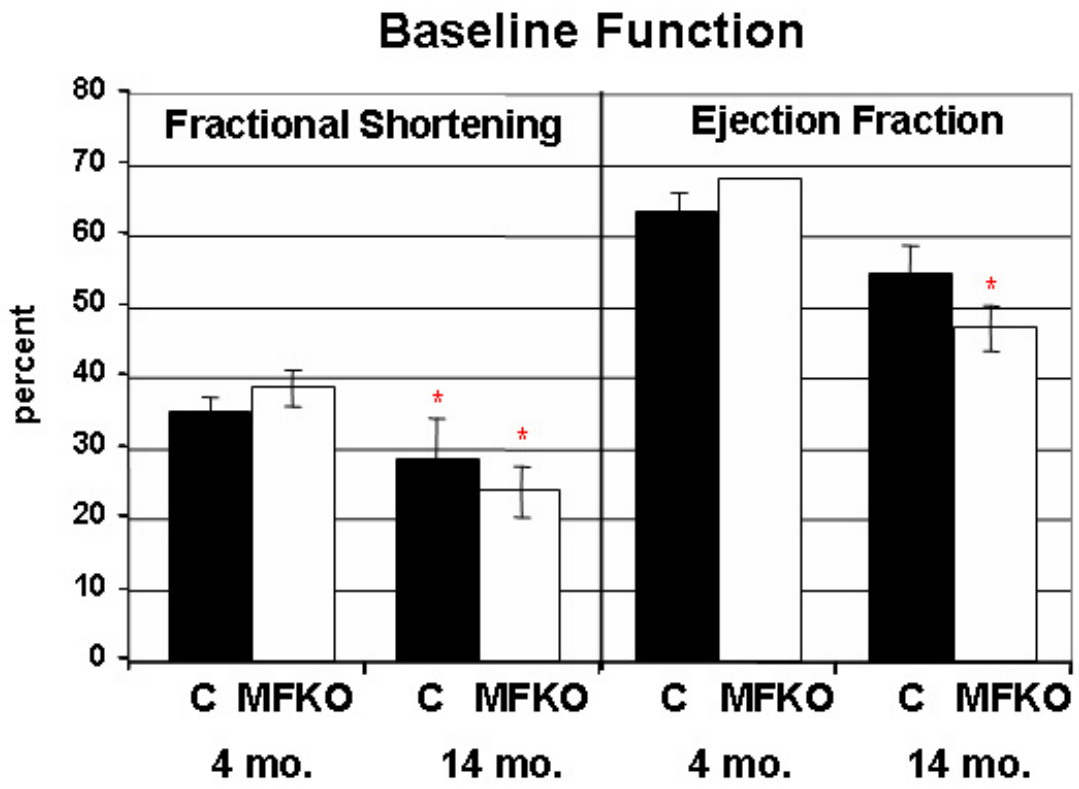
Baseline Function
Fractional Shortening
Ejection Fraction
percent
80
70
60
50
40
30
20
10
0
C MFKO C MFKO C MFKO C MFKO
4 mo. 14 mo. 4 mo. 14 mo.

b.

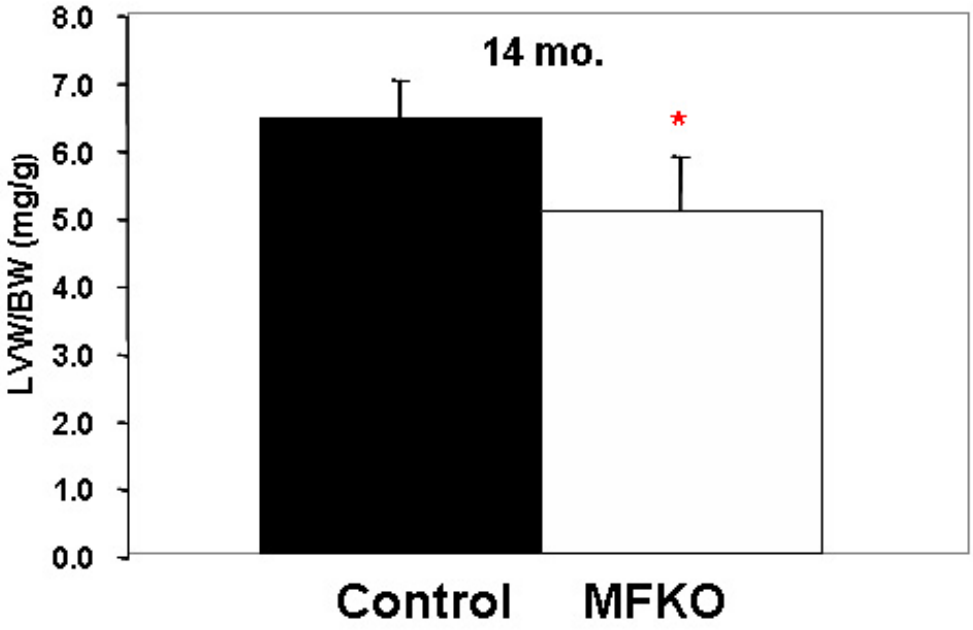
14 mo.
LVW/BW (mg/g)
8.0
7.0
6.0
5.0
4.0
3.0
2.0
1.0
0.0
Control MFKO

c.

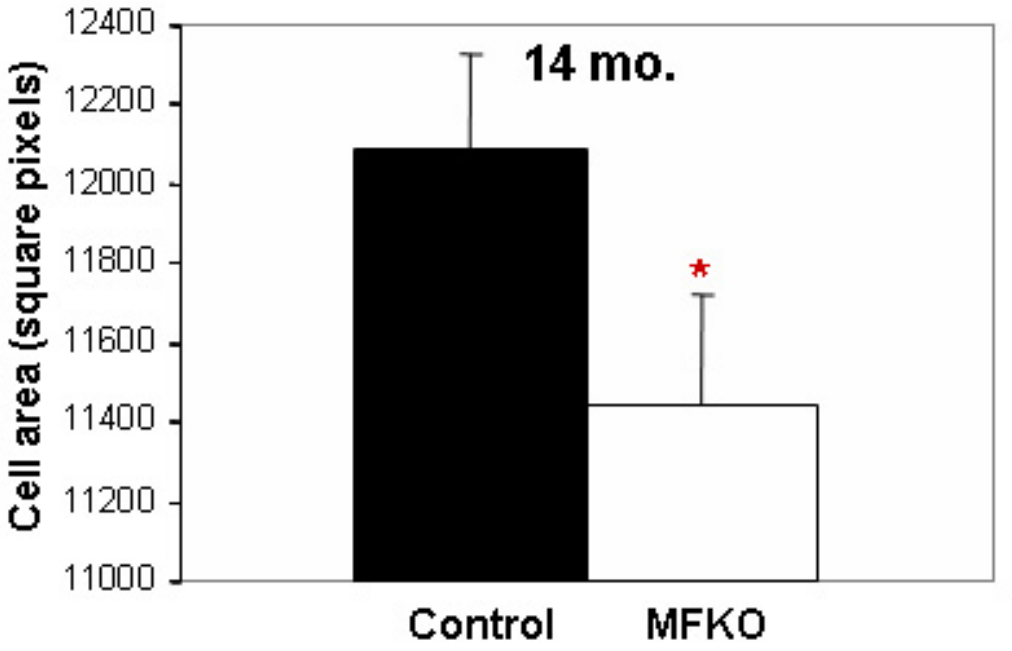
14 mo.
Cell area (square pixels)
12400
12200
12000
11800
11600
11400
11200
11000
*
Control
MFKO

d.

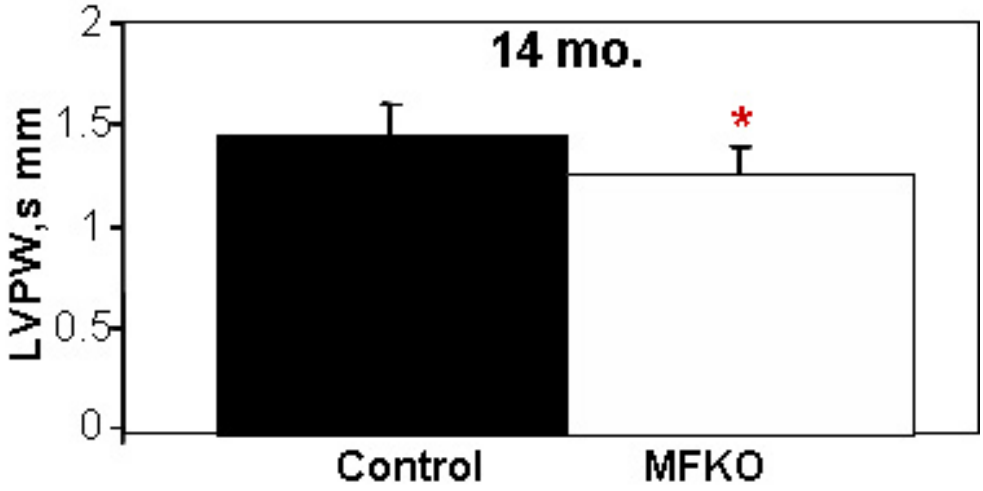
14 mo.
LVPW,s mm
2
1.5
1
0.5
0
*
Control
MFKO

Table 2.2 Baseline Contractility in Control and MFKO Mice

	CONTROL	MFKO
dp/dt max	3987.8 + 315.8	3595.8 + 255.7
dp/dt min	-3026.0 + 437.7	-3265.8 + 344.0
%EF	70.2 + 11.8	62.6 + 6.2
CO	6570.2+ 1623.6	7235.5 + 884.9
SV	18.2 + 4.8	21.1 + 3.1
ESP	55.5 + 3.2	56.1 3.5
EDP	4.2+ 0.7	6.0+ 1.3
SW	789.7 + 226.9	959.0 + 173.4
ESV	10.2 + 2.5	16.7 + 3.25
EDV	33.2 + 7.0	30.8 + 4.0

4-month old control (n=6) and MFKO (n=12). dp/dt=LV pressure over time, EF=ejection fraction, CO=cardiac output, SV=stroke volume, ESP=end systolic pressure, EDP=end diastolic pressure, SW=stroke work, ESV=end systolic volume, EDV=end diastolic volume.

Figure 2.3. FAK is Not Required for Maintenance of Myocyte Cyto-Architecture. ***a,*** Left ventricles from indicated ages of control and MFKO mice were processed for histology as described in the Materials and Methods section and stained with Masson's Trichrome to reveal myocyte organization and level of fibrosis (blue). ***b,*** Sections of left ventricle from control and MFKO mice were stained with an anti-cardiac troponin T antibody to reveal myofibrillar organization. ***c,*** Immunoblot of protein extracts from 4-month control or MFKO ventricles were probed with anti-Pyk2 (top) or anti-ERK antibodies (bottom). Densitometry quantification of Pyk2 expression compared to an ERK loading control (right, n=4).

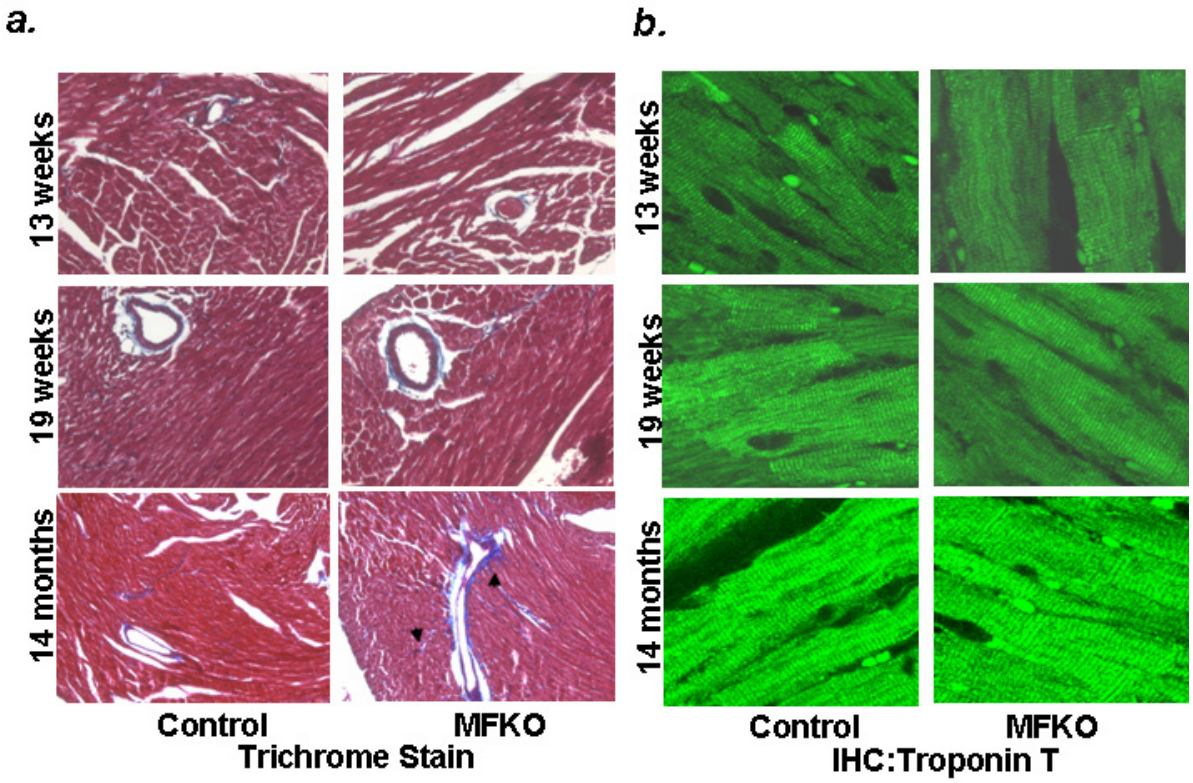
a.
b.
13 weeks
19 weeks
14 months
Control
MFKO
Trichrome Stain
IHC:Troponin T

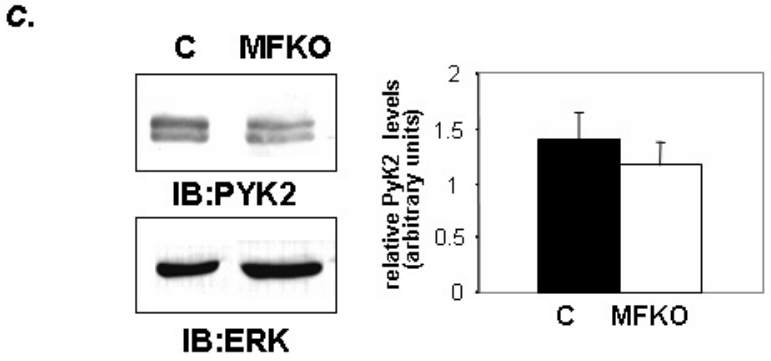
c.
C
MFKO
IB:PYK2
IB:ERK
relative PyK2 levels (arbitrary units)
2
1.5
1
0.5
0

Table 2.3 Fibrosis in Control and MFKO mice

	0	+	++	+++
CONTROL Baseline (n=6)	83.3	16.7	0.0	0.0
MFKO Baseline (n=4)	75.0	25.0	0.0	0.0
CONTROL 4wk TAC (n=6)	0.0	50.0	33.3	16.7
MFKO 4wk TAC (n=18)	11.1	22.2	50.0	16.7
CONTROL 8wk TAC (n=5)	20.0	40.0	20.0	20.0
MFKO 8wk TAC (n=7)	14.3	14.3	28.6	42.9
CONTROL 12wk TAC (n=5)	20.0	60.0	20.0	0.0
MKKO 12wk TAC (n=6)	16.7	33.3	50.0	16.7
CONTROL 14 mo. (n=10)	40.0	50.0	10.0	0.0
MFKO 14 mo. (n=6)	0.0	50.0	50.0	0.0

Percentage of control and MFKO mice with vascular and interstitial fibrosis at baseline, after 4, 8, or 12 weeks of aortic constriction, or at 14 months of age. Cross sections of Trichrome stained hearts were quantitated as follows: 0 = no presence of peri-vascular or interstitial fibrosis. + = 1-25% of vessels contained peri-vascular fibrosis. ++ = 26-75% of vessels contained fibrosis and/or presence of interstitial fibrosis. +++ = 76-100% of vessels contained fibrosis and/or the presence of significant interstitial fibrosis.

Figure 2.4. FAK is Essential for Pressure-Overload-Induced Hypertrophy. ***a,*** M-mode echocardiograph measurements of the left ventricles from baseline and banded control and MFKO mice during diastole (d) and systole (s) were analyzed for percent change from pre to post TAC. *, $p<0.05$ when compared to percent change in control mice. ***b,*** Ventricles from sham and 4-week banded control and MFKO hearts were stained with Trichrome to reveal gross changes in wall thickness and chamber dimensions following 4-weeks of TAC.

a.

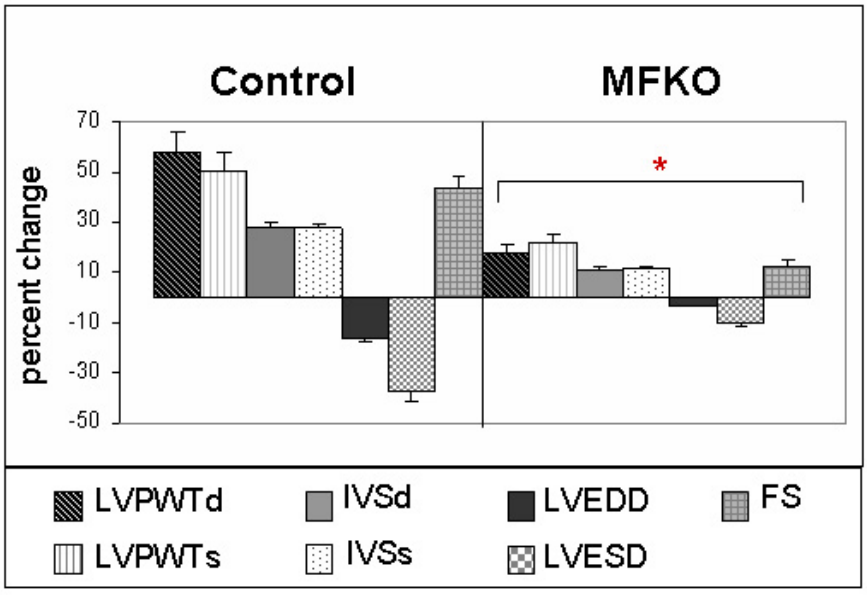
Control
MFKO
70
50
30
10
-10
-30
-50
percent change
*
LVPWTd
LVPWTs
IVSd
IVSs
LVEDD
LVESD
FS

b.

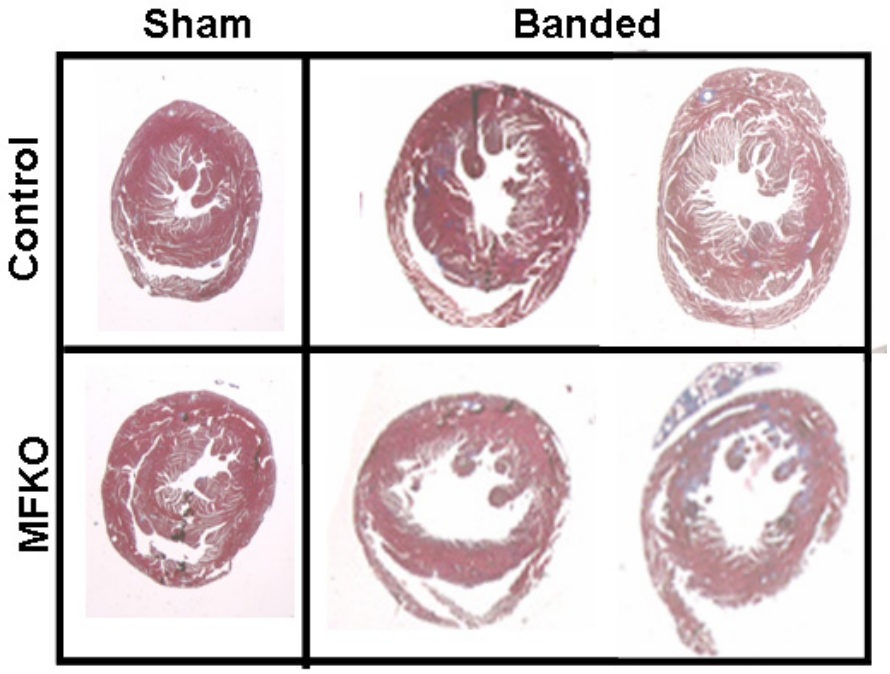
Sham
Banded
Control
MFKO

Figure 2.5. FAK is Required for Increased Posterior Wall Thickness. Relative wall thickness (RWT) measured in 15/19 MFKO hearts show a significant reduction compared to control. *p,<0.05.

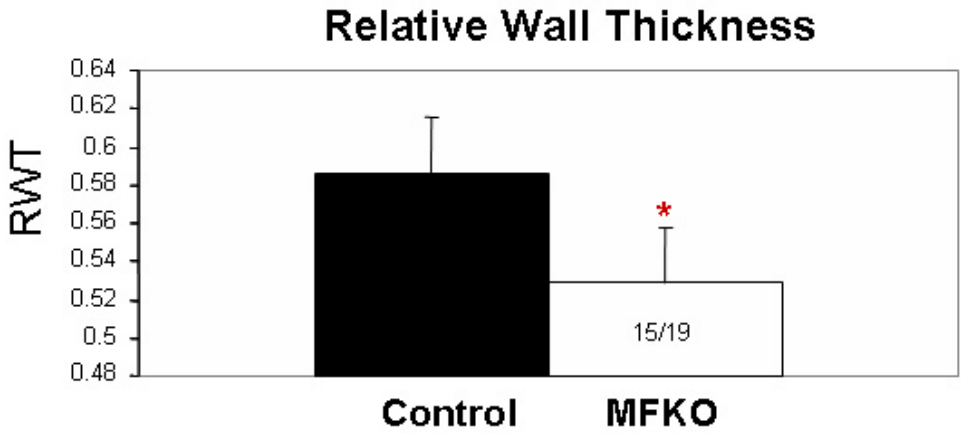
Relative Wall Thickness
RWT
0.64
0.62
0.6
0.58
0.56
0.54
0.52
0.5
0.48
*
15/19
Control
MFKO

Figure 2.6. MFKO Hearts Have Reduced Myocyte Area. ***a,*** Left ventricular weight (LVW) to body weight (BW) ratio. ***b.*** Cross-sectional myocyte area of sham and 4 week banded control and MFKO myocytes (middle, n=at least 175 per condition). *, $p<0.05$ for indicated comparison. Representative LV sections stained with lectin reveals reduced cross-sectional area in MFKO myocytes compared to controls following 4-weeks of TAC (bottom).

a.

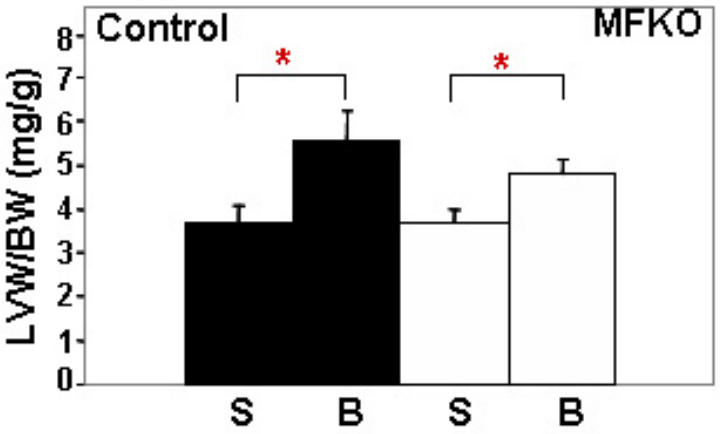
Control
MFKO
LVW/BW (mg/g)
0
1
2
3
4
5
6
7
8
*
*
S
B
S
B

b.

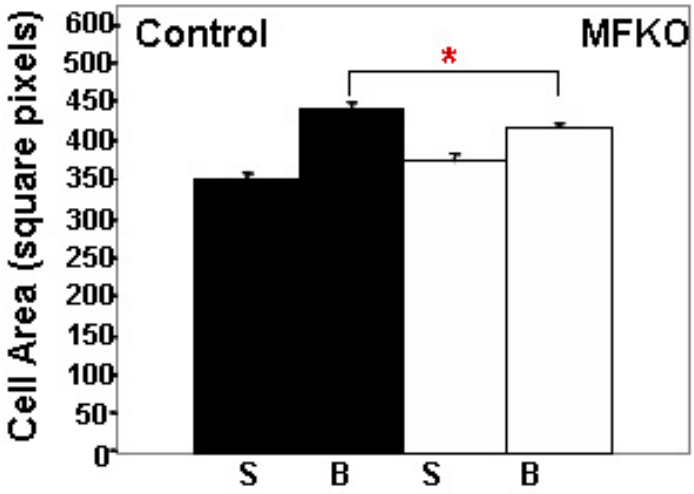
Control
MFKO
Cell Area (square pixels)
0
50
100
150
200
250
300
350
400
450
500
600
*
S
B
S
B

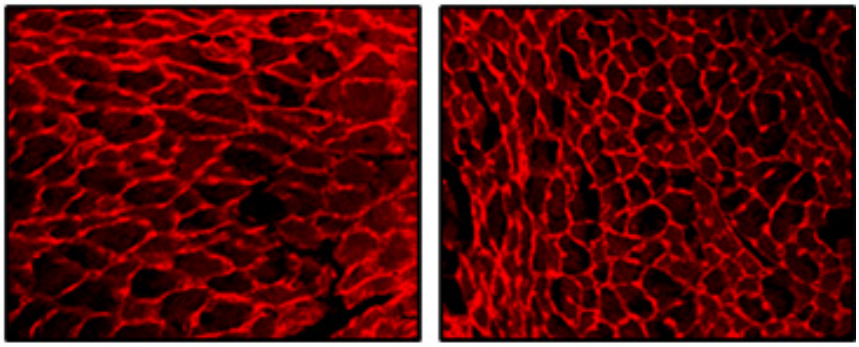
Control
MFKO

Figure 2.7. Functional and morphological changes induced by TAC in control and MFKO mice. ***a,*** Doppler measurements from the left and right carotid arteries prior to and immediately following aortic constriction were compared for changes in peak velocity. Similar changes were measured in both control (C) and MFKO mice. ***b,*** Comparison of left ventricular posterior wall and chamber size in both control and MFKO mice. *, p=0.01 versus control 4-week banded control.

a.

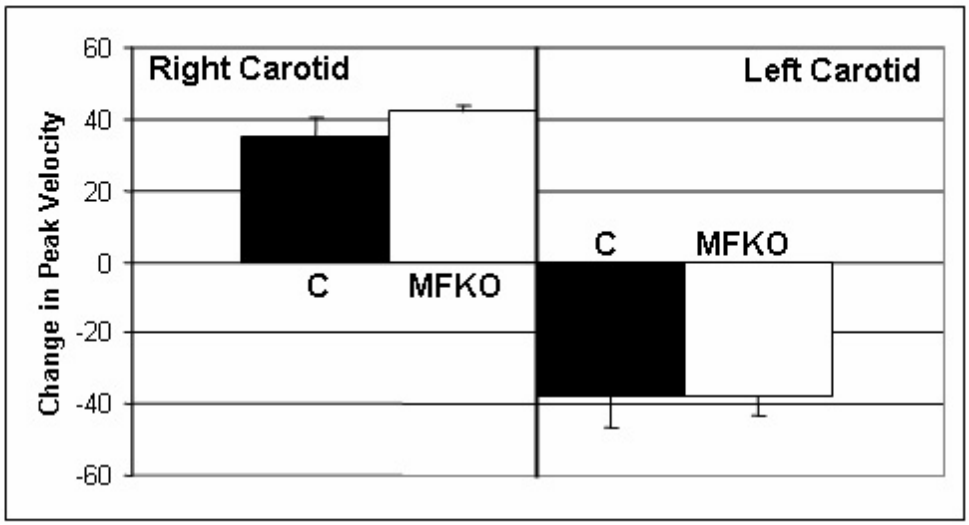
Right Carotid
Left Carotid
Change in Peak Velocity
60
40
20
0
-20
-40
-60
C
MFKO
C
MFKO

b.

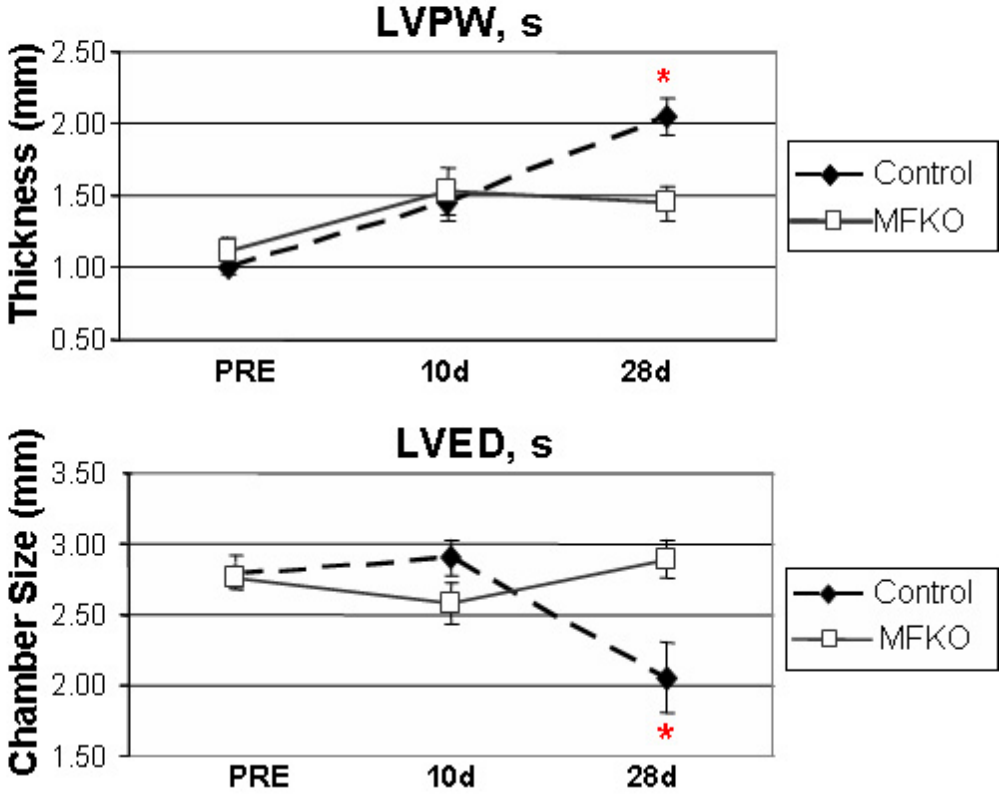
LVPW, s
Thickness (mm)
2.50
2.00
1.50
1.00
0.50
PRE
10d
28d
*
Control
MFKO
LVED, s
Chamber Size (mm)
3.50
3.00
2.50
2.00
1.50
PRE
10d
28d
*
Control
MFKO

Table 2.4 Echocardiographic Analysis in Baseline and Banded Mice

	CONTROL			MFKO		
	Baseline	**10d**	**28d**	**Baseline**	**10d**	**28d**
LVEDD(mm)	3.9 ± 0.1	3.8 ± 0.1	3.6 ± 0.2	3.8 ± 0.1	3.5 ± 0.1 *	3.9 ± 0.2
LVESD (mm)	2.8 ± 0.1	2.9 ± 0.1	2.1 ± 0.3	2.8 ± 0.1	2.6 ± 0.2	2.9 ± 0.1
LVPWTd (mm)	0.9 ± 0.04	1.2 ± 0.1 *	1.8 ± 0.2 * ‡	1.0 ± 0.1	1.2 ± 0.1 *	1.2 ± 0.1 * †
LVPWTs(mm)	1.0 ± 0.1	1.5 ± 0.1 *	2.1 ± 0.1 * ‡	1.1 ± 0.1	1.5 ± 0.2 *	1.5 ± 0.1 * †
IVSd (mm)	0.9 ± 0.1	1.2 ± 0.1 *	1.3 ± 0.1 *	0.87 ± 0.1	1.2 ± 0.05 *	1.1 ± 0.1 *
IVSs(mm)	1.32 ± 0.1	1.6 ± 0.1 *	1.6 ± 0.1 *	1.3 ± 0.1	1.6 ± 0.1 *	1.5 ± 0.1 *
%FS	26.1 ± 1.7	21.9 ± 4.0	24.1 ± 2.4	23.8 ± 3.7	20.8 ± 2.5 *	24.4 ± 1.7
HR	507 ± 17	500 ± 24	497 ± 28	500 ± 14	489 ± 14	491 ± 19

*, p< 0.05 versus baseline Control. †, p< 0.05 versus 28d Control. ‡, p<0.05 versus 10d geneticcontrol. LVEDD, left ventricular end-diastolic diameter; LVESD, left ventricular end-systolic diameter; LVPWTd, left ventricular posterior wall thickness in end diastole; LVPWTs, left ventricular posterior wall thickness in end systole; IVSd, interventricular septum thickness in end systole; IVSs, interventricular septum thickness in end systole; %FS, percent fractional shortening; HR, heart rate. Baseline Control and MFKO n=8, 10d Control and MFKO n=7, 28d Control and MFKO n=7.

Figure 2.8. Post TAC MFKO Hearts Have Increased Fibrosis but MFKO Myocytes Display Normal Cyto-Architecture. ***a,*** 10X images of Trichrome-stained sections (top) or 40X images of sections stained with cardiac troponin T antibody (bottom) reveal increased fibrosis but normal cell-cell interactions and myofibrillar organization in control and MFKO hearts. ***b,*** Western blot analysis of Pyk2 protein levels following 4-week TAC of control (C) and MFKO mice. Densitometry quantification of Pyk2 expression compared to an ERK loading control (right, n=5).

a.

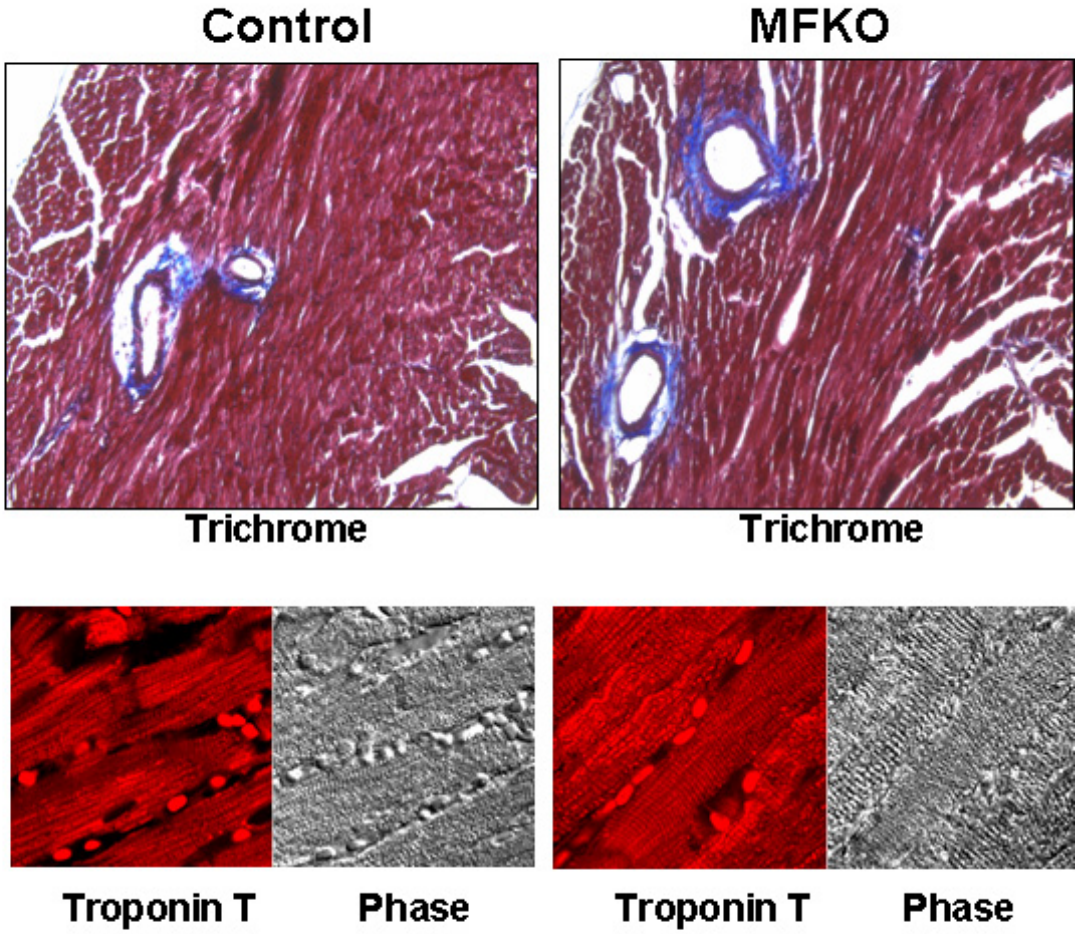
Control
MFKO
Trichrome
Trichrome
Troponin T
Phase
Troponin T
Phase

b.

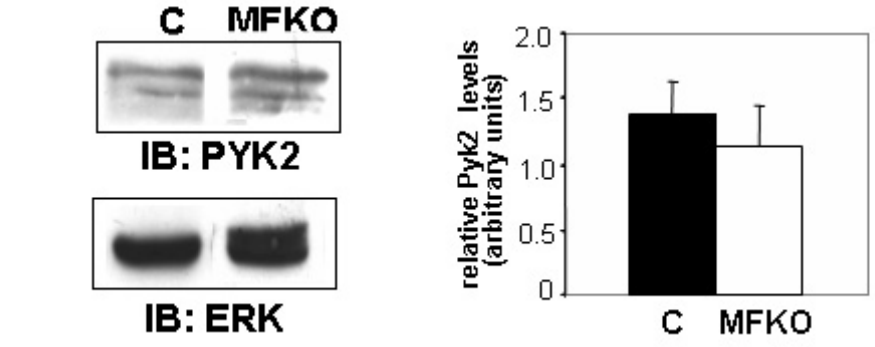
C
MFKO
IB: PYK2
IB: ERK
relative Pyk2 levels (arbitrary units)
2.0
1.5
1.0
0.5
0
C
MFKO

Figure 2.9. MFKO Hearts Have Similar Ultra-Structure as Controls. Transmission electron micrographs from the mid-wall region of the left ventricle of 4-week banded control and MFKO mice taken at 4000x, 10000x and 20000x magnification.

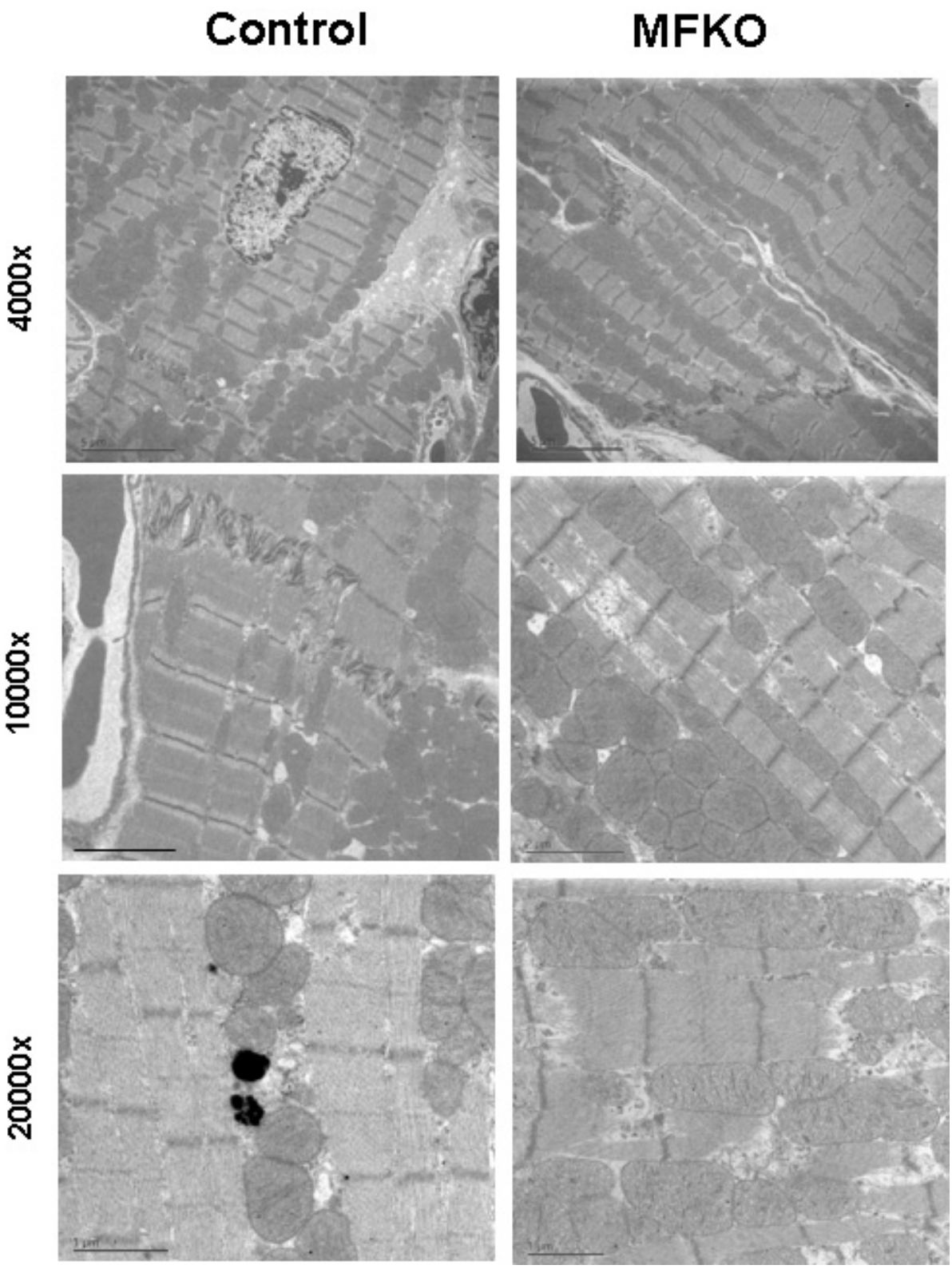
Control
MFKO
4000x
10000x
20000x

Figure 2.10. FAK Deletion Does Not Alter Expression of Apoptotic Markers. ***a,*** Ventricular lysate from baseline and 4 week TAC control (C) and MFKO mice was processed for Western analysis using anti-PARP antibody. Amount of cleaved PARP was quantified by densitometry. Data are presented in comparison to an ERK loading control (n=4). ***b,*** Top panel shows RTPCR analysis of Bax and Bcl-2 mRNA from sham and 28d banded control (C) and MFKO (M) mice. Bottom panel shows Western blot analysis of Bax and Bcl-2 protein levels from control and MFKO mice following 4 weeks of TAC. Right panel shows quantification of Bax to Bcl-2 protein levels (n=4).

a.

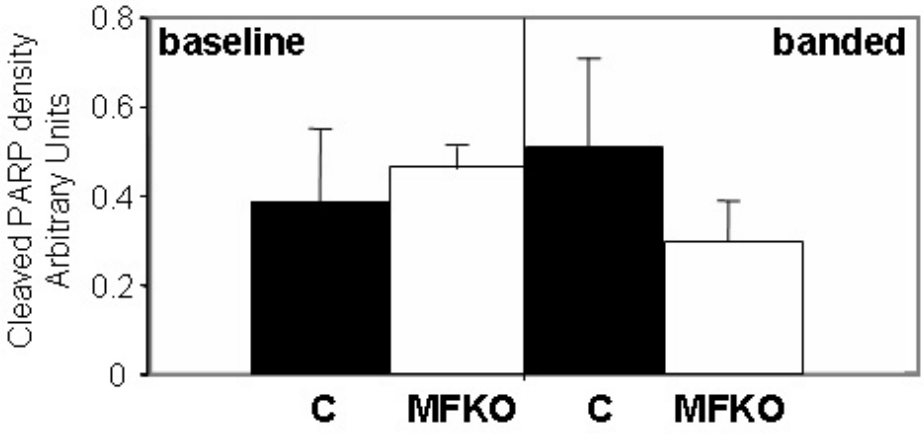
baseline
banded
Cleaved PARP density
Arbitrary Units
0.8
0.6
0.4
0.2
0
C
MFKO
C
MFKO

b.

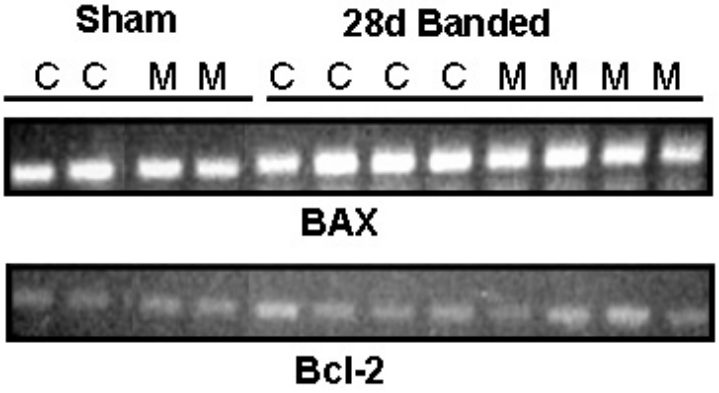
Sham
28d Banded
C C M M C C C C M M M M
BAX
Bcl-2

c.

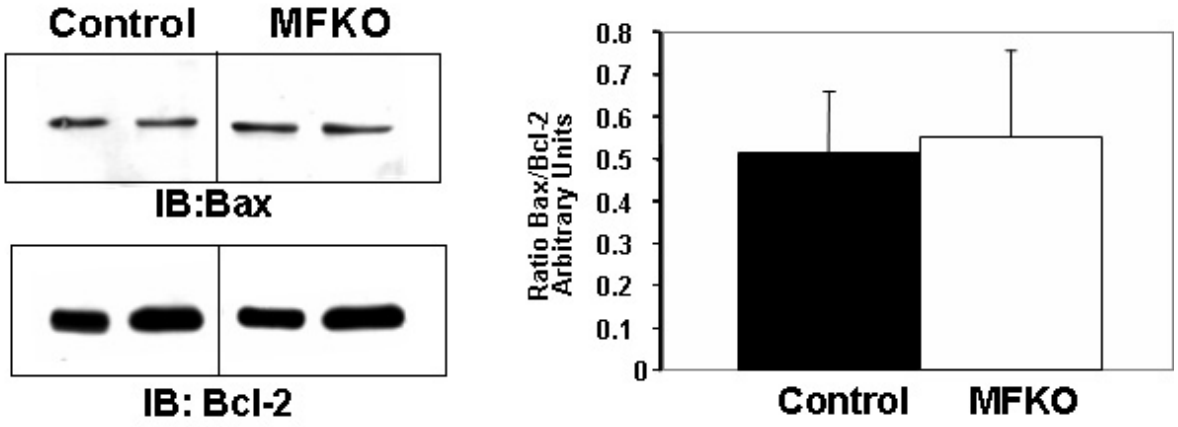
Control
MFKO
IB:Bax
IB: Bcl-2
Ratio Bax/Bcl-2
Arbitrary Units
0.8
0.7
0.6
0.5
0.4
0.3
0.2
0.1
0
Control
MFKO

Figure 2.11. FAK Modulates ANF Expression Following TAC. Quantitative RT-PCR analysis for ANF (**a**) and αMHC (**b**) RNA levels from sham and banded control and MFKO hearts. Data were normalized to β-actin levels and presented as fold over values from sham control mice. *, p = 0.03 versus banded control.

a.

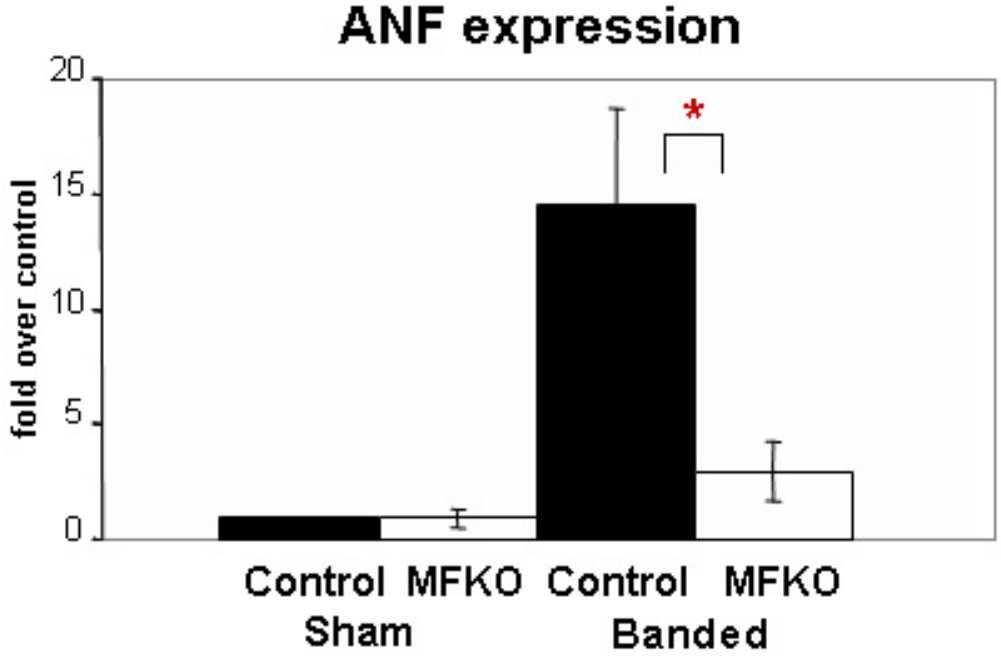
ANF expression
fold over control
20
15
10
5
0
*
Control
MFKO
Control
MFKO
Sham
Banded

b.

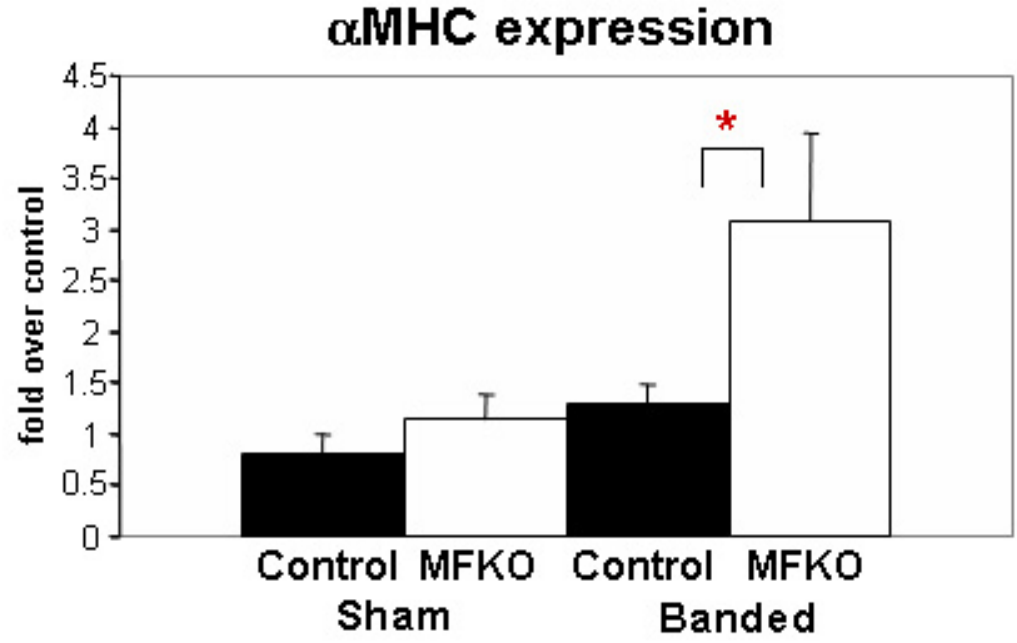
αMHC expression
fold over control
4.5
4
3.5
3
2.5
2
1.5
1
0.5
0
*
Control
MFKO
Control
MFKO
Sham
Banded

Figure 2.12. Chronic Banding Leads to Systolic Dysfunction in MFKO Mice. *a,* Wet lung and body weight measurements were taken from control and MFKO sham-treated mice or mice banded for 4 or 8-weeks. *, p=0.03 versus experimental control n=4 (or more) for each group. ***b,*** Sham or 12-week banded control and MFKO mice were subjected to cardiac catheterization as described in the Materials and Methods section to examine contractile function. n=at least 4 for each group. *, p=0.03 versus 12-week banded control.

a.

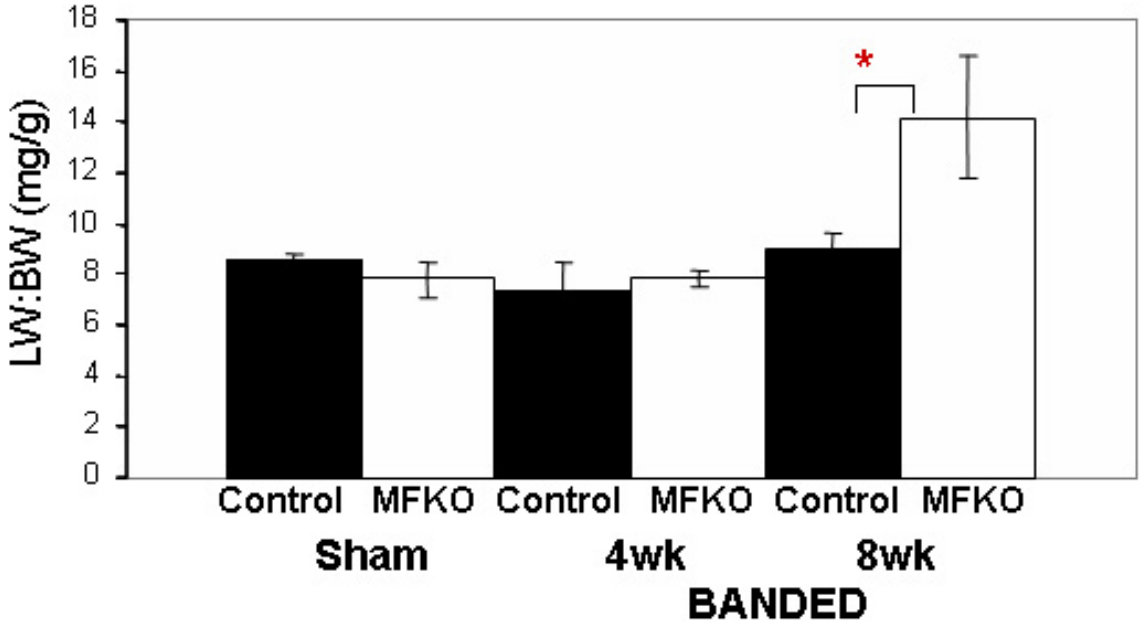
LW:BW (mg/g)
18
16
14
12
10
8
6
4
2
0
*
Control
MFKO
Control
MFKO
Control
MFKO
Sham
4wk
8wk
BANDED

b.

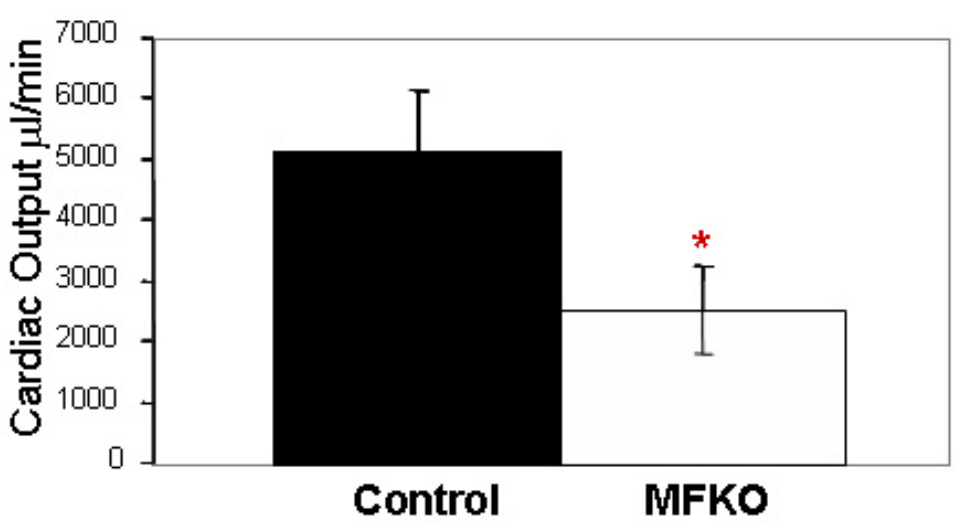
Cardiac Output µl/min
7000
6000
5000
4000
3000
2000
1000
0
*
Control
MFKO

Figure 2.13. FAK is Required for Maximal ERK Activation Induced by Banding and Adrenergic Stress. ***a,*** Western blot analysis of phopspho-ERK1/2 following one or four days of aortic constriction in control and MFKO mice. Densitometry quantification of phospho-ERK1/2 compared to an ERK loading control (right, n=3). ***b,*** Control (C) and MFKO mice were injected with a adrenergic cocktail for 7 min containing PE and isoproterenol (30 mg/kg each) or PBS into the intraperitoneal cavity. Ventricular lysate was processed for Western blot analysis using anti-FAK, phospho-ERK1/2, and total ERK 1/2 (loading control) antibodies. Densitometry quantification of phospho-ERK1/2 compared to an ERK loading control (right, n=3). **c,** RNA was extracted from control and MFKO hearts at days 0, 4, and 7 following banding and processed for quantitative RT-PCR using the c-*fos* probe and primers detailed in the Materials and Methods section *, p = 0.03 versus 4-day banded control mice.

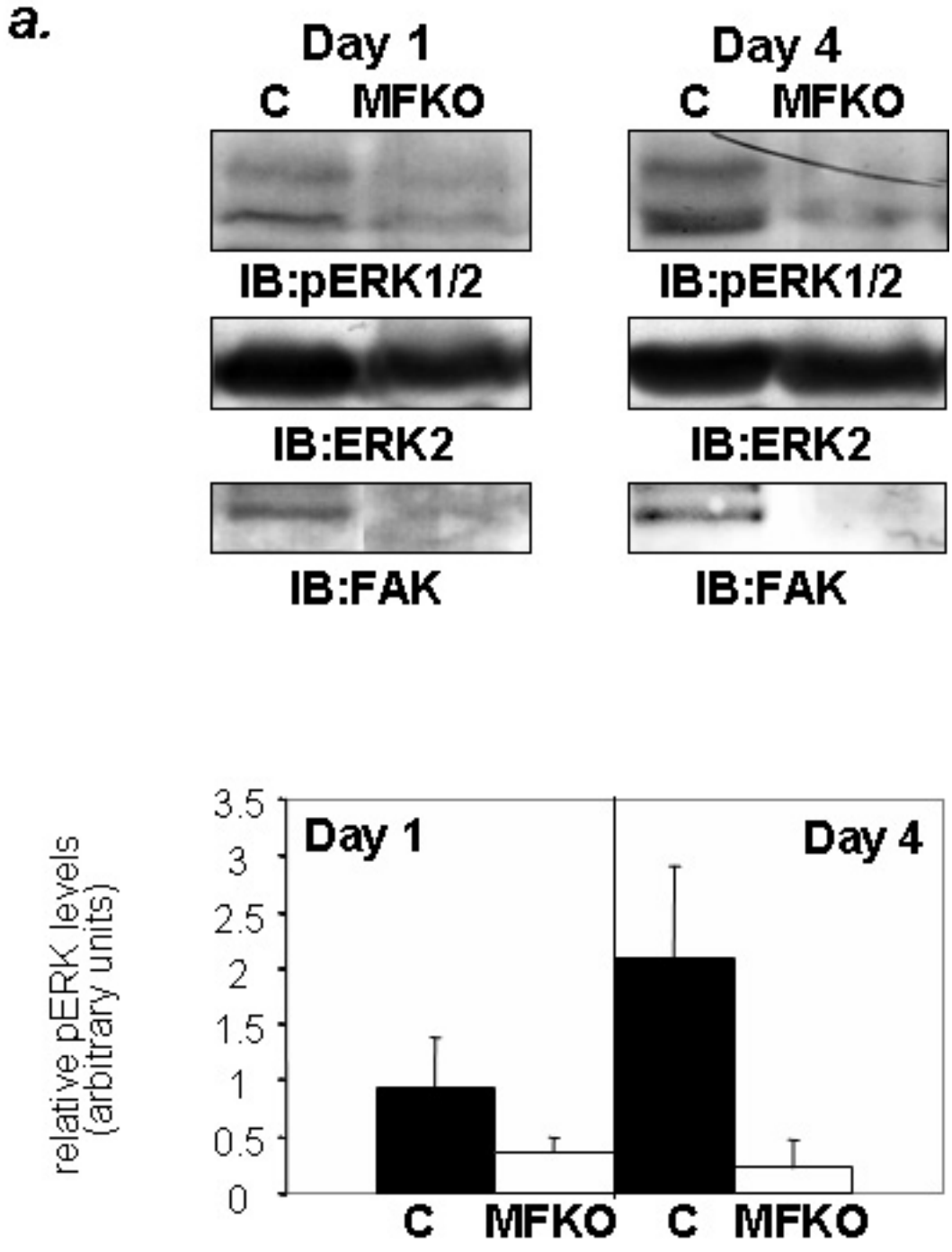
a.
Day 1
C MFKO
Day 4
C MFKO
IB:pERK1/2
IB:pERK1/2
IB:ERK2
IB:ERK2
IB:FAK
IB:FAK
relative pERK levels (arbitrary units)
3.5
3
2.5
2
1.5
1
0.5
0
Day 1
Day 4
C MFKO C MFKO

b.

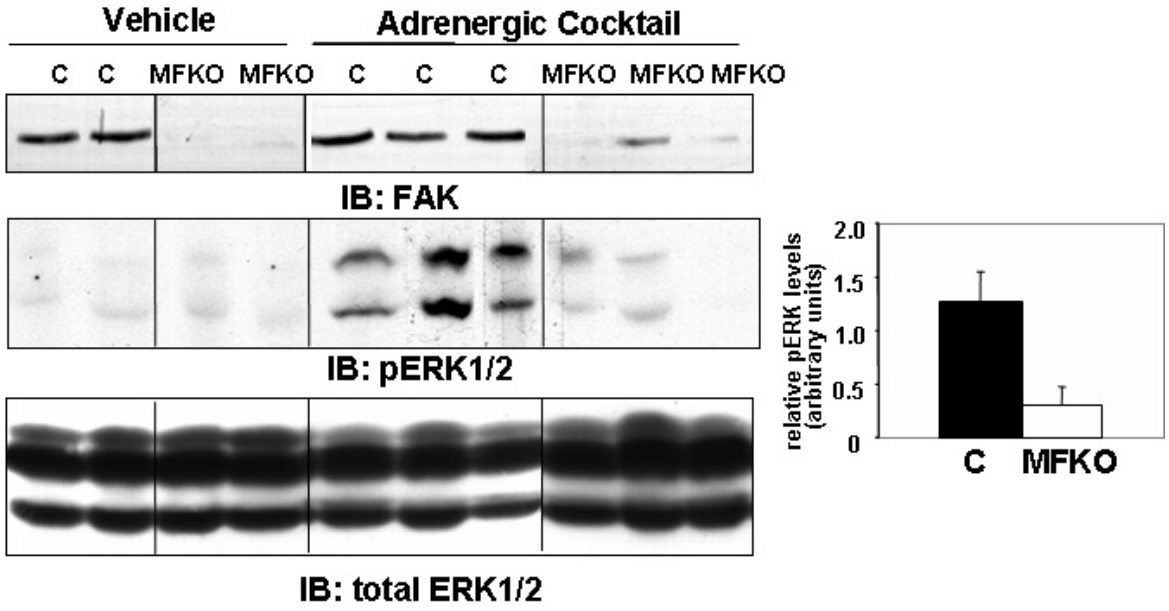
Vehicle
Adrenergic Cocktail
C C MFKO MFKO C C C MFKO MFKO MFKO
IB: FAK
IB: pERK1/2
IB: total ERK1/2
relative pERK levels (arbitrary units)
2.0
1.5
1.0
0.5
0
C
MFKO

c.

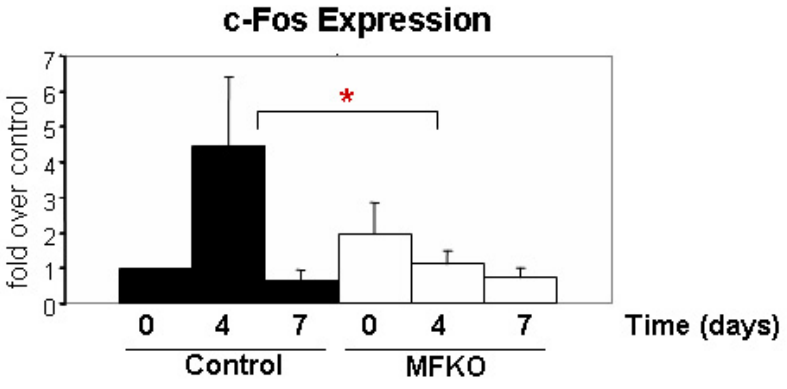
c-Fos Expression
fold over control
7
6
5
4
3
2
1
0
*
0 4 7 0 4 7
Time (days)
Control
MFKO

Chapter III

FAK ACTIVITY IS NECESSARY AND SUFFICIENT TO INDUCE CARDIAC HYPERTROPHY

A. Introduction

Hypertrophy, broadly described as an increase in growth, can manifest in distinct pathologies in the heart. Chronic exercise training can induce a beneficial adaptive response on the cardiovascular system causing cardiac hypertrophy which is referred to as an athletic heart or physiological hypertrophy [171]. These adaptations help the heart meet the increased hemodynamic demands, enhancing normal cardiac function [172]. On the other hand, chronic pressure overload induced by neuroendocrine and autocrine factors leads to a distinct form of cardiac hypertrophy termed pathological hypertrophy. Initially, this response is compensatory as the increased heart size can help maintain function in response to the increased demand [173]. However, over time this leads to decreased left ventricular cardiac function and subsequent heart failure [173]. The latter is likely due to changes in gene expression that do not occur in physiological hypertrophy including alterations in a number of calcium handling proteins. The differential responses observed in physiological and pathological hypertrophy are likely due to differential signaling pathways at the cellular level [174]. Although many molecules have been defined to have a specific role in either pathological or physiological

hypertrophy, the further delineation of the distinct signaling pathways is critical for the treatment of heart disease (Figure 1.4).

Normal cardiac growth and physiological hypertrophy are largely mediated through insulin growth factor-1 (IGF-1) and growth hormone (GH). IGF-1 activates the PI3K subunit a (p110a) which activates downstream effectors such as the serine/threonine kinase AKT and its activator 3-phosphoinositide-dependent protein kinase-1 (PDK-1) [81-83]. AKT is required for normal heart growth and regulates the hypertrophic response through signals to mTOR and GSK3β, which regulate the synthesis of proteins involved in hypertrophy [92, 93].

A variety of cellular receptors are responsible for the initiation of pathological hypertrophy. Ligands such as phenylephrine (PE), angiotensin II (AngII), and endothelin-I activate GPCR's, specifically $G_{q,}$ and trigger the induction of cardiac hypertrophy *in vitro* [100-102]. *In vivo* studies have also implicated a role for GPCR's in pressure overload ventricular hypertrophy[103]. Transgenic mice that over express either Gα_q, α1-adrenergic receptors (ARs), or AngII receptors in myocytes all develop cardiac hypertrophy [104-106]. The specific downstream pathways initiated in the pathological hypertrophic response have been reviewed earlier in this thesis.

Although precise characterization of the pathways that lead to detrimental versus compensatory responses and the plethora of gene expression changes are not clear at present, data from our lab and others indicate that Focal Adhesion Kinase (FAK), a ubiquitously expressed cytoplasmic tyrosine kinase, may play a key role in cardiomyocyte hypertrophy. As noted previously in this thesis, pathological

hypertrophy is characterized by an increased accumulation of extracellular matrix (ECM) proteins, such as fibronectin(FN) [107]. The deposition of ECM proteins is thought to contribute an additional layer of stiffness to the heart as well as to enhance signaling cascades. FAK is strongly activated by integrins and neurohumoral factors, and a variety of *in vitro* and *in vivo* studies have implicated FAK in the progression of cardiac hypertrophy following mechanical and adrenergic stimuli.

Past *in vitro* work from our laboratory demonstrated that cells expressing the dominant negative of FAK, FRNK, displayed an inhibition of PE induced cardiomyocyte hypertrophy as assessed by cell size, sarcomeric reorganization, and endogenous ANF staining [38]. Subsequent reports showed that over expression of FRNK also attenuated endothelin-I and stretch/AngII stimulation of hypertrophy [129, 130]. Following pressure overload in the adult rat heart, FAK tyrosine phosphorylation is increased [145]. Further examination showed that in addition to activation of FAK, a variety of downstream effectors of FAK including p130Cas, Grb2, ERK1/2, AKT, and PI3K were activated [145, 175]. Work described in Chapter III of this thesis demonstrates that *in vivo* deletion of FAK is able to block the pressure-overload induced hypertrophic response.

Although past work has established a role for FAK protein in the progression of hypertrophy, it is presently unclear whether FAK activity is necessary and sufficient for the initiation of pathological cardiac hypertrophy. We recently generated a line of mice that enabled us to examine the effect of FAK deletion in the progression of pathological hypertrophy. This model utilized Cre/loxP technology to

specifically delete FAK protein from the myocardium and led to maximal protein deletion at 3-months postnatal [33]. The delay in recombination, due to (suboptimal) gene accessibility of the endogenous gene as well as a relatively long half life of FAK protein, made it impossible to study the role of FAK in anabolic growth and early stages of cardiac development. To circumvent these problems, we inhibited FAK activity in the adult myocardium using a transgenic mouse which expresses MycFRNK in the myocardium to determine if FAK activity is necessary for the progression of hypertrophy. This model will target FAK activity earlier than the FAK deletion model in Chapter II (MFKO) since Cre initiated gene recombination and expression of protein (in this case MycFRNK), will occur earlier than recombination of a floxed allele and deletion of the gene of interest. We reasoned that ectopic expression of this endogenous dominant negative would be a good model to study the effect of FAK activity on cardiac development and anabolic growth.

Our studies reveal that inhibition of FAK in the postnatal heart does not alter anabolic growth, but attenuates pressure overload induced hypertrophy. To test the possibility that active FAK is sufficient to induce cardiac hypertrophy *in vivo*, we next generated a novel mouse model that produces cardiomyocyte-specific expression of a constitutively active form of FAK, termed SuperFAK. We show that expression of this protein is sufficient to induce cardiac hypertrophy in the absence of surgical manipulation. Initial gene expression data from one of the SuperFAK transgenic lines reveals that the hypertrophy observed resembles a classic pathological hypertrophic response. However, further studies are required to distinguish between the pathological and physiological hypertrophic response in these mice.

B. Materials and Methods

Generation of MycFRNK Mouse. A 1.4kb fragment of MycFRNK was amplified out of the pRK5MycFRNK vector to incorporate 3' and 5' Not1 sites with an internal Kpn site [38]. This fragment was then ligated into a cassette in which a piece of the βactin promoter is fused to cDNA containing GFP flanked by loxP sites. Ultimately, the CX1-MycFRNK fragment was cut out using Kpn, linearized, and submitted for pronuclear microinjection into 0.5 day fertilized embryos which was performed within the UNC Animal Models Core Transgenic Facility at the University of North Carolina at Chapel Hill. All mice were backcrossed to the C57black6 background at least 8 generations prior to subsequent breeding. DNA isolated from tail snips or tissues was subjected to PCR analysis using primers specific for the MycFRNK transgene (CGCGGTACCATCCAGACATGATAAGATACATTGATGAG and CGCCTCGAGGCTGCCACCATGGAGCAGAAGCTGATC). Dr. Kenneth Chien (Harvard) graciously provided the *mlc2v*^{Cre} knock-in mice. Mice were housed in an AAALAC accredited University Animal Care Facility.

Generation of the SuperFAK Mouse. A 3.2 kb Not1 fragment comprising the modified βMHC promoter was amplified from a vector and ligated into a pBKS plasmid [32]. SuperFAK was amplified from a pBKS plasmid and cloned into a flag vector with BamHI and XhoI sites using standard procedure [176]. FlagSuperFAK was subsequently cut from the flag vector using NotI and SpeI to place it downstream of the βMHC promoter in the pBKS plasmid. Pronuclear microinjection of the linearized βMHCflagSuperFAK plasmid into 0.5 day fertilized embryos was performed at the UNC Animal Models Core Transgenic Facility at the University of

North Carolina at Chapel Hill. Transgene expression in C57/Bl6 X C3H hybrid strain founders and F1 progeny mice were confirmed by PCR analysis using primers specific for the SuperFAK transgene (CCGGCATGGAGATGCTACTG, and GCGGCCGCAAGCTGCCACCATGGACTACAAGG). Six founder mice tested positive for the βMHCflagSuperFAK transgene. However, of these six, two expressed the flag-SuperFAK protein in the heart. These lines were breed with black6 mice and F1 progeny characterized. All transgenic mouse procedures were performed in accordance with guidelines set forth by the Institutional Animal Care and Use Committee (IACUC).

***Western Blotting*.** Tissues were lysed in modified radioimmune precipitation assay buffer (50 mM Hepes, 0.15 M NaCl, 2 mM EDTA, 0.1% Nonidet -40, 0.05% sodium deoxycholate, pH7.2) containing 1 mM 4-(2-amnionethyl)benzenesulfonyl fluoride hydroxychloride, 0.02 mg/ml aprotonin containing 5% Triton-X. Proteins were boiled in a sample buffer and resolved using SDS-PAGE and transferred to nitrocellulose. Western blots were preformed using a 1:1000 dilution of the appropriate primary antibody. Blots were washed in Tris-buffered saline, pH 7.4 plus 0.05% Triton-X, followed by incubation with either horseradish peroxidase-conjugated protein A-Sepharose (Amersham Bioscience) or horseradish peroxidase-conjugated rabbit anti-mouse antibody (Amersham Biosciences) at a 1:2000 dilution. Blots were visualized after incubation with chemiluminescence reagents (ECL, Amersham Biosciences)[155].

Histological Analysis and Immunohistochemistry. Paraffin-embedded hearts were sectioned into 8 μm slices and stained with Masson's Trichrome stain (Sigma-

Aldrich), to assess overall morphology and presence of fibrosis, and hematoxylin and eosin for overall morphology. Following the block of endogenous peroxidases with 0.3% H_2O_2 in methanol, sections were permeabilized with phosphate buffered saline containing 3% BSA w/ 0.2% Triton-X and then incubated with cardiac troponin T or GFP antibody in 1%BSA/PBS overnight at 4 degrees C. The sections were then washed with TBST (TBS plus 0.05% Triton-X), incubated with Texas Red-conjugated donkey anti-mouse antibody or horseradish peroxidase conjugated anti-mouse antibody for 90 min. at room temperature (RT), rinsed, and mounted with Vectamount (Vector Labs). Cell area measurements were conducted on TRITC-Lectin (Sigma-Aldrich) stained cross sections of the compact zone of the heart muscle using Image J software (NIH).

Antibodies and Reagents. The FAK, ERK2 (1B3B9), and cortactin (4F11) antibodies were purchased from Upstate Biotechnology, Inc. The phosphospecific ERK1/2 (p42/p44) antibody and monoclonal Myc antibody was purchased from Cell Signaling. The caspase-3 antibody was purchased from Cell Signaling. The GFP (AV polyclonal) antibody was purchased from ClonTech. The phosphospecific tyrosine-397 antibody was purchased from Biosource. The monoclonal M2 flag antibody was purchased from Sigma-Aldrich. The cardiac troponin T monoclonal antibody (13-11) was a gift from Nadia Malouf (UNC, Chapel Hill). Unless specified, antibodies were used at 1:1000 dilution.

***Transthoracic Echocardiography*.** Echocardiograph measurements were taken at the indicated time points using previously described methods[177]. Briefly, following light sedation with isoflurane, hair was removed from the chest and abdomen, and

the mice were placed on a water-jacketed, warmed table in the left lateral decubitus position for imaging. A Visualsonic Ultrasound System (Vevo 660) ultrasound machine containing a 30 MHz variable frequency pediatric probe with a 1 cm offset was used to capture the echocardiogram. Standard long axis and short axis M-mode views were recorded when the mouse possessed a target heart rate between 450 and 650 beats per minute. End-diastolic and end-systolic interventricular septum (IVSd, IVSs), posterior wall thickness (PWTd, PWTs) and left ventricular internal diameters (LVEDD, LVESD) were calculated and averaged from three consecutive contractions using Visual Sonics software. Percent fractional shortening was calculated using: %FS=(LVEDD-LVESD)/LVEDD (x 100).

***Quantitative RT-PCR*.** Ventricles were harvested from end stage mice, homogenized, and RNA was extracted using Trizol reagent (Invitrogen). Each sample of RNA was diluted to 50 ng/μl in DEPC treated H_20. Each 30 μl RNA reaction mixture contained 0.5 μl of 0.1 μg/μl of primer, 1 μl of 20 μmol of probe 15μl of AB Gene one step master mix, and 0.1μl of RT enzyme. The primers and probes used were as follows: ANF forward GAGAAGATGCCGGTAGAAGA, ANF reverse AAGCACTGCCGTCTCTCAGA, ANF probe FAM-ATGCCCCCGCAGGCCCTG-TAMARA, βMHC forward AGCTCAGCCATGCCAACCGT, βMHC reverse TGAGTGTCCTTCAGCAGACT, βMHC probe FAM-AGGCTCTTCACTTGTTTCTGGGCCTCA-TAMARA, αMHC forward AGCTCAGCCAGGCCAATAGA, αMHC reverse TGGGTGTCCTTCAAGTGAGC, αMHC probe FAM-AGAATTCTTCAGGTGTTTCTGTGCCTCAG-TAMARA, 18s forward AGAAACGGCTACCACATCCA, 18s reverse

CTCGAAAGAGTCCTGTATTGT, 18s probe TET-AGGCAGCAGGCGCGCAAATTAC-TAMARA**.** The real time-RT-PCR was performed using the ABI prism 7500 Sequence Detection System (PE Applied Biosystems) in 96-well plates under the following conditions: 30 minutes at 48 ˚C, 10 minutes at 95 ˚C, 40 cycles of 95 ˚C for 15 seconds, and then 60 ˚C for one min.

Statistics. Data are presented as mean ± SEM. Means were compared by 2-tailed Student's *t* test. $p<0.05$ was considered statistically significant.

C. Results

Generation of CX1^{frnk} Mice.

Our success with using FRNK over-expression to inhibit FAK activity in the neonatal cell culture model prompted us to use the same approach to study the role of FAK signaling in the myocardium *in vivo*. To this end we have generated a Cre recombinase-based transgenic mouse model in which FRNK can be over-expressed in a time and tissue-restricted fashion under the *indirect* control of Cre expression. In this expression system the gene of interest (e.g. MycFRNK) is cloned downstream of a region of the β-actin promoter that drives high level expression in all tissues. However, a GFP reporter followed by a transcriptional 'stop' site has been inserted upstream of the transgene, preventing expression of MycFRNK. Importantly, the GFP-'stop' codon region is flanked as a unit by loxP sites, which direct Cre-mediated excision (Figure 3.1a). Thus the CX1-stop-transgenic mice can be crossed with a second line of mice that express the Cre recombinase under the control of a cell or tissue-specific promoter.

To test the MycFRNK construct, cultured cells were transfected with the MycFRNK transgene and then infected using a Cre recombinase adenovirus. Cell lysates were acquired at various time points following infection and immunoblot analysis was performed on the lysate for both FRNK and GFP. As expected, in the presence of Cre, FRNK expression was induced and the expression of GFP decreased over time (Figure 3.1b).

Results shown in Figure 3.1c demonstrate that this approach enabled tight control of MycFRNK expression *in vivo*. Western blot analysis revealed moderate

levels of GFP in all tissues examined including aorta, brain, heart, lung, esophagus, bladder, stomach, intestine, kidney, skeletal muscle, and uterus, while MycFRNK was undetectable in these lysates. Immuonhistochemistry for GFP expression revealed uniform expression throughout the heart, confirming that the transgene does not result in a variegated expression pattern (Figure 3.1d).

Ventricle targeted expression of FRNK

To explore the role of FAK in cardiac development and anabolic growth of the heart, we generated an inducible transgenic line with myocyte restricted FAK expression (Figure 3.1a). The MycFRNK transgenic mouse, herein termed CX1^{frnk} was bred to the previously described MLC2v^{Cre} line to generate a line of myocyte-restricted FRNK expressing mice (Figure 3.2a) [159, 178]. CX1^{frnk}MLC2v^{Cre} mice are born with Mendelian frequency, have a normal life expectancy and do not have any overt abnormalities (Figure 3.2b). As shown in Figure 3.3d, comparable levels of FRNK are expressed in cardiac lysates from 1 day to 10 months postnatal. However, expression of FRNK in embryonic heart lysate was undetectable. Accordingly, histological analysis revealed that these hearts developed normally. Notably, in the presence of Cre, MycFRNK expression was restricted to heart and was not expressed in the skeletal muscle or stomach, indicating that unwanted "read-through" expression did not occur *in vivo* (Figure 3.2e). Importantly, hearts from CX1^{frnk}MLC2v^{Cre} mice exhibit decreased FAK activity relative to hearts from control mice (CX1^{frnk}MLC2v$^{wt/wt}$) as determined by Western blotting with an anti-pFAK Y-397 antibody (Figure 3.2f).

Histological and Functional analysis of CX1^{frnk}MLC2v^{Cre} hearts

Histological analysis revealed that hearts from MycFRNK mice had similar cardiomyocyte size, myofibrillar organization, and extent of collagen deposition as compared to hearts from littermate control mice from 2 to 8 months of age (Figure 3.3a). Sarcomeric organization was intact and comparable in both control and MycFRNK mice as demonstrated by cardiac troponin T staining. Cardiomyocyte area was not significantly different between 8 week old control and MycFRNK hearts (Figure 3.3b,c). Additionally, heart weight versus body weight measurements taken from CX1^{frnk}Mlc2v^{cre} and control mice at 2 months postnatal was similar between the two groups (Figure 3.4a). Physiological evaluation of CX1^{frnk}Mlc2v^{cre} mice via echocardiography revealed that FRNK overexpression does not alter cardiac development or function (Table 3.1). These data imply that the presence of FRNK in the cardiomyocytes does not affect anabolic growth of the heart.

CX1^{frnk}MLC2v^{Cre} Mice Exhibit a Delayed Hypertrophic Response

We recently published a report showing that myocyte-restricted FAK deletion attenuates compensatory hypertrophic remodeling following pressure-overload [33]. This finding highlights the possibility that FAK activity is required for the initiation of this compensatory response. The utilization of FRNK as a dominant negative for FAK will enable us to dissect FAK's role as a scaffold compared to its role as a signaling molecule to further explore the requirement for full FAK activity in the progression of cardiac hypertrophy *in vivo.* Thus, we next subjected CX1^{frnk}MLC2v^{Cre} and wild type littermate control mice to a minimally invasive aortic banding

procedure that provides an approximate 50% reduction in the lumen of the ascending aorta [177].

Following chronic aortic constriction, we inspected the mice for a variety of hypertrophic changes. At 14 days post banding, there was a significant increase in heart weight versus body weight in both genetic control and CX1^{frnk}MLC2v^{Cre} mice. However, the CX1^{frnk}MLC2v^{cre} mice had significantly lower heart weight versus body weight in comparison to genetic controls following banding (Figure 3.4a). In addition, the genetic control mice exhibited significant increases in the diameters of the left ventricular wall (LVPW) and interventricular septum (IVS) at the expense of the left ventricular chamber following 14d of aortic banding. By contrast, we saw no significant changes in these parameters in the CX1^{frnk}MLC2v^{Cre} mice, as expected from our previously published account in MFKO mice (Figure 3.4b) [33]. The decreased wall thickness was likely due to decreased cardiomyocyte cell hypertrophy, since prolonged aortic constriction revealed a significant decrease in myocyte cross sectional area in CX1^{frnk}MLC2v^{Cre} hearts compared to wild type (Figure 3.4c). In addition, the fold increase in ANF expression via quantitative RTPCR analysis in these hearts following banding was significantly decreased (66 fold increase, control; 3.8 fold increase, FRNK; data not shown). Overall, these findings corroborate our previous studies in the MFKO mice (Chapter II) and collectively our data confirms that FAK activity in the developing myocardium is dispensable for anabolic growth of the heart, but is essential for hypertrophic progression, supporting previous data in which absence of FAK attenuated the hypertrophic response.

Generation of the SuperFAK Mouse

We next examined whether increased FAK activity was sufficient to promote hypertrophic growth. To this end, I created a transgenic mouse which expressed constitutively active FAK under the control of a shortened 3.2kb piece of the cardiac specific βMHC promoter. This modified promoter induced ventricle specific expression that, unlike the full length promoter, is not downregulated after birth (Figure 3.6, *personal communication* and [179]). Constitutive activation of FAK was achieved by engineering glutamic acid substitutions for two lysine residues in the activation loop of FAK (K578E, K581E) to create a variant termed SuperFAK. As previously described theses mutations increased the catalytic activity of FAK (Figure 3.5a) [176]. As shown in Figure 3.5b, in comparison to non-transfected cells as well as cells transfected with Flag-FAK, FlagSuperFAK induced a significant increase in autophosphorylation of FAK as assayed by tyrosine 397 phosphorylation.

Characterization of the Two βMHCSuperFAK Transgenic Lines

We obtained two founder lines that expressed ventricle specific SuperFAK protein. The gene was transmitted in both lines were with Mendelian frequency and the founders have survived out to eight months thus far without any noticeable morbidity. Following Western analysis of cardiac lysate taken from the two lines (SuperFAK 1 and 2) we determined that FAK activity, as assayed by tyrosine 397 phosphorylation, was increased in both lines compared to wildtype levels of active FAK in littermate controls (Figure 3.6). Therefore, to distinguish the expressing lines, we named them SuperFAK 1 for the lower expressing line (SF1) and SuperFAK 2 (SF2) for the higher expressing line. Thus far, both lines have been characterized

out to 10 weeks postnatal and the SF1 line has additional data from 16 weeks postnatal. We hypothesize that different levels of activated protein in these lines will enable us to determine whether there is a dose dependent effect of FAK activity on the progression of cardiac hypertrophy.

Characterization of the SF2 Mouse Line

Given the substantial increase in tyrosine 397 observed at four weeks of age in the SF2 mice, we hypothesized that the SF2 mice would induce cardiac hypertrophy in the absence of a pathological challenge. To date, two groups of SF2 mice have been examined: an end stage group at four weeks postnatal, and an end stage group at ten weeks postnatal. To determine the cardiac specificity of the transgene, various tissue lysates from SF2 and littermate control mice were compared for expression of flag protein. As expected, flag protein was present specifically in the heart and was not observed in skeletal muscle, stomach and aorta (Figure 3.7b). To evaluate FAK activity in the SF2 mice at four and ten weeks postnatal, cardiac lysates from transgenic and control mice were examined for an increase in phospho-397 via Western analysis (Figure 3.7a). Immunoblot analysis revealed an increase in FAK activity in the SF2 hearts relative to control hearts. Despite the increased FAK activity, there was no difference in heart weight versus body weight measurements or heart weight versus tibia length in the SF2 mice at ten weeks postnatal relative to controls (data not shown).

To look for hypertrophic cardiac remodeling at the cellular level, SF2 hearts were paraffin embedded, sectioned, and examined for any histological changes. Both control and SF2 trichrome stained heart sections displayed an increase in

fibrosis from four to ten weeks of age. Interestingly, there is a slight increase in the degree of vascular fibrosis noted in the SF2 mice likely due to cardiomyocyte remodeling (Figure 3.8). In addition, cardiomyocyte cross-sectional area was significantly increased in SF2 hearts at ten weeks of age compared to littermate controls indicating that at the cellular level, increased FAK activity leads to an increased growth response (Figure 3.9).

As assayed by quantitative RT-PCR, the SF2 mice exhibited an increase in pathological gene expression compared to controls. RNA extracted from ten week postnatal SF2 hearts displayed a significant increase in βMHC expression compared to control hearts. This pathologic change was also accompanied by an increase in ANF and a decrease in αMHC in the SF2 hearts. The change of the gene expression in the heart indicates that these mice are undergoing a pathological hypertrophic change significant enough to result in changes in fetal gene expression (Figure 3.10). Although we observed the hypertrophic progression as indicated by an increase in cell area and alterations in gene expression, there were no significant changes in heart size as assayed by echocardiography at ten weeks postnatal.

Characterization of the SF1 Mouse Line

To date, three groups of SF1 mice have been examined: an end stage group at four weeks, an end stage group at ten weeks, and a current group at 16 weeks postnatal which were analyzed by echocardiography. Examination of cardiac lysate taken at four and ten weeks postnatal showed a significant increase in FAK activity via Western analysis similar to the SF2 mice (data not shown). We found that left ventricle heart weights at ten and 16 weeks postnatal were increased compared to

littermate controls (Figure 3.11c). In accordance with this data, echocardiograph measurements completed at this time showed a significant increase in LVPW,d at 10 weeks postnatal. At 16 weeks postnatal, there was a significant increase of the LVPWs,d and IVS,s in the SF1 mice relative to controls, indicative of a hypertrophic response in these animals (Figure 3.11a,b). In addition, the SF1 mice displayed an increase in cardiac function as determined by a significant increase in fractional shortening and ejection fraction (Figure 3.11d). Although there was a significant increase in LVPW,d at the 10 week time point, this change was not accompanied by any pathological genetic changes in ANF or βMHC as assayed by quantitative RTPCR. Gene profiles will be completed at later time points to determine if prolonged exposure to low levels of active FAK will indeed induce pathological hypertrophy in these mice.

D. Discussion

FAK is an important regulator of cardiac hypertrophy; however, the critical question of whether FAK activity is necessary and sufficient to induce cardiac hypertrophy *in vivo* was heretofore not known. Herein, we have described two novel mouse models which enabled us to explore the consequence of myocardium restricted inhibition or overexpression of active FAK during anabolic growth and pathologic hypertrophy. The cardiac expression of MycFRNK in the $CX1^{frnk}Mlc2v^{Cre}$ mice resulted in mice that were born with Mendelian frequency and that were phenotypically comparable to controls from birth to adulthood. In this model, although the presence of FRNK was able to decrease ventricular FAK activity it did not affect anabolic growth of the heart nor did it affect baseline cardiac function. However, following chronic aortic constriction, decreased FAK activity attenuates the hypertrophic response similar to previously published data [33]. Thus, the presence of FAK protein, as well as full activation of FAK is critical for mediating the pathological hypertrophic response *in vivo.* Our results from the SuperFAK mice suggest that constitutively active FAK is sufficient to induce cardiac hypertrophy in the absence of any mechanical stimuli. These studies demonstrate that FAK activation is both necessary and sufficient for the induction of cardiac hypertrophy.

The traditional germline deletion of FAK results in embryonic lethality and makes studying the effect of FAK activity in heart development and in the progression of cardiac disease impossible. Therefore, we generated a MycFRNK transgenic mouse that can be crossed with various Cre expressing lines to enable us to study the effect of decreased FAK activity from development to adulthood. In

our model, Cre recombinase is able to initiate recombination between pairs of loxP sites that flank a stop signal in the transgene leading to Cre-mediated expression of MycFRNK. This results in FRNK expression days and weeks before we are able to see knockout of the FAK protein using the floxed FAK gene with identical Cre mice. This is because we do not have to wait for gene abrogation of both floxed alleles and subsequent protein degradation [33]. This model additionally allows us to study the fundamental difference between FAK expression and activity throughout cardiac development and disease.

Since FAK is an integral part of the focal adhesion complex which serves to connect the ECM to sarcomeres, it is possible that the effects observed in our past knock-out models were due to disruptions of this structural complex and not simply due to blocking FAK activity. However, in this current model, although FAK's kinase activity has been dampened due to the presence of FRNK, FAK protein is still present and can still serve as a structural scaffold within the cell. Therefore, in addition to elucidating a role for FAK activity during anabolic growth of the heart, the use of MycFRNK enables us to study the potential role of FAK as a critical pathological hypertrophy signal transducer.

It is reported that FAK can promote cell growth and proliferation in a variety of cell types *in vitro* [180, 181]. Thus, in our model, it is presumed that increased FAK activation would lead to increased cell growth. Our results from echocardiography and cardiomyocyte cross sectional area indicate that FAK is an important signal transducer in the cell growth signal cascade regulating the pathological hypertrophic response but not anabolic growth. In the SF1 line, echocardiograph measurements

revealed the transformation of the heart into a more hypertrophic state. This was also supported by increased LV mass in the gender-matched SF1 mice at both ten and sixteen weeks postnatal. Additionally, myocyte area measurements in the SF2 mice demonstrated an increase in overall cell size relative to control cells. However, due to non-gender matched controls in the ten week end stage group of the SF2 mice, heart weight versus body weight measurements did not show an increase in cell size. Future end stage studies at a variety of time points will determine if, in the presence of increased active FAK, overall heart weight increases in proportion to body weight and whether active FAK induces gene expression changes indicative of pathological remodeling.

A reversion in the gene expression to a fetal gene profile is a hallmark of pathological cardiac hypertrophy. At ten weeks postnatal we observed increased expression of in ANF and βMHC, and a decreased expression of αMHC in SF2 hearts. Notably, levels of expression of these genes correlate directly with the extent of hypertrophy observed in other mouse models [162]. Collectively, we observed that increased FAK activation alters the structural framework and molecular profile of the heart, indicative of a hypertrophic response in the absence of hypertrophic stimuli.

Additional studies will confirm the extent of hypertrophy in both SuperFAK lines, as well as any additional structural and functional changes indicative of pathological hypertrophy. Hearts from end stage experiments with gender matched controls at a variety of time points throughout adulthood will be examined for changes in gene expression, extent of fibrosis and cell size. In addition to structural changes, we will explore through cardiac catheterization any functional changes that

are occurring in the heart. Examination of pressure-volume loops from both SuperFAK and control hearts will determine if, in the presence of active FAK, the SuperFAK hearts have increased contractility and function.

In addition to proliferation, FAK has also been implicated in cell survival in a variety of cell types. Although no increase in apoptosis was found in *fak-/-* embryos or in the cardiac-specific FAK deleted mouse, it is possible that the presence of active FAK is protective against apoptotic injury [33, 182]. To examine this possibility, we plan on inducing apoptosis by ligating the left anterior descending artery of the heart. Since studies in the MFKO mice revealed a significant increase in ischemia-reperfusion infarct size accompanied by an increase in apoptosis we hypothesize that the SuperFAK mice will display decreased ischemic injury relative to control hearts, indicating that FAK signaling is protective in the heart (unpublished observations).

Cardiac lysates taken from SuperFAK expressing hearts will be inspected for changes in activity and expression of downstream effectors of FAK. Our previous work reported a decrease in ERK activation in the absence of FAK protein following adrenergic stimulation [33]. Therefore, it will be interesting to determine whether, in the absence of other external stimuli, ERK activation is increased in hearts containing increased FAK activation. Work completed in this thesis showed that FAK is important in regulating the hypertrophic response following pathological stimuli. However, it is also known that FAK can activate proteins involved in the physiological hypertrophic pathway (Figure 3.1). Therefore, other downstream

effectors involved in both the pathological and physiological hypertrophic pathway will be examined for changes in activation and expression.

It is possible that the different levels of active FAK in these hearts is causing varying hypertrophic responses. The SF1 mice may require a longer exposure to FAK activity to result in the changes in gene expression noted in the SF2 mice. Further analyses including echocardiography and examination of changes in fetal gene changes in aged mice, histological inspection for increased fibrosis, increased cell size and disorganized myocytes will help to determine the timing and extent of pathological hypertrophy in these mice. In addition, further characterization of these lines will allow us to explore the possibility that moderate levels of FAK activity will lead to physiological hypertrophy while dramatically increased levels may result in a pathological hypertrophic response. The exploration of specific pathways involved in both physiological and pathological signaling and further genetic studies at later adult time points will help to elucidate the specific changes that are occurring.

In summary, our findings highlight an important role for FAK signaling in mediating cardiac hypertrophy. Our models which increase or decrease FAK activity in the myocardium demonstrated that FAK signaling is both necessary and sufficient to induce cardiac hypertrophy and may be a promising target for the treatment of heart disease**.**

Figure 3.1. Characterization of the MycFRNK Transgenic Mouse. ***a,*** Diagrammatic representation of the CX1^{frnk} transgene. ***b,*** Cultured cells were transfected with the CX1^{frnk} transgene and infected with an adenovirus driving expression of the Cre recombinase. Lysates taken before infection and 24, 48, 72, and 96 hours post-infection were processed by SDS-PAGE and probed with anti-FAK or anti-GFP antibodies. ***c,*** Immunoblots of tissue lysates from the CX1^{frnk} transgenic mice (tg) and wildtype mice (wt) were probed with anti-GFP, anti-Myc, and anti-ERK antibodies. ***d,*** Left ventricles from 2 month old CX1^{frnk} mice were processed for immunohistochemistry using anti-GFP antibodies.

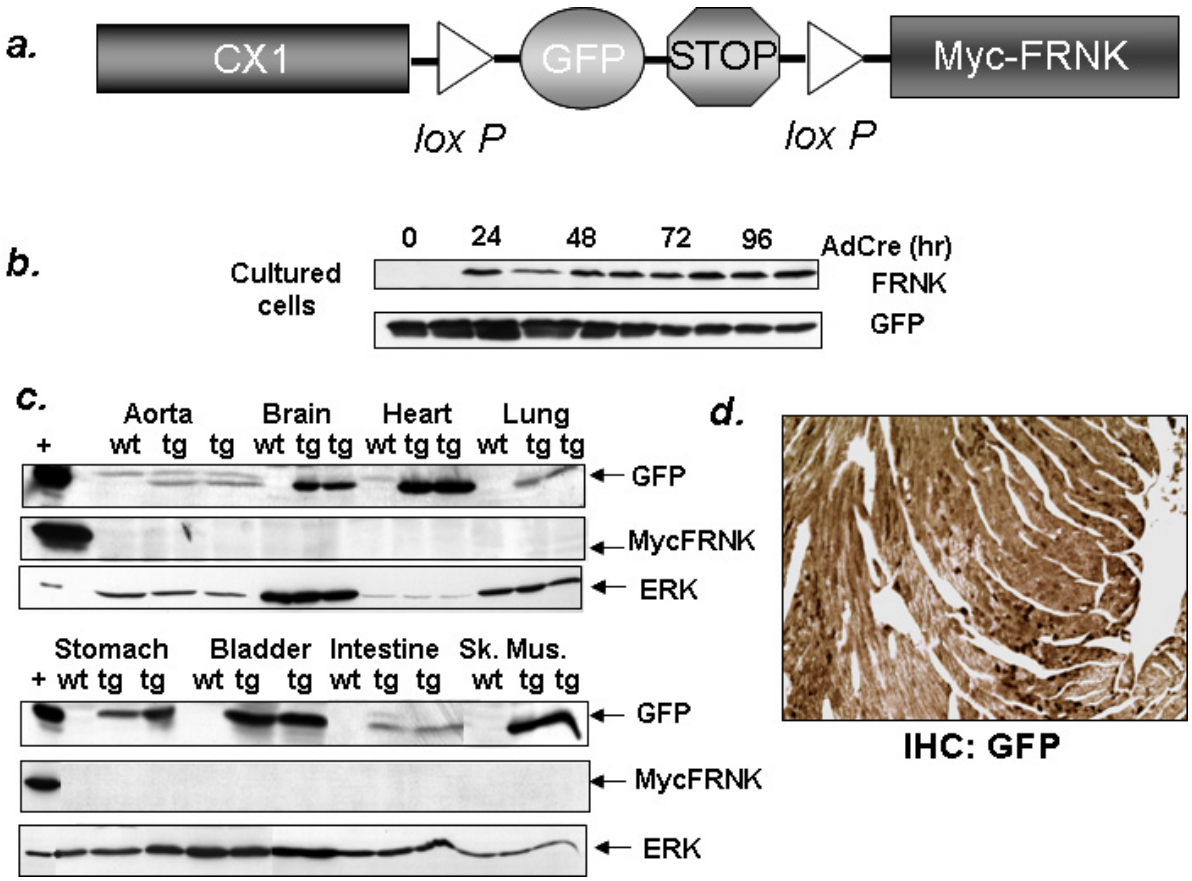
a.
CX1
GFP
STOP
Myc-FRNK
lox P
lox P
b.
0
24
48
72
96
AdCre (hr)
Cultured cells
FRNK
GFP
c.
Aorta
Brain
Heart
Lung
+
wt tg tg wt tg tg wt tg tg wt tg tg
GFP
MycFRNK
ERK
Stomach
Bladder
Intestine
Sk. Mus.
+ wt tg tg wt tg tg wt tg tg wt tg tg
GFP
MycFRNK
ERK
d.
IHC: GFP

Figure 3.2. Targeted Myocyte Specific Inhibition of Focal Adhesion Kinase. ***a,*** Illustrative representation of the $CX1^{frnk}$ and $Mlc2v^{cre}$ breeding strategy. ***b,*** Percentage of mice positive for both $CX1^{frnk}$ and $Mlc2v^{cre}$ at three weeks and one year postnatal. ***c,*** Ventricle lysate from control (C) and MycFRNK (F) mice were separated by SDS-PAGE and probed with anti-FAK antibody. ***d,*** Cardiac lysates taken from E14.5, E18.0, 1 day, 3 month, 6 month and 9 month $CX1^{frnk}Mlc2v^{cre}$ mice were separated by SDS-PAGE and probed with anti-FAK antibody to visualize MycFRNK. MycFRNK transfected Cos cell lysate shown as positive control. ***e,*** Western blot analysis of MycFRNK levels in heart, skeletal muscle, and stomach from control (C) and MycFRNK (F) expressing mice. ***f,*** Immunoblots of control (C) and MycFRNK (F) heart lysate were probed with anti-FAK and anti-phosphotyrosine 397 antibodies.

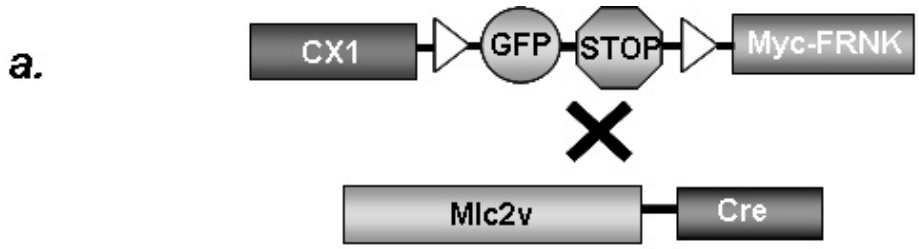

b.

	3wks	1yr
CX1 ^{frnk} Mlc2v ^{cre}	27%	27%

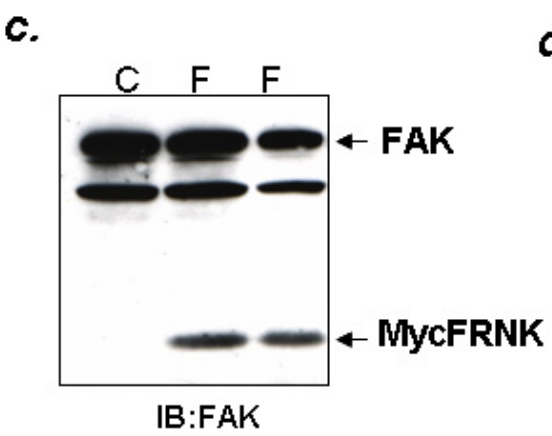

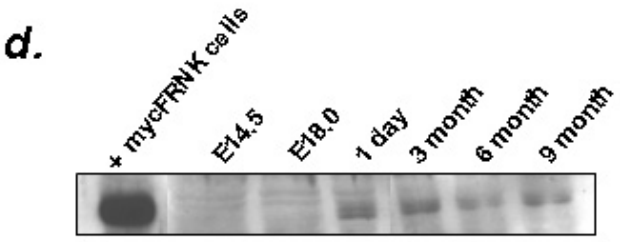

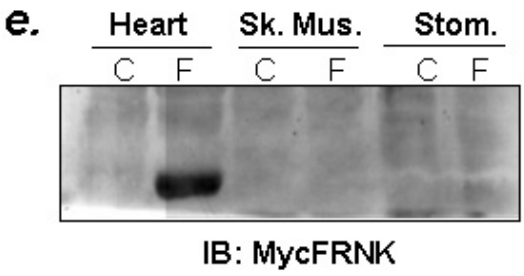

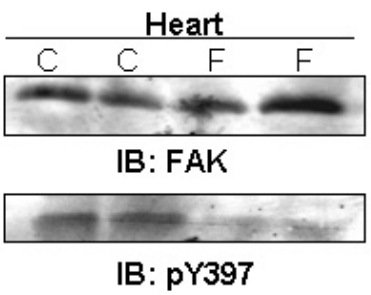

Figure 3.3. Inhibition of FAK in the Postnatal Heart Does Not Alter Anabolic Growth. ***a,*** Left ventricles from two month old CX1^{frnk}Mlc2v^{cre} and CX1^{frnk}Mlc2v$^{wt/wt}$ mice were processed for histology and stained with Masson's Trichrome to reveal myocyte organization and levels of fibrosis (blue). ***b,*** Sections of left ventricles from two month old CX1^{frnk}Mlc2v^{cre} and CX1^{frnk}Mlc2v$^{wt/wt}$ mice were stained with an anti-cardiac troponin T antibody to reveal myofibrillar organization. ***c,*** Cross sectional cardiomyocyte area from two month old control and CX1^{frnk}Mlc2v^{cre} (FRNK) myocytes (n=at least 300 cells per condition).

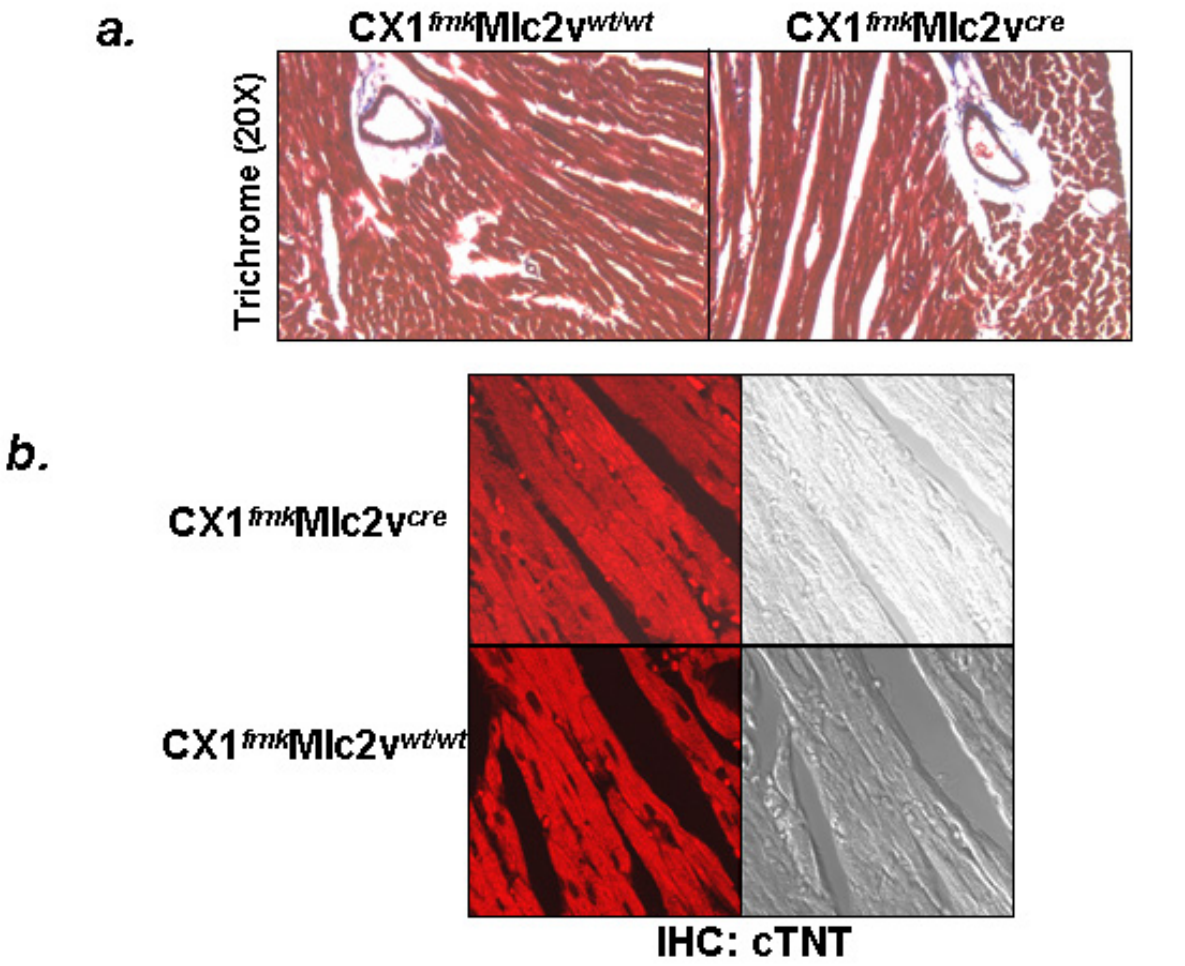
a.
CX1fnkMlc2vwt/wt
CX1fnkMlc2vcre
Trichrome (20X)
b.
CX1fnkMlc2vcre
CX1fnkMlc2vwt/wt
IHC: cTNT
c.
Cardiomyocyte area square pixels
0.15
0.1
0.05
0
Control
FRNK

Table 3.1. Baseline Echocardiography in CX1^{frnk}Mlc2v^{cre} and Control mice

	Control	FRNK
LVEDD(mm)	2.77 ± 0.11	2.82 ± 0.13
LVESD (mm)	1.45 ± 0.14	1.60 ± 0.16
LVPWTd (mm)	0.90 ± 0.05	0.91 ± 0.08
LVPWTs(mm)	1.36 ± 0.09	1.25 ±0.12
IVSd (mm)	1.00 ± 0.04	1.01 ± 0.05
IVSs(mm)	1.48 ± 0.05	1.45 ± 0.06
%FS	50.00 ± 3.06	45.48 ± 3.69
%EF	79.9 ± 3.3	75.2 ± 3.5
HR	515.02 ± 14.65	538.76 ± 18.03

%FS, percent fractional shortening; HR, heart rate; d, diastole; s, systole. Baseline control n=26, Baseline FRNK n=19.

Figure 3.4. Cardiac Expression of MycFRNK Attenuates the Hypertrophic Response Following Aortic Banding. ***a****,* Heart weight versus body weight ratios at baseline and following 14d of aortic constriction in control, CX1^{frnk}Mlc2v$^{wt/wt}$ (n=5) and FRNK, CX1^{frnk}Mlc2v^{cre} mice (n=6) hearts. ***b*****,** Percent change in cardiac dimensions following 14 days of aortic constriction in control, CX1^{frnk}Mlc2v$^{wt/wt}$ and FRNK, CX1^{frnk}Mlc2v^{cre} mice (n= at least 8 mice). *, $p<0.05$ compared to baseline. ***c*****,** Cardiomyocyte cell area following 8 weeks of aortic constriction. *, $p<0.05$.

a.

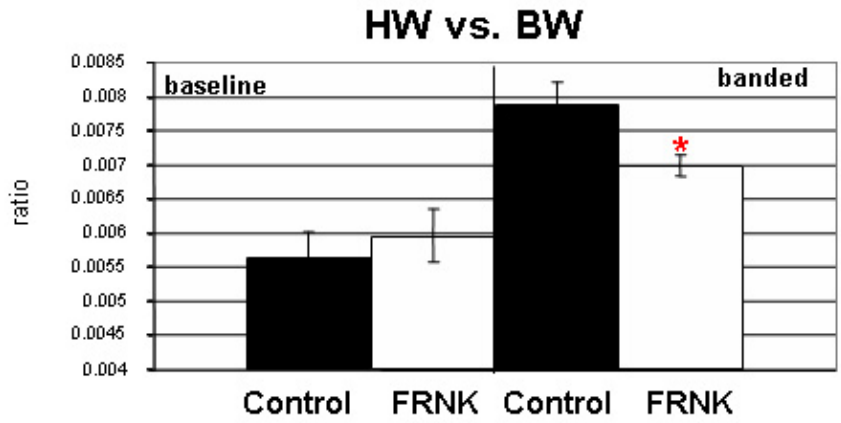
HW vs. BW
baseline
banded
ratio
0.0085
0.008
0.0075
0.007
0.0065
0.006
0.0055
0.005
0.0045
0.004
Control
FRNK
Control
FRNK

b.

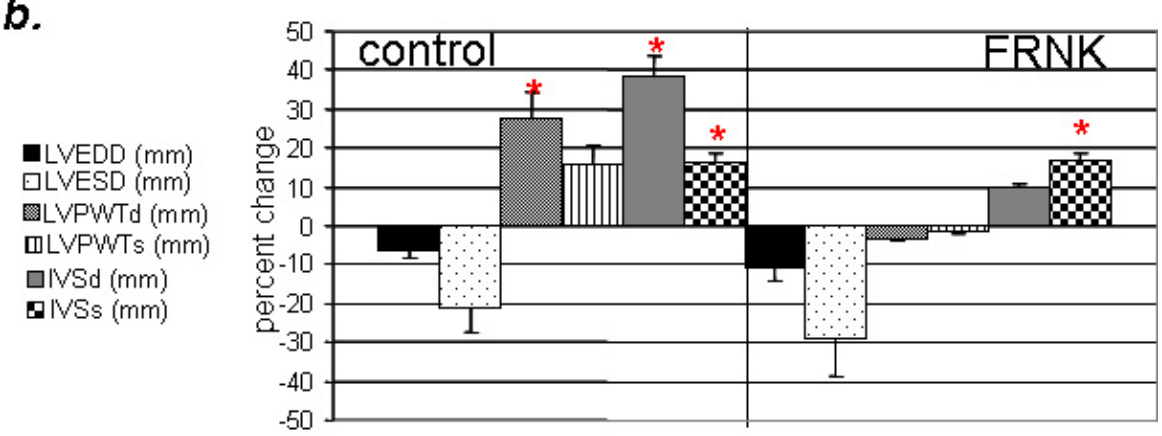
control
FRNK
percent change
50
40
30
20
10
0
-10
-20
-30
-40
-50
LVEDD (mm)
LVESD (mm)
LVPWTd (mm)
LVPWTs (mm)
IVSd (mm)
IVSs (mm)

c.

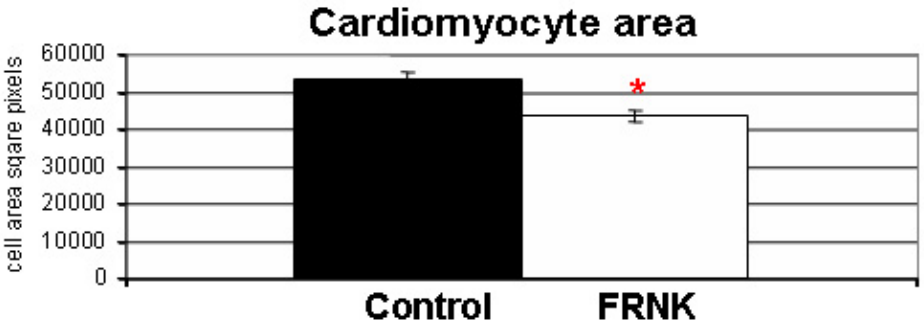
Cardiomyocyte area
cell area sqare pixels
60000
50000
40000
30000
20000
10000
0
Control
FRNK

Figure 3.5. Construction of SuperFAK. ***a,*** A diagrammatic image of FAK showing the activation loop of the kinase domain. To create SuperFAK, two lysines (K578, K581) were substituted with glutamic acids (E). Figure modified from [176]. ***b,*** Cultured cell lysate from cells transfected with flag-FAK or flag-SuperFAK and control non-transfected cells (NT) were processed for Western blot analysis and probed with anti-FAK, anti-flag, and anti-phospho-397 antibodies.

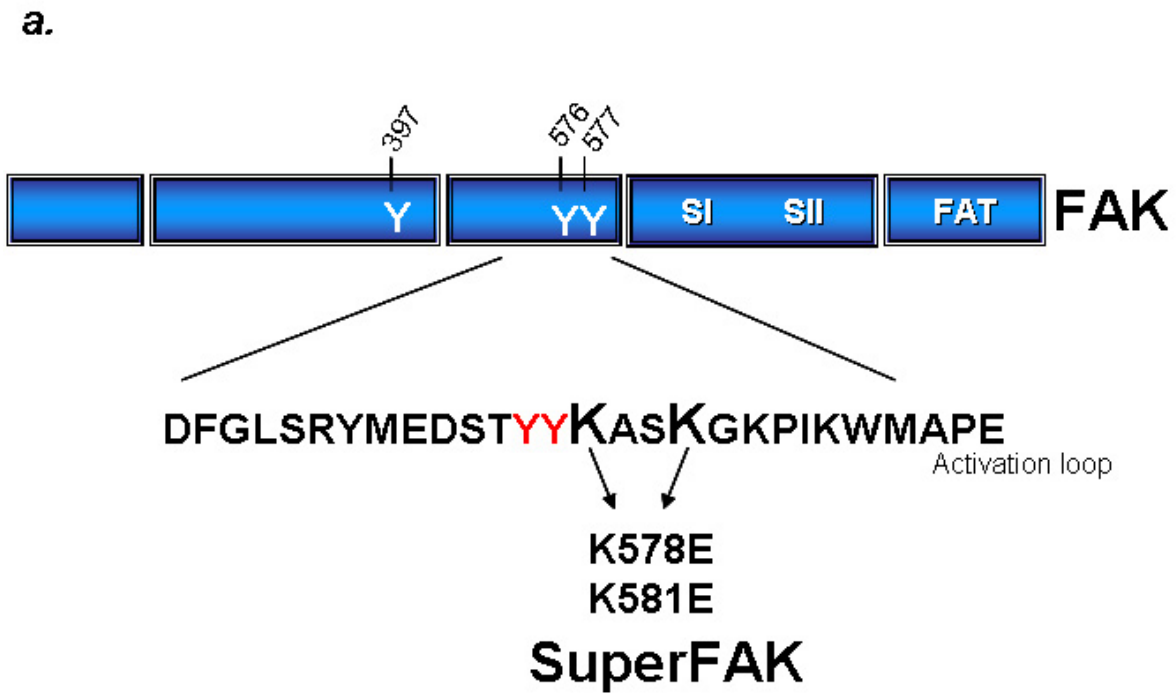
a.
397
576
577
Y
YY
SI
SII
FAT
FAK
DFGLSRYMEDSTYYKASKGKPIKWMAPE
Activation loop
K578E
K581E
SuperFAK

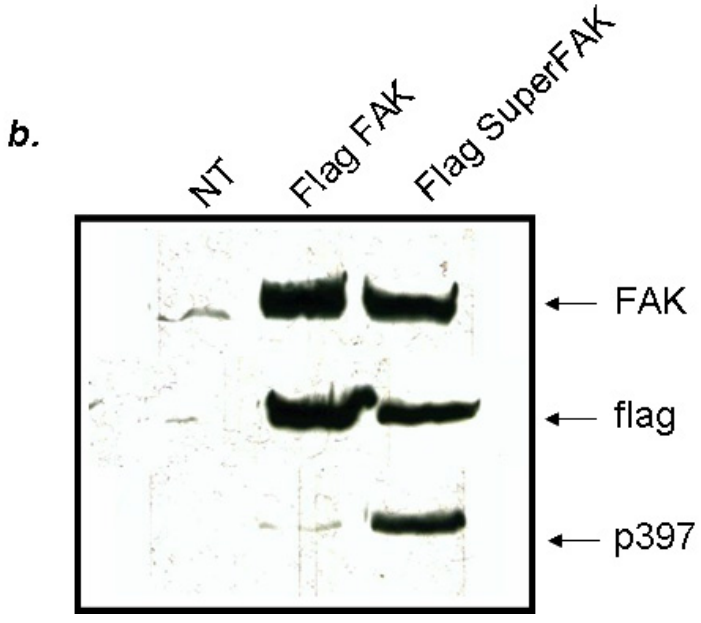
b.
NT
Flag FAK
Flag SuperFAK
FAK
flag
p397

Figure 3.6. Identification of the Two SuperFAK Transgenic Mouse Lines. *a*, Illustration of the βMHC-flag-SuperFAK transgenie. ***b,*** Cardiac lysate from four week old SuperFAK 1 (SF1) and four week old SuperFAK 2 (SF2) mice were analyzed by Western blot and probed with antibodies for anti-phospho-397 and anti-cortactin. Levels of phopho-397 were compared to littermate controls (C) for each line.


βMHC
flag
SuperFAK

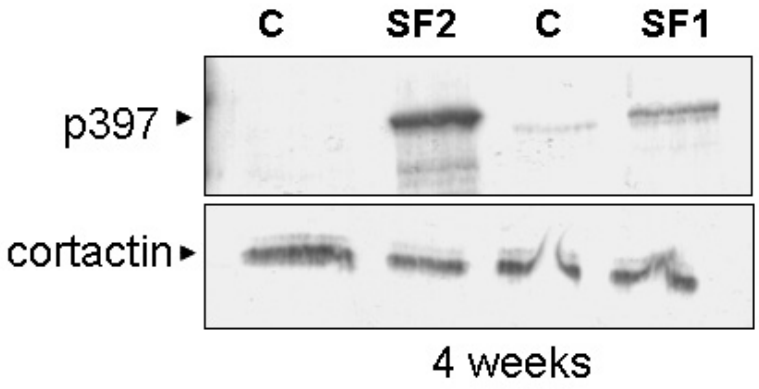
C
SF2
C
SF1
p397
cortactin
4 weeks

Figure 3.7. Characterization of the SuperFAK Mouse. ***a,*** Cardiac lysate from four and ten week old littermate control (C) and SuperFAK 2 (SF) mice were separated via SDS-PAGE and probed with anti-phospho-397, anti-flag, and anti-ERK antibodies. ***b,*** Tissue lysates from SuperFAK 2 (SF) heart, skeletal, stomach, and aorta were analyzed by Western analysis using anti-flag and anti-ERK antibodies.

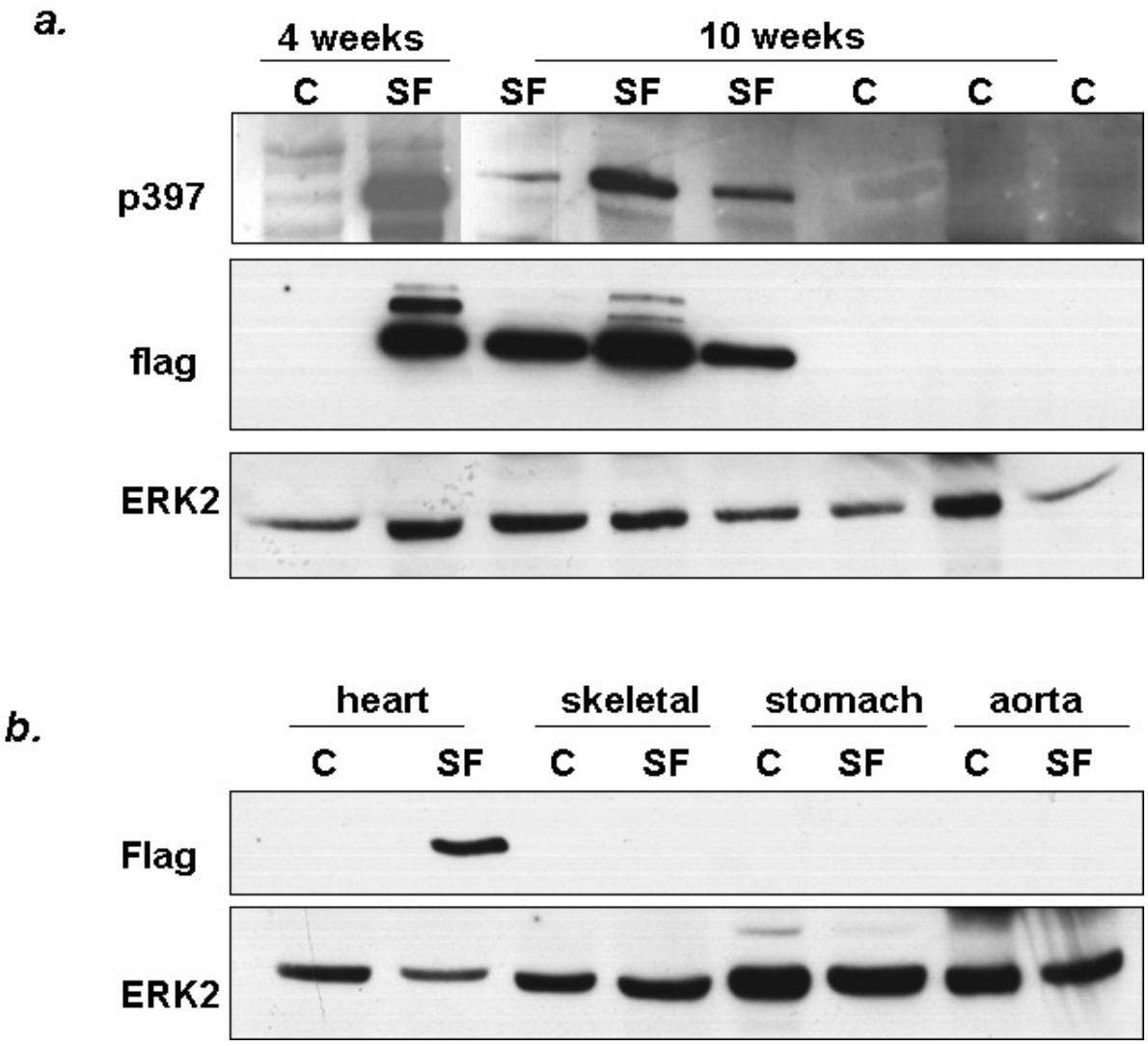
a.
4 weeks
10 weeks
C
SF
SF
SF
SF
C
C
C
p397
flag
ERK2
b.
heart
skeletal
stomach
aorta
C
SF
C
SF
C
SF
C
SF
Flag
ERK2

Figure 3.8. Histological Analysis of SuperFAK Hearts. ***a***. Ventricles from ten week old control and SuperFAK 2 (SF2) hearts were processed for histology and stained with Masson's Trichrome to determine myofibrillar organization and collagen deposition (blue, visible at higher magnification. Top panel=1x, bottom panel=20x). Black arrows indicate areas of significant fibrosis. ***b.*** Quantification of fibrosis in SuperFAK 2 (SF2) hearts. Cross sections of Trichrome stained hearts were quantitated as follows: 0 = no presence of fibrosis, 1 = 0-15% of vessels contained peri-vascular fibrosis, 2 = 15-30% of vessels contained peri-vascular fibrosis, 3 = 30-45% of vessels contained peri-vascular fibrosis. Values of vascular fibrosis were added to score for interstitial fibrosis: 1 = presence of interstitial fibrosis, 2 = increased interstitial fibrosis, 3 = very significant amount of interstitial fibrosis.

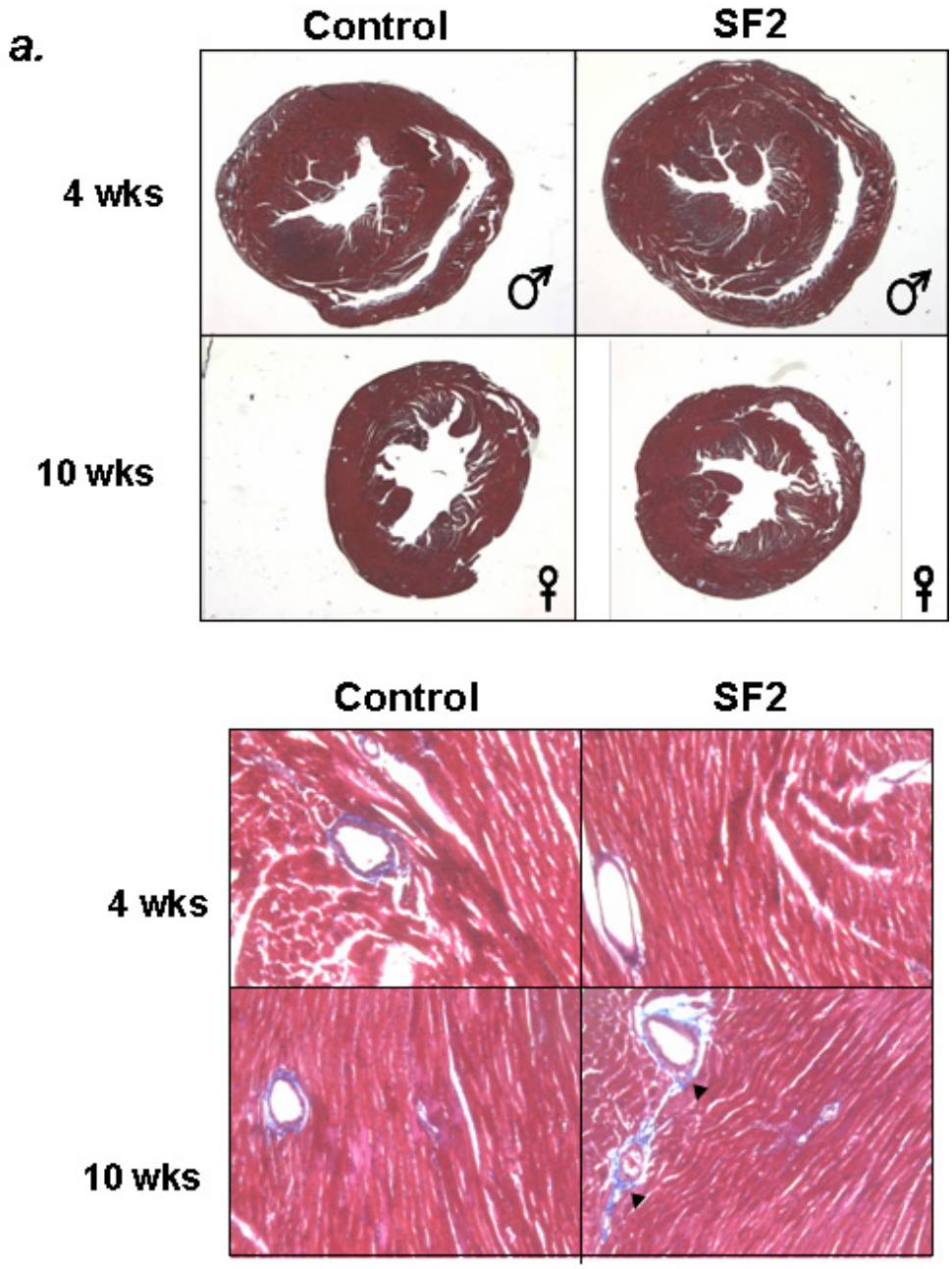
a.
Control
SF2
4 wks
10 wks
♂
♀
Control
SF2
4 wks
10 wks
b.
degree of fibrosis
4.5
4
3.5
3
2.5
2
1.5
1
0.5
0
Control
SF2

Figure 3.9. Increased FAK Activity Results in increased Cardiomyocyte Cell Area. Ventricles from control and SuperFAK 2 (SF2) hearts were processed for histology and stained with lectin (bottom panel). Cross-sectional area of control and SuperFAK 2 myocytes were analyzed (n=at least 300 cells per condition). *$p<0.05$ for indicated comparison.

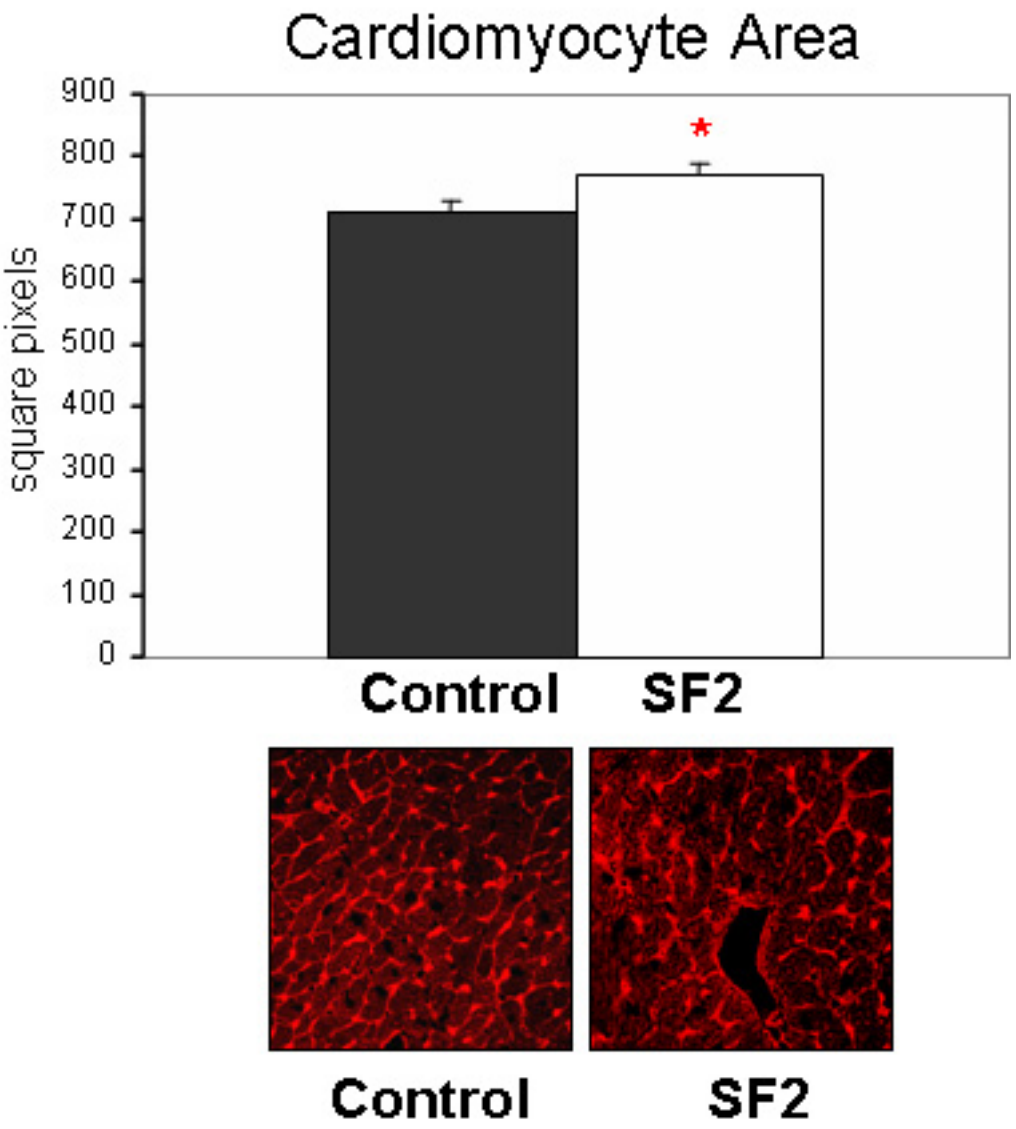
Cardiomyocyte Area
square pixels
900
800
700
600
500
400
300
200
100
0
*
Control
SF2
Control
SF2

Figure 3.10. FAK Activity Modulates Hypertrophic Gene Expression. Quantitative RT-PCR analysis for ANF, βMHC, and αMHC RNA levels in control and SuperFAK 2 (SF) hearts. Data was normalized to 18s RNA and presented as fold over values from control mice (n=3 per condition). *p<0.05 versus control.

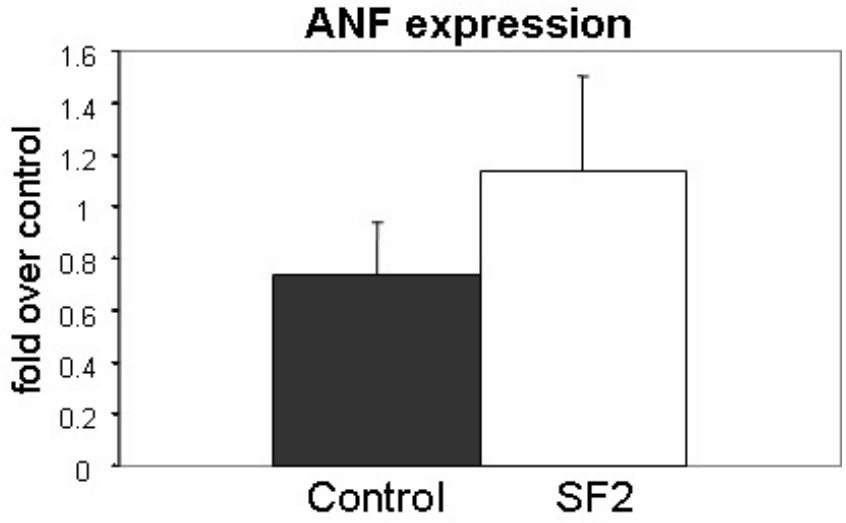
ANF expression
fold over control
1.6
1.4
1.2
1
0.8
0.6
0.4
0.2
0
Control
SF2

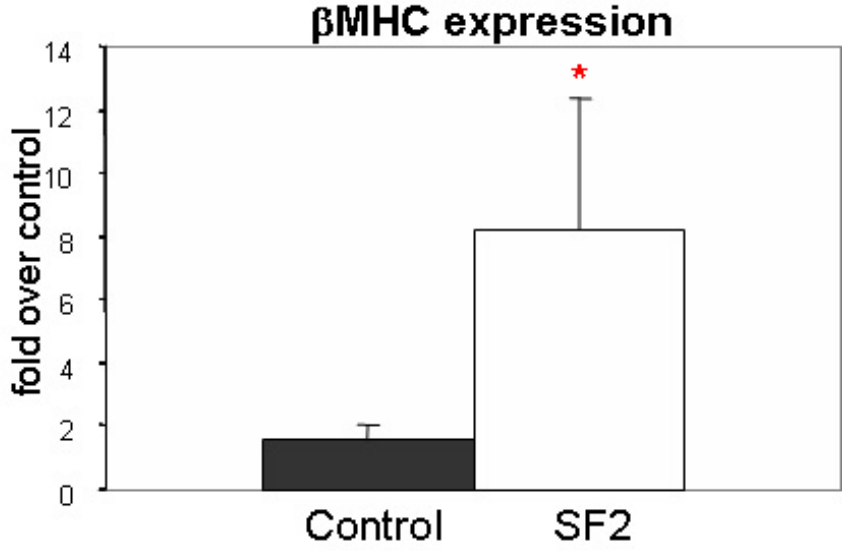
βMHC expression
fold over control
14
12
10
8
6
4
2
0
*
Control
SF2

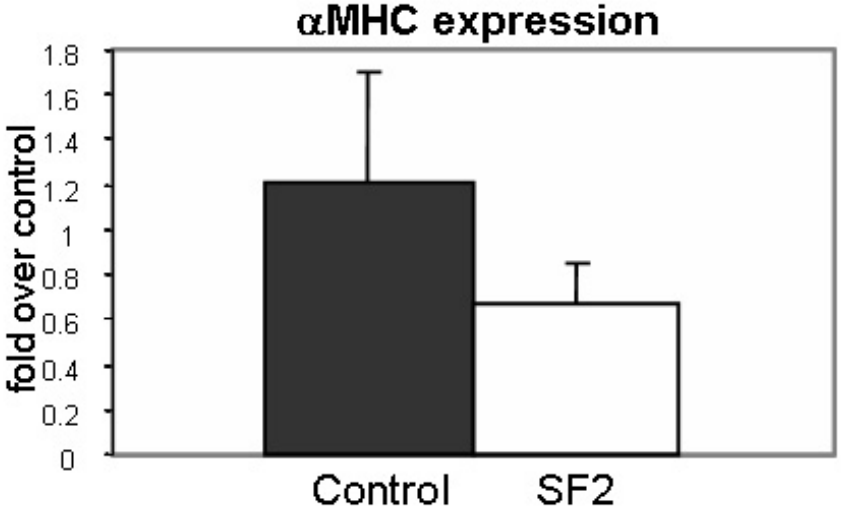
αMHC expression
fold over control
1.8
1.6
1.4
1.2
1
0.8
0.6
0.4
0.2
0
Control
SF2

Figure 3.11. Prolonged Exposure to SuperFAK Increases Cardiac Size and Function. ***a,*** Left ventricular posterior wall (LVPW) thickness in diastole (top) and systole (bottom) taken from ten, and 16 week old Control and SuperFAK 1 (SF) mice. ***b,*** Representative echocardiography from Control and SuperFAK 1 (SF1) mice at 10 and 16 weeks postnatal. ***c,*** Gender matched control and SuperFAK 1 (SF1) left ventricular measurements taken from echocardiography at ten and 16 weeks postnatal. ***d,*** Percent fractional shortening (%FS) and percent ejection fraction (%EF) from 16 week old SuperFAK 1 (SF1) mice. *,$p<0.05$ compared to control at indicated time points.

a.

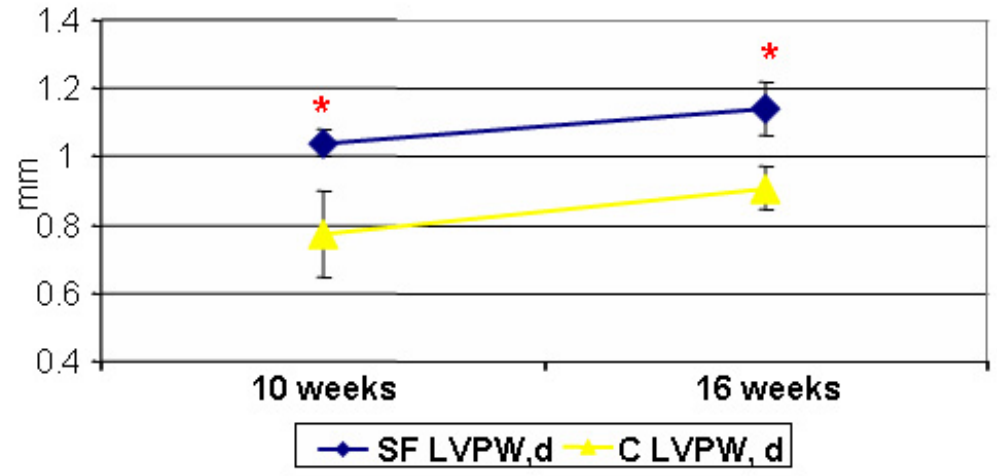
1.4
1.2
1
0.8
0.6
0.4
mm
*
*
10 weeks
16 weeks
SF LVPW,d
C LVPW, d

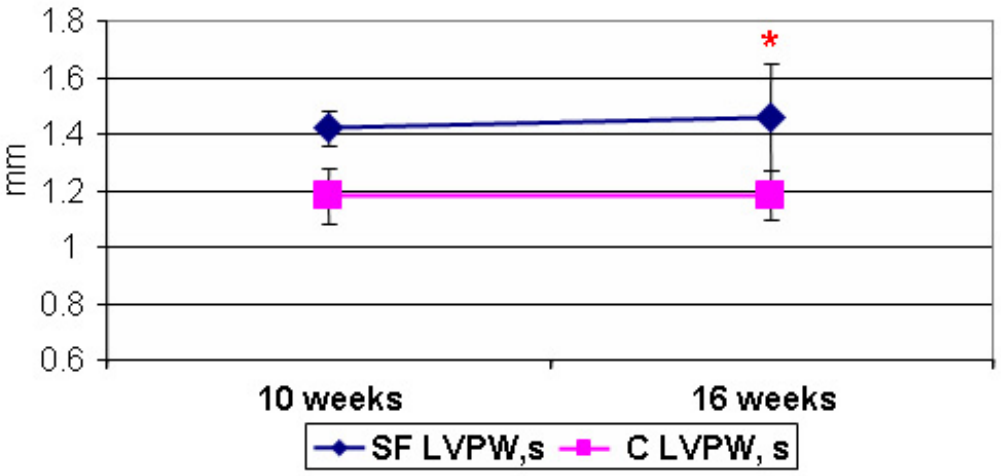
1.8
1.6
1.4
1.2
1
0.8
0.6
mm
*
10 weeks
16 weeks
SF LVPW,s
C LVPW, s

b.

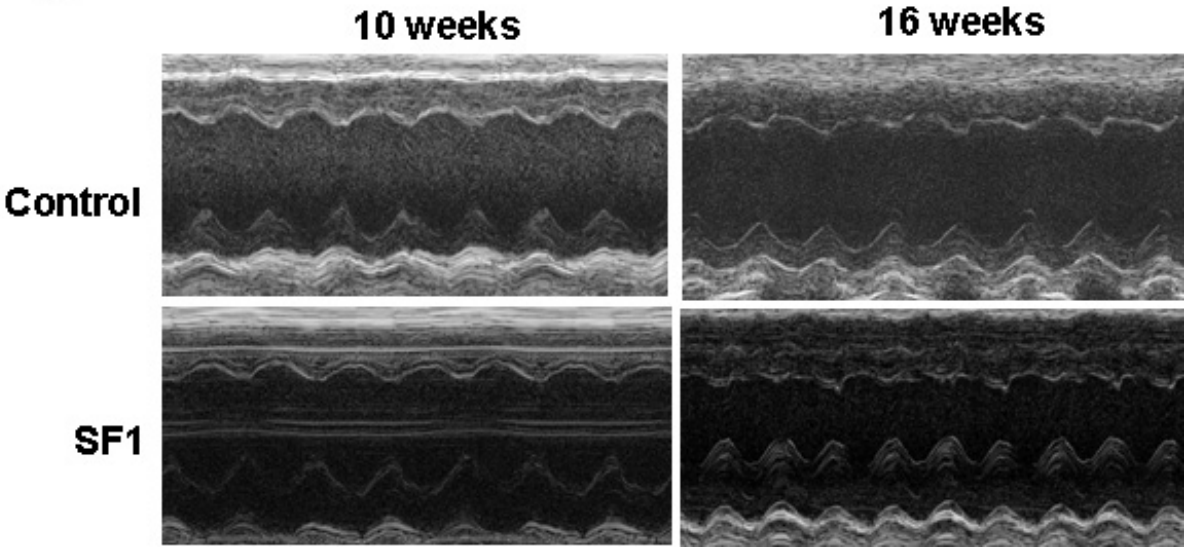
10 weeks
16 weeks
Control
SF1

c.

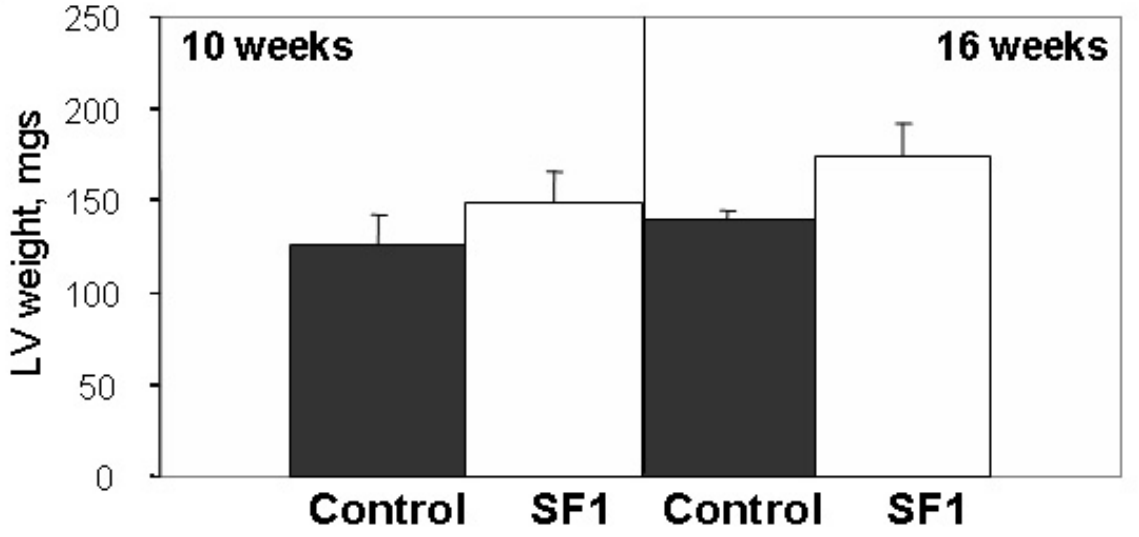
10 weeks
16 weeks
LV weight, mgs
250
200
150
100
50
0
Control
SF1
Control
SF1

d.

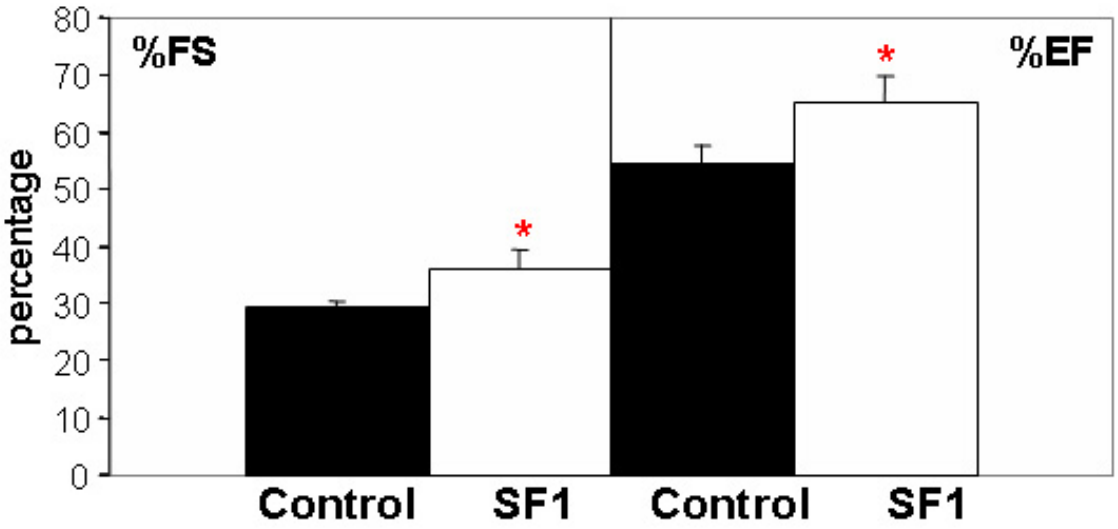
%FS
%EF
percentage
80
70
60
50
40
30
20
10
0
*
*
Control
SF1
Control
SF1

CHAPTER IV

FAK ACTIVITY IS REQUIRED FOR PROPER CARDIAC DEVELOPMENT

A. Introduction

Recent genetic evidence indicates that the integrin class of fibronectin (FN)-binding adhesion receptors ($\alpha_5\beta_1$ and others) can regulate the form and function of the heart [60, 134, 139, 183-185]. Integrin ligation drives recruitment of a number of structural and signaling molecules to the ventral plasma membrane. This complex is collectively termed a focal adhesion. These focal adhesions link the force-generating actin cytoskeleton inside the cell to the extracellular matrix (ECM), and coordinate activation of downstream signaling pathways [3]. The non-receptor tyrosine kinase, Focal Adhesion Kinase (FAK), is strongly activated by both integrins and growth factors, and is a likely candidate to mediate downstream signals from these diverse pathways during cardiac growth and development [136]. Germline deletion of FAK results in mesodermal defects and embryonic lethality between E8.5-10 similar to the phenotype observed in both FN-null, and α5-null mice, supporting an important role for FAK in mediating integrin dependent processes during development [27, 139]. In addition, FAK is predominantly expressed in the mesoderm of wildtype embryos at embryonic day 8.5 [26]. Indeed, hearts from FAK-null embryos revealed a lack of separate mesocardial and endocardial layers, suggesting that FAK may play a role in cardiac morphogenesis [26].

The heart forms from two separate progenitor cell populations or heart fields referred to as the primary and secondary heart fields. These fields divide from a common progenitor at gastrulation [45-47]. The primary heart field arises from the anterior splanchnic mesoderm and is responsible for the formation of the cardiac crescent and ultimately the left ventricle and atria [48]. The secondary heart field originates from the pharyngeal mesoderm and contributes to the right ventricle and outflow tract [45, 46, 49]. The primary heart field is distinguished by expression of specific transcription factors Tbx5, bhHLH and Hand2 whereas the secondary heart field is mediated by the transcription factor Isl1 and Fgf10 [45, 46]. The homeobox gene Nxk2.5 is expressed in both heart fields [50].

The heart is the first organ to form and is crucial for embryonic viability. A significant number of fetal and childhood mortalities can arise from defects in the carefully orchestrated steps that govern cardiac development can contribute significantly to fetal and childhood mortality [40]. Cardiac organogenesis is initiated by the formation of the cardiac crescent by cardiac precursors. Following crescent formation, a linear heart tube is formed. The heart tube undergoes a rightward looping, giving rise to the ventricular and atrial chambers, thus forming a four chambered heart.

Genetic studies in drosophila, zebrafish, xenopus, and mice have been critical for the understanding of the specific factors required for vertebrate heart development [186]. For example, GATA mediates heart tube formation, NF-ATc and Smad6 direct the formation of valves, and ErbB2, ErbB4, and neuregulin are required for the growth and maturation of cardiomyocytes [58, 59, 187, 188] .

Although a basic genetic blueprint of transcription factors for cardiac development is known, questions still remain regarding the signaling pathways mediating cardiogenesis. Based on past studies involving FAK binding partners and upstream activators in cardiac development, we reasoned that FAK signaling is likely an important step in the intricate morphogenesis process.

In order to study a role for FAK in the developing myocardium, we generated a transgenic mouse model which enables tissue-specific expression of a dominant interfering mutant for FAK termed Focal Adhesion Related Non-Kinase (FRNK), In this model, MycFRNK is expressed downstream of a region of the β-actin promoter that drives high levels of expression in all tissues and induces conditional expression of MycFRNK in the presence of a tissue specific Cre recombinase. Previous *in vitro* experiments demonstrated the effective inhibition of FAK activity with FRNK in isolated cardiomyocytes [37]. Therefore, we rationalized that FAK activity is necessary for cardiac morphogenesis and used FRNK *in vivo* to elucidate a role for FAK activity in the developing myocardium. To target development, we used the Nxk2.5-Cre knock-in mouse line which facilitates robust expression of Cre recombinase as early as E7.5 [189]. The recent use of the Nxk2.5-Cre mouse line with the floxed FAK mouse revealed peri-natal lethality due to malformations in the outflow tract, a sub-aortic ventricular septal defect with overriding aorta or double outlet right ventricle. The malformations in the Nkx2.5-Cre driven FAK knockout mouse were due to an impaired cardiomyocyte migration [32]. In addition, significant protein depletion was not observed in the FAK knockout model until E13.5, days after the heart has completed formation. Unlike this FAK knockout

model, the MycFRNK transgenic mouse enables more precise control of protein expression since the expression of a protein will occur days before homozygous gene inactivation and subsequent protein degradation present in a floxed loxP/Cre model [32]. Of interest, this model will allow us to note the potential differences in decreased FAK activity in these mice compared to previously published deletion of FAK protein and enable us to examine the role of FAK as a kinase and as a molecular scaffold [32]. We found that decreased FAK activity during cardiac development results in embryonic lethality between E14-E15 due to a significant cardiomyocyte proliferation defect. Hearts with Nkx2.5 driven expression of MycFRNK resulted in a significant reduction in heart size, and cardiomyocyte proliferation accompanied by a ventricular septation defect.

B. Material and Methods

Generation of MycFRNK Mice. A 1.4kb fragment of MycFRNK was amplified out of the pRK5mycFRNK vector to incorporate 3' and 5' Not1 sites with an internal Kpn site[38]. This fragment was then ligated into a vector containing a cassette in which a piece of the βactin promoter is fused to cDNA containing GFP flanked by loxP sites. Ultimately, the CX1-MycFRNK fragment was cut out using Kpn, linearized, and submitted for pronuclear microinjection into 0.5 day fertilized embryos at the UNC Animal Models Core Transgenic Facility which was preformed within the University of North Carolina at Chapel Hill. DNA isolated from tail snips or tissues was subjected to PCR analysis using primers specific for the MycFRNK transgene (5'-CGCGGTACCATCCAGACATGATAAGATACATTGATGAG-3' and 5'-CGCCTCGAGGCTGCCACCATGGAGCAGAAGCTGATC-3'). Dr. Robert Schwartz (Institute of Biotechnology, Houston) provided the *Nkx2.5*^{Cre} knock-in mice [29, 189]. Both lines of mice were backcrossed to the C57black6 background at least 6 generations prior to subsequent breeding. DNA isolated from tail snips or tissues was subjected to PCR analysis using primers specific for Cre (5-ACCCTGACCCAGCCAAAGAC-3' and 5'-CTAGAGCCTGTTTTGCACGTTC-3'). Mice were housed in an AALAC accredited University Animal Care Facility.

Generation of the SuperFAK Mice. A 3.2 kb Not1 fragment comprising the modified βMHC promoter was amplified from a vector and ligated into a pBKS plasmid [32]. SuperFAK was amplified from a pBKS plasmid and cloned into a flag vector with BamHI and XhoI sites using standard procedure [176]. FlagSuperFAK was subsequently cut from the flag vector using NotI and SpeI to place it

downstream of the βMHC promoter in the pBKS plasmid. Pronuclear microinjection of the linearized βMHCflagSuperFAK plasmid into 0.5 day fertilized embryos was performed at the UNC Animal Models Core Transgenic Facility at the University of North Carolina at Chapel Hill. Transgene expression in C57/Bl6 X C3H hybrid strain founders and F1 progeny mice were confirmed by PCR analysis using primers specific for the SuperFAK transgene (5'-CCGGCATGGAGATGCTACTG-3', and 5'-GCGGCCGCAAGCTGCCACCATGGACTACAAGG-3'). Six founder mice tested positive for the βMHCflagSuperFAK transgene. However, of these six, two expressed the flag-SuperFAK protein in the heart. These lines were breed with black6 mice and F1 progeny characterized. All transgenic mouse procedures were performed in accordance with the guidelines set forth by the Institutional Animal Care and Use Committee (IACUC).

Western Blotting. Tissues were lysed in modified radioimmune precipitation assay buffer (50 mM Hepes, 0.15 M NaCl, 2 mM EDTA, 0.1% Nonidet -40, 0.05% sodium deoxycholate, pH7.2) containing 1 mM 4-(2-amnionethyl)benzenesulfonyl fluoride hydroxychloride, 0.02 mg/ml aprotonin containing 5% Triton-X. Proteins were boiled in a sample buffer and resolved using SDS-PAGE and transferred to nitrocellulose. Western blots were performed using a 1:1000 dilution of the appropriate primary antibody. Blots were washed in Tris-buffered saline, pH 7.4 plus 0.05% Triton-X, followed by incubation with either horseradish peroxidase-conjugated protein A-Sepharose (Amersham Bioscience) or horseradish peroxidase-conjugated rabbit anti-mouse antibody (Amersham Biosciences) at a 1:2000 dilution. Blots were

visualized after incubation with chemiluminescence reagents (ECL, Amersham Biosciences). [155].

Histological Analysis and Immunohistochemistry. Paraffin-embedded hearts were sectioned into 8 μm slices and stained with hematoxylin and eosin (Sigma-Aldrich) to assess overall morphology. Cell area measurements were conducted on TRITC-Lectin (Sigma-Aldrich) stained cross sections of the compact zone of the heart muscle using Image J software (NIH).

Antibodies and Reagents. The FAK, ERK2 (1B3B9) and cortactin (4F11) antibodies were purchased from Upstate Biotechnology, Inc. The caspase-3 antibody was purchased from Cell Signaling. The phosphospecific Pky2 antibody was purchased from BioSource International and total Pyk2 antibody was purchased from BD transduction laboratories. Unless specified, antibodies were used at a 1:1000 dilution.

Quantitative RT-PCR. Hearts were harvested from E13.5 embryos, pooled in groups of 3 based on genotype, homogenized, and RNA was extracted using Trizol reagent (Invitrogen). Each sample of RNA was diluted to 50 ng/μl in DEPC treated H_20. Each 30 μl RNA reaction mixture contained 0.5 μl of 0.1 μg/μl of primer, 1 μl of 20 μmol of probe, 15μl of AB Gene one step master mix, and 0.1μl of RT enzyme. The primers and probes used were as follows: βactin forward CTGCCTGACGGCCAAGTC, βactin reverse CAAGAAGGAAGGCTGGAAAAGA, βactin probe FAM-CACTATTGGCAACGAGCGGTTCCG-TAMARA. c-Fos forward CAGTCAGAGAAGGCAAGGCA, c-fos reverse TCCTCTCTGTAATGCACCAG, c-Fos probe FAM-CATCCAGACGTGCCACTGCCCGA-TAMARA. The real time-RT-

PCR was performed using the ABI prism 7500 Sequence Detection System (PE Applied Biosystems) in 96-well plates under the following conditions: 30 minutes at 48 ˚C, 10 minutes at 95 ˚C, 40 cycles of 95 ˚C for 15 seconds, then 60 ˚C for one min.

For semi-quantitative RT-PCR analysis, each 20μl reaction contained 250ng of cardiac RNA from end stage mice, 4μl reaction mix and 1μl reverse transcriptase using the iScript cDNA synthesis kit (BioRad). Each reaction was performed under the following conditions: 5 minutes at 25 ºC, 30 minutes at 42 ºC, then 5 minutes at 85 ºC. Each 50 μl PCR reaction mixture contained 2.5 μl of 10μM of primer, 4μl of dNTP mixture, 5μl of reaction buffer and 0.5 μl of TaKaRa Ex Taq enzyme. The reaction was performed under the following conditions: 5 minutes at 94 ºC, 29 cycles of one minute at 94 ºC, one minute at 61 ºC, 2 minutes at 72 ºC, and a final extension of 10 minutes at 72 ºC. The primers used were as follows: Bax forward GCGTCCACCAAGAAGCTGAG, Bax reverse ACCACC CTGGTCTTGGATCC, Bcl-2 forward TGTGGCCTTCTTTGAGTTCG, Bcl-2 reverse TCACTTGTGGCCCAGGTATG.

Apoptosis and Cell Proliferation Assays. Apoptosis was assessed on paraffin-embedded tissue sections using a DNA fragmentation detection kit, FragEL™ DNA (Calbiochem) according to the manufacturer's protocol. Cardiac cell proliferation was determined by BrdU labeling which was achieved by administering 100 mg/Kg of BrdU (Sigma) to pregnant mice intraperitoneally. Embryos were harvested 3-4 hours later, fixed, and embedded in paraffin. BrdU incorporation was detected by immunohistochemistry using a commercially available kit (Zymed). Apoptosis and

cell proliferation were quantified by scoring the number of FragEL- and BrdU-positive nuclei in the muscular IVS per unit area using NIH Image J software.

Statistics. Data are presented as mean ± SEM. Means were compared by 2-tailed Student's *t* test. $p<0.05$ was considered statistically significant.

C. Results

FRNK Protein is Not Detectible in the Developing or Postnatal Heart

Previous studies suggest that FAK was highly expressed in mesodermal tissues throughout embryonic development. Therefore, we examined FAK expression in the heart and found that high levels of FAK were observed from E10.5 to postnatal day 7. These time points correlate with the window of cardiomyocyte proliferation. We also examined whether FRNK might be expressed since several smooth muscle specific genes are transiently expressed in the embryonic heart. Detection of FAK and FRNK from aortic SMC lysate and various heart lysate was examined using a C-terminal anti-FAK antibody that recognizes both proteins. Although FAK is expressed in high levels during development and in lower levels in the adult heart, FRNK is undetectable at all stages of heart development and limited to the SMC lysate (Figure 4.1).

Nkx2.5 Targeted Expression of FRNK

Since FRNK is not expressed in the heart, we utilized our CX1^{frnk} transgenic mouse line in combination with the Nkx2.5-Cre knock-in mouse line to study the effect of FAK activity in early stages of heart development (Figure 4.2a). The CX1^{frnk} mouse was created following successful inhibition of FAK activity with FRNK *in vitro* [38]. The CX1^{frnk} mouse was designed such that the MycFRNK gene is driven by a region of the β-actin promoter that induces high expression in all tissues. However, a GFP reporter followed by a transcriptional stop site has been inserted upstream of the transgene, thus preventing expression of MycFRNK. Importantly, the GFP-stop codon region is flanked as a unit by loxP sites, which direct Cre recombinase-

mediated excision (Figure 4.2a). Thus, the CX1-stop-MycFRNK-transgenic mice can be crossed with a second line of mice that express the Cre recombinase under the control of a cell or tissue specific promoter to render specific MycFRNK expression and subsequent decreased FAK activity. A detailed characterization of the CX1^{frnk} transgenic mouse can be found in Chapter III. In this study, we crossed the CX1^{frnk} with the Nxk2.5-Cre promoter since this is a robust promoter that turns on around mid-gestation (E7.5) and has a fairly broad expression pattern. Unlike the Mlc2v-Cre mouse utilized in Chapter II and III, the Nkx2.5-cre recombination is induced in the primary and secondary heart fields and in the epithelium and endothelium of the first pharyngeal arch [189].

Histological and Morphological Analysis of CX1^{frnk}Nkx2.5^{cre} Mice

Viable offspring expressing both the CX1^{frnk} and Nkx2.5^{cre} transgenes were not detected and subsequent studies revealed that CX1^{frnk}Nkx2.5^{cre} mice died between embryonic day 14.5 and 15.5 (Figure 4.2b). By embryonic day E14.5, CX1^{frnk}Nkx2.5^{cre} embryos showed a significant increase in overall edema, potentially due to cardiac failure in these animals (Figure 4.2c). Western analysis of embryonic hearts from CX1^{frnk}Nkx2.5^{cre} mice showed the presence of MycFRNK in the myocardium as early as E10.5 and continued high expression at E12.5 and E13.5 (Figure 4.2d, data not shown). The expression of MycFRNK occurs shortly after the onset of FAK expression in the embryo. In wildtype embryos, FAK expression gradually increased from E8.0 onward in all tissues, although expression was most predominant in the mesoderm at midgestation (E8.5) [26]. Therefore, expression of

MycFRNK in the CX1^{frnk}Nkx2.5^{cre} embryos should be able to inhibit FAK activity shortly after it is expressed in the embryo.

Histological examination of coronal sections through the CX1^{frnk}Nkx2.5^{cre} hearts revealed similar heart size and ventricular wall thickness at E10.5. In addition, we found similar morphologies of the endocardial cushion relative to genetic controls. However, as development progressed from E10.5 to E13.5, the ventricular walls expanded in the control hearts and the interventricular septum (IVS) grew and fused with the outflow tract (OFT) in the control hearts while little growth was observed in the CX1^{frnk}Nkx2.5^{cre} hearts (Figure 4.3). Cardiac sections from E14.5 CX1^{frnk}Nkx2.5^{cre} embryos revealed a significant reduction in ventricular wall size compared to controls as well as endocardial cushion defects resulting in malformation of the bicuspid and tricuspid valves. Histological analysis of E14.5 coronal heart sections revealed a 48% reduction in overall ventricular cellular area in the CX1^{frnk}Nkx2.5^{cre} hearts compared to aged matched controls (Figure 4.4).

We also examined non-cardiac tissues known to express Nkx2.5 for any defects [189]. CX1^{frnk}Nkx2.5^{cre} embryos at embryonic day 14.5 revealed normal craniofacial development and no indication of cleft palate (Figure 4.2, data not shown). In addition, there were no overall histological differences observed in the tongue, spleen, and thymus compared to genetic controls at E13.5 (tongue) or E14.5 (spleen, thymus) (Figure 4.5).

MycFRNK Expression Results in Decreased Cell Proliferation but Does Not Affect Apoptosis

As previously indicated, FAK can regulate a variety of biological processes. In some cell types, activation of FAK has been shown to be important for cell survival, and inhibiting FAK activity can lead to apoptosis [12, 24, 25]. We examined E13.5 MycFRNK hearts for increased DNA fragmentation at the cellular level and for increased apoptotic markers. Although hearts with decreased FAK activity displayed a significant reduction in ventricular mass, this phenotype was not attributed to increased apoptosis. Figure 4.6a shows a similar percentage of TUNEL positive cells in both control and MycFRNK hearts. We also examined cleaved caspase-3, since the presence of its cleaved 12 and 17kDa subunits associate to form an active enzyme and are key indicators of apoptosis [190]. Cardiac lysate from both control and MycFRNK hearts showed similar levels of the uncleaved 32 kDa caspase-3 while the cleaved 17 and 12 kDa pieces were undetected by immunoblot (Figure 4.6b). In addition, we examined RNA for increased expression of genes important in pro-apoptotic pathways such as Bax or a decrease in genes involved the pro-survival pathway involving Bcl-2. In accordance with the previous data, there was no change in Bax or Bcl-2 expression as detected by semi-quantitative RT-PCR (Figure 4.6c). Overall, our data suggest that the cardiac phenotype associated with the MycFRNK hearts is not due to an increase in apoptosis.

Data from the *fak-/-* mouse revealed that FAK may regulate cell proliferation in some cell types [26]. Therefore, we examined cell proliferation in the MycFRNK hearts to determine if the significantly smaller heart size was due to a proliferation

defect. Following maternal BrdU injection, we noted that there was significantly less BrdU incorporation in the hearts containing MycFRNK relative to control hearts indicative of a proliferation defect (Figure 4.7a). These data were supported by quantitative RT-PCR data from E13.5 MycFRNK and control hearts that showed a significant decrease in cardiac cFos expression, an early immediate gene involved in cell growth (Figure 4.7b). In summary, the expression of MycFRNK in the heart does not increase apoptosis, but does result in a proliferation defect.

Embryonic Lethality is Due to a Cardiomyocyte Specific Growth Defect

Since Nkx2.5 is not limited to the primary heart field, it is possible that the myocyte proliferation defect observed in the MycFRNK hearts is due to aberrant growth signals from surrounding non-myocyte NXK2.5 expressing cells derived from the secondary heart field and in the endocardium and endocardial cushions [189]. To determine if the defects observed in $CX1^{frnk}Nkx2.5^{cre}$ were due to a cardiomyocyte autonomous effect we bred the $Nkx2.5^{cre}$ mice with a novel mouse model that expresses constitutively active FAK, termed SuperFAK, under the control of the heart-specific βMHC promoter. The βMHC promoter is activated between E7.5 and 8 and is restricted to ventricular cardiomyocytes by E10 [191]. A detailed characterization of the SuperFAK mouse is available in Chapter III. For these studies we used the SuperFAK 1 line of mice. The resultant $\beta MHC^{SuperFAK}Nkx2.5^{cre}$ mouse was then crossed with the MycFRNK transgenic to create a mouse that expresses MycFRNK in Nkx2.5 expressing cells and active FAK in the cardiomyocytes (Figure 4.8a). The resultant mice, termed SuperFAK rescue mice (SFR), were born with no gross morphological phenotype at neonatal day 1. The pups were sacrificed at day 2

postnatal and we examined their hearts for gross and microscopic morphological abnormalities. Although viable, gross examination of the heart revealed an abnormal shape with apparent dilated left and right ventricles (Figure 4.8b, top panel). Interestingly, the SFR mice demonstrated a substantial, although not complete, reversal of the proliferation defect and ventricular septation defect noted in the CX1^{frnk}Nkx2.5^{cre} embryos (Figure 4.8b, bottom panel). In addition, bicuspid and tricuspid valve formation in the SFR hearts was similar to control sections (data not shown). High power images reveal that there was still a left ventricular compaction defect in the SFR hearts (Figure 4.9). Taken together, these data confirm that FRNK acts as a specific dominant negative to block FAK activity and that FAK activity is necessary for cardiomyocyte proliferation during development.

D. Discussion

The germline deletion of FAK results in embryonic lethality, precluding an assessment of the requirement of FAK throughout heart development. We recently published that deletion of FAK in Nkx2.5 expressing cells causes significant deletion of FAK protein at E13.5. FAK deletion in late gestation results in peri-natal lethality due to a profound ventricular septal defect due to a cardiomyocyte migration defect [32]. Herein to examine earlier time points in cardiac morphogenesis, we generated a MycFRNK transgenic mouse line that was crossed with a heart specific Cre expressing line to enable us to study the effect of decreased FAK activity in the heart during development. This model results in expression of FRNK, the dominant negative of FAK, days before we are able to see reduction of the FAK protein using the Nxk2.5-floxed FAK model. This is because we do not have to wait for Cre-mediated recombination of both floxed alleles and subsequent protein degradation of FAK (which has a relatively long half-life, 24hrs), allowing us to examine the role of FAK at different points in development [32].

Since the Nkx2.5 promoter is capable of inducing higher expression of Cre at an earlier stage of development than the Mlc2v promoter, it is not surprising that we observe a vastly different phenotype compared to the CX1^{frnk}Mlc2v^{cre} model (Chapter III). Briefly, the CX1^{frnk}Mlc2v^{cre} mouse showed ventricular specific expression of MycFRNK at postnatal day 1. This expression of MycFRNK, and subsequent decrease of FAK activity, was dispensable for proper anabolic growth, but was required for pressure-overload induced pathological cardiac hypertrophy. Unlike the CX1^{frnk}Mlc2v^{cre} model, we see robust expression of MycFRNK at E10.5 in

the CX1^{frnk}Nxk2.5^{cre} embryonic hearts. At this point in development, the hearts have undergone looping and formation of trabeculae along the inner myocardial layer, near the curvature of the primitive ventricle [192]. Additionally, the superior and inferior cushions in the AV canal have formed by epithelial to mesenchymal transformation (EMT) [193]. Also at this time (E10.5), epicardial cells invade the myocardium and may play a role in myocardial maturation [194]. At the E10.5 stage, CX1^{frnk}Nxk2.5^{cre} mice have similar histology compared to their littermate controls. At E12.5-13.5 the cushions fuse to form the valve primordia, the ventricular septum fuses, and there is proliferation of the compact myocardial layer and continuing formation of trabeculae [195]. It is during these changes that we observe a proliferation and ventricular and atrial septation defect in the CX1^{frnk}Nxk2.5^{cre} mice. These defects become more pronounced at E14.5 when there is subsequent compaction of the left ventricle. This coincides with invasion of the developing coronary vasculature from the epicardium in the control embryos [196]. This significant decrease in proliferation in the CX1^{frnk}Nxk2.5^{cre} hearts is supported by the overall decrease in cellular area and considerable decrease in cFos expression.

Endogenous wildtype FRNK is expressed primarily in SMCs and functions as a dominant negative of FAK. Although we have yet to show definitively by Western analysis that FAK activity is decreased in the CX1^{frnk}Nkx2.5^{cre} hearts, we are confident that the expression of MycFRNK in these mice is inhibiting FAK activity. Numerous western blots were unable to determine differences in levels of active FAK in the MycFRNK containing hearts compared to controls. It is possible that there is a significant decrease FAK activity in the Nxk2.5 expressing cells, but the

high levels of FAK activity in cardiac fibroblasts during development are masking this signal. Previous work by our lab showed that overexpressing FRNK in SMCs by adenoviral infection of these cells with GFP-FRNK inhibited autophosphorylation of FAK on tyrosine 397, as well as the Src-dependent phosphorylation sites in FAK-pY556, pY557, and pY861 [37, 155]. In addition, data in Chapter III of this thesis supported that *in vivo* expression of MycFRNK in the myocardium was also able to inhibit autophosphorylation of FAK (Figure 3.3f). However, because we were unable to definitively show that FRNK was functioning as an inhibitor of FAK activity in the CX1^{frnk}Nkx2.5^{cre} hearts and that the proliferation defect was not a secondary effect to exogenous expression of MycFRNK, we crossed the CX1^{frnk}Nkx2.5^{cre} mice with the SuperFAK mouse. The SuperFAK mouse contained cardiomyocyte specific constitutively active FAK under the control of the βMHC promoter. The use of these mice demonstrated that the CX1^{frnk}Nkx2.5^{cre} hearts had a decreased level of FAK activity causing the cardiac phenotype.

The MycFRNK model also allows us to study the fundamental difference between FAK expression and activity throughout cardiac development. Our recently published paper addressing deletion of FAK using the Nkx2.5-floxed FAK mouse (termed, FAK^{nk} mouse) showed a significantly different phenotype than the CX1^{frnk}Nkx2.5^{cre} embryos. In the FAK^{nk} animals, the mice died shortly after birth due to a profound sub-aortic ventricular septal defect and associated mal-alignment of the outflow tract [32]. Unlike the MycFRNK model, the FAK^{nk} hearts revealed no significant difference in proliferation. This is possibly due to a time dependent requirement for FAK activity on proliferation during midgestation, but not late

gestation. Notably, inhibiting FGFR signaling with adenoviral dominant-negative mutants of FGFR1 or with translation of endogenous FGFR1 antisense RNA during the first week of chicken embryonic development inhibited myocyte proliferation and/or survival [197]. However, the inhibition of FGFR1 during the second week of embryonic development had much less effect on myocyte growth suggesting that proliferation and survival are FGF dependent in early cardiac development, but myocyte growth in later stages of development is FGF-independent [197]. Interestingly, the FAK^{nk} model also shows no difference in apoptosis relative to controls, indicating that FAK expression and FAK activity are not essential for cell survival during cardiac development.

The use of constitutively active FAK was able to alleviate the cardiac phenotype in the MycFRNK mouse but was not able to completely rescue the phenotype. This is most likely due to the amount of SuperFAK expression compared to MycFRNK expression. The SuperFAK mouse we used in these experiments was the lower expressing line, SuperFAK1 (see Chapter III). Therefore it is likely that there is sufficient FAK activity to improve cardiomyocyte proliferation, but no enough to reverse it. It will be of interest to examine the rescue effects of the higher expressing SuperFAK line, SuperFAK 2, to determine if increased FAK activity will completely rescue the phenotype. Additionally, the expression of βMHC driven SuperFAK is limited to ventricular cardiomyocytes whereas Nkx2.5 drives expression of FRNK in myocyte and non-myocyte cells. Therefore the resultant phenotype may be due to a combination of abnormalities in the non-myocyte cells that express FRNK but not SuperFAK. Further studies need to be completed

including the examination of SuperFAK expression during development as well as the ratio of SuperFAK to FRNK expression at this time.

Several studies have examined the expression and activity of Pyk2 in models of FAK deletion or inhibition. Previous *in vitro* work with *fak*$^{-/-}$ fibroblasts indicated that in the absence of FAK, expression and activation of Pyk2 are elevated [157]. However, overexpression of FRNK in cultured cardiomyocytes inhibited Pyk2 phosphorylation [198]. Interestingly, our recent *in vivo* work showed comparable Pyk2 protein levels (and activity) in control and MFKO hearts (Chapter II) as well as in the FAK^{nk} hearts indicating that Pyk2 does not compensate for loss of FAK in these models [32, 33]. Therefore, given the differential results from *in vitro* studies with FAK deletion or inhibition as well as the differential results between the *in vitro* and *in vivo* experiments, it will be of interest to examine the levels of Pyk2 expression and activity in the CX1^{frnk}Nkx2.5^{cre} hearts. If Pyk2 expression and/or activity is altered in these mice, it will also be of interest to examine the rescue hearts to determine if the presence of SuperFAK would reverse this change.

In summary, our findings highlight the importance of FAK activity in the developing myocardium. Further studies involving the SuperFAK mouse, including those proposed in Chapter III of this thesis will help to elucidate the specific functions of FAK activity in adult cardiomyocytes. Increased FAK activity in the adult myocardium may result in increased proliferation of cardiomyocytes which suggests that FAK may be a potential therapeutic target for heart disease.

Figure 4.1. Expression of FAK and FRNK During Heart Development. Hearts were isolated from embryos or mice at various time points as indicated. Cardiac and smooth muscle cell (SMC) extracts were analyzed by SDS-PAGE and immunoblotted using anti-FAK antibody to detect both FAK and FRNK, and anti-tubulin antibody. FAK is expressed in high levels during development and low levels in the adult heart, while FRNK is undetectable at all stages of heart development.

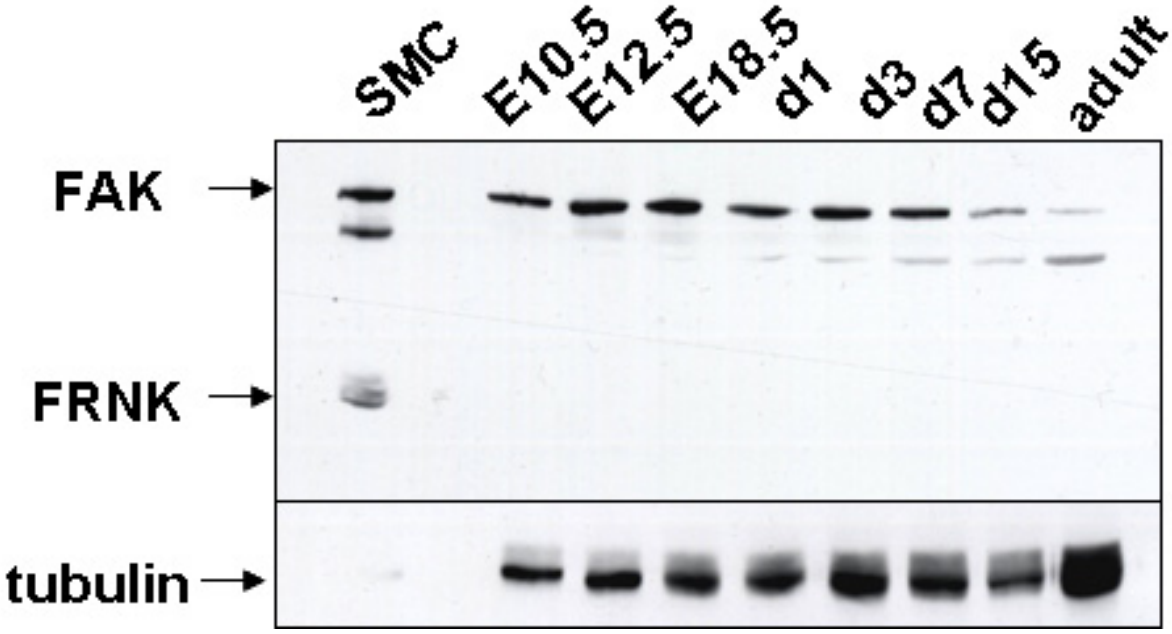
SMC
E10.5
E12.5
E18.5
d1
d3
d7
d15
adult
FAK
FRNK
tubulin

Figure 4.2. Generation of CX1^{frnk}Nkx2.5^{cre} Mice. ***a*****,** CX1^{frnk} transgenic mice were bred with Nkx2.5-Cre knock-in mice to produce progenies with or without cardiac expression of MycFRNK. ***b,*** Number of progeny that were positive for the MycFRNK transgene and for Cre over total number of progeny. ***c,*** Gross morphological analysis of control and FRNK embryos taken at E14.5. ***d,*** Western analysis of E13.5 cardiac lysate from control (C) and MycFRNK (F) hearts using anti-FAK and anti-ERK antibodies.

a.

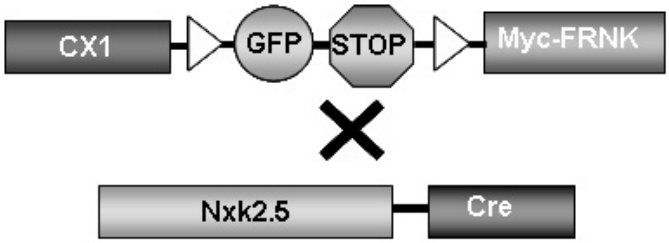

b.

	E10.5	E11.5	E12.5	E13.5	E14.5	E18.5	3wks
$CX1^{frnk}$ $Nkx2.5^{cre}$	3/12	14/40	11/62	33/147	8/31	0/14	0/63
Percentage (expect 25%)	25	35	18	22	26	0	0

c.

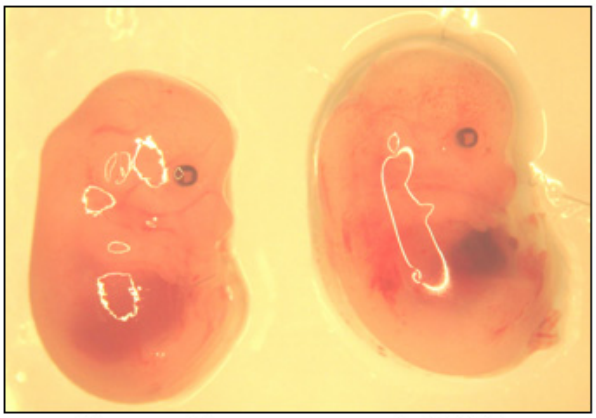

Control FRNK

d.

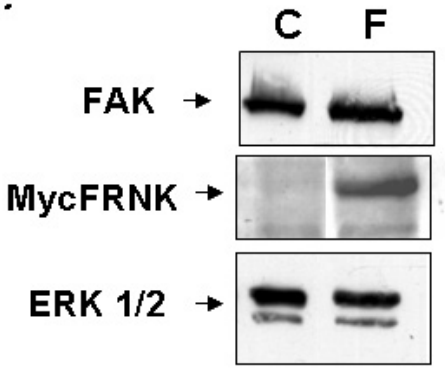

Figure 4.3. Histological Analysis of CX1^{frnk}Nkx2.5^{cre} Mice. Histological analysis of hematoxylin and eosin stained coronal heart sections from E10.5, E12.5 and E13.5 from control CX1^{wt}Nxk2.5^{cre} hearts and CX1^{frnk}Nxk2.5^{cre} MycFRNK expressing hearts.

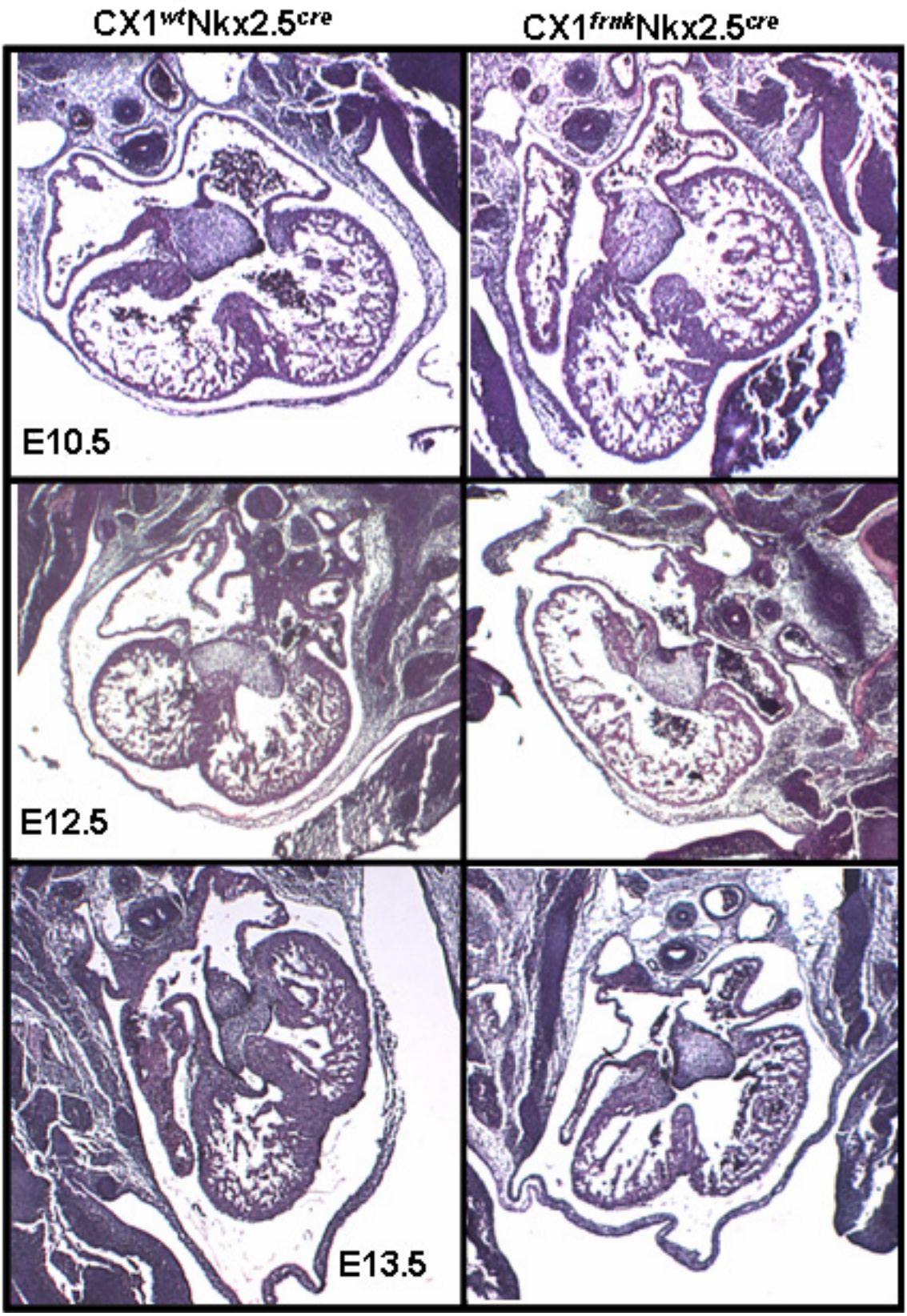
CX1wtNkx2.5cre
CX1frnkNkx2.5cre
E10.5
E12.5
E13.5

Figure 4.4. Decreased FAK Activity in CX1^{frnk}Nxk2.5^{cre} Hearts Results in a Cardiomyocyte Proliferation Defect. ***a,*** Control CX1^{wt}Nxk2.5^{cre} hearts and CX1^{frnk}Nxk2.5^{cre} MycFRNK at E14.5 are stained with hematoxylin and eosin to observe any histological differences in the ventricular walls of the hearts at 2x, 10x, and 40x. ***b,*** Cellular area measured in Control and MycFRNK hearts at E14.5. *p<0.05 versus control.

a.

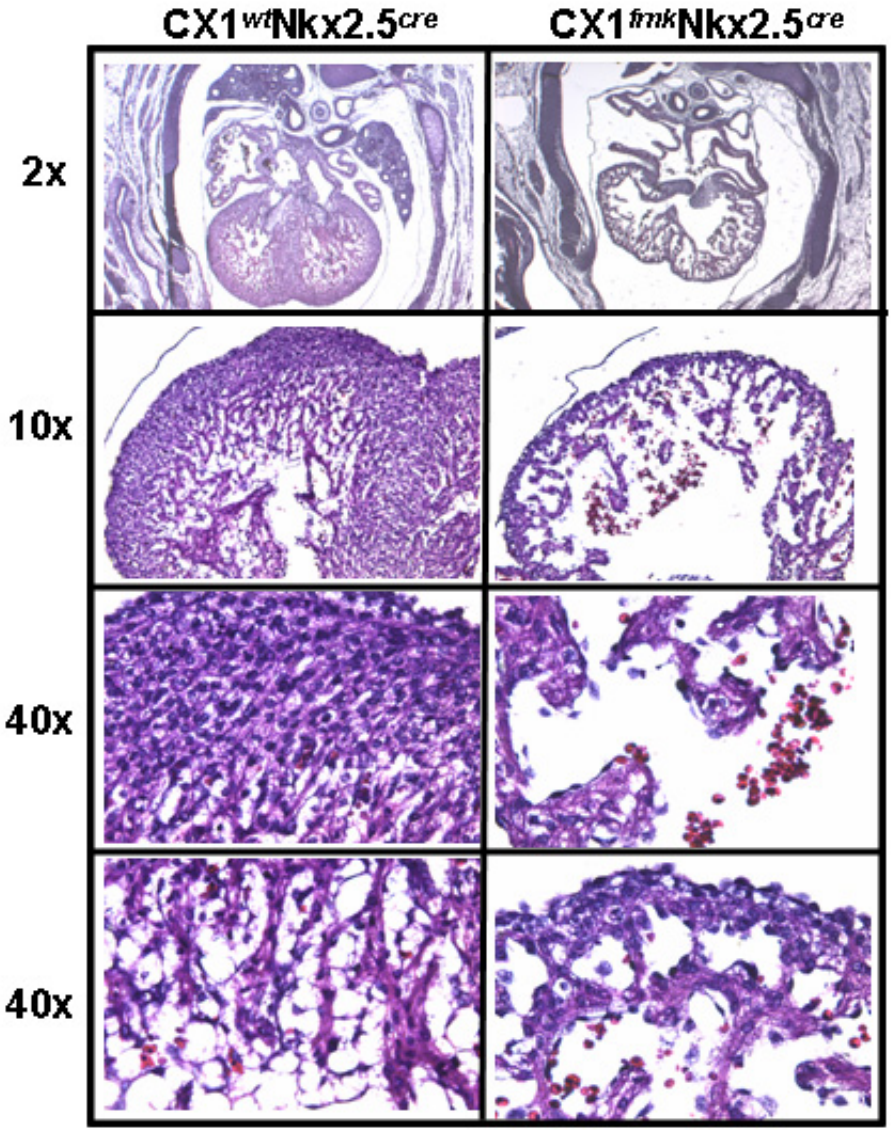
CX1wtNkx2.5cre
CX1frnkNkx2.5cre
2x
10x
40x
40x

b.

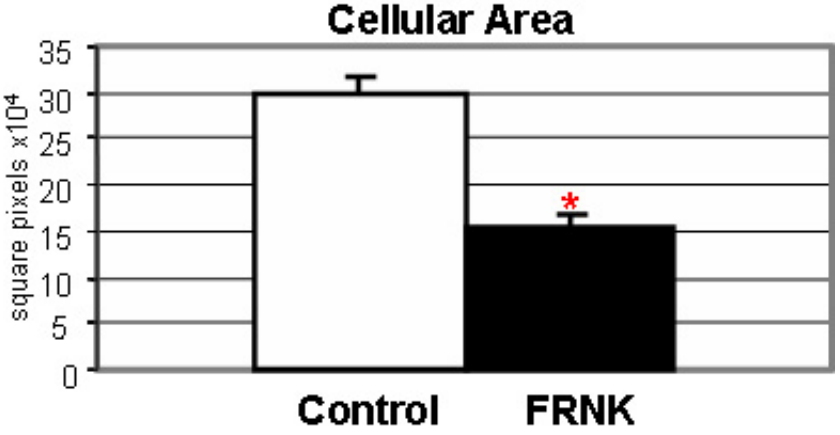
Cellular Area
square pixels x10^4
35
30
25
20
15
10
5
0
*
Control
FRNK

Figure 4.5. Comparable Histology in Other Tissues with Nkx2.5 Expressing Cells. Hematoxylin and eosin stained spleen (E14.5,100x), thymus (E14.5, 40x) and tongue (E13.5, 10x) sections from control and CX1^{frnk}Nxk2.5^{cre} embryos.

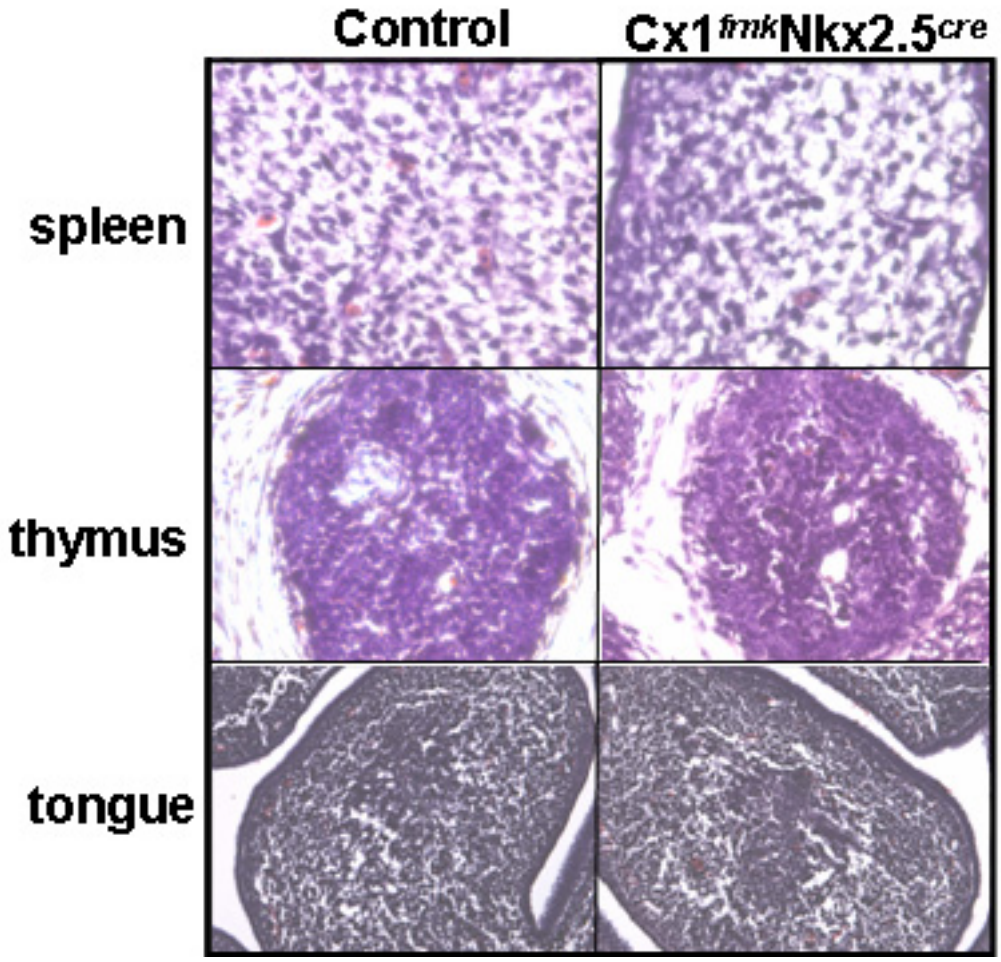
Control
Cx1fmkNkx2.5cre
spleen
thymus
tongue

Figure 4.6. Inhibition of FAK Activity Does Not Increase Apoptosis. ***a,*** Quantification of FragEL stained apoptotic cells of the ventricles in control and MycFRNK expressing hearts at E13.5. ***b*****,** Western analysis of total and cleaved caspase 3 levels in genetic control (C) and MycFRNK (F) hearts at E13.5. ***c,*** RNA from pools of 3 hearts each from genetic controls and MycFRNK expressing E13.5 hearts were examined for expression of Bax and Bcl-2 by RT-PCR. Control samples consist of MycFRNK transgene only (F), Nxk2.5-Cre only (C), and wildtype (W) samples. Densitometry quantification of Bax compared to Bcl-2 (right panel).

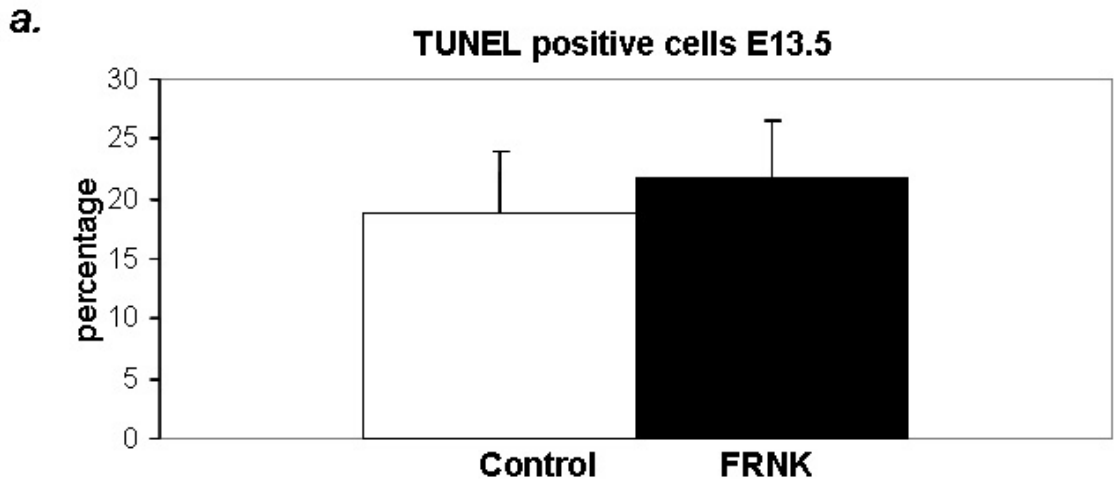
a.
TUNEL positive cells E13.5
30
25
20
15
10
5
0
percentage
Control
FRNK

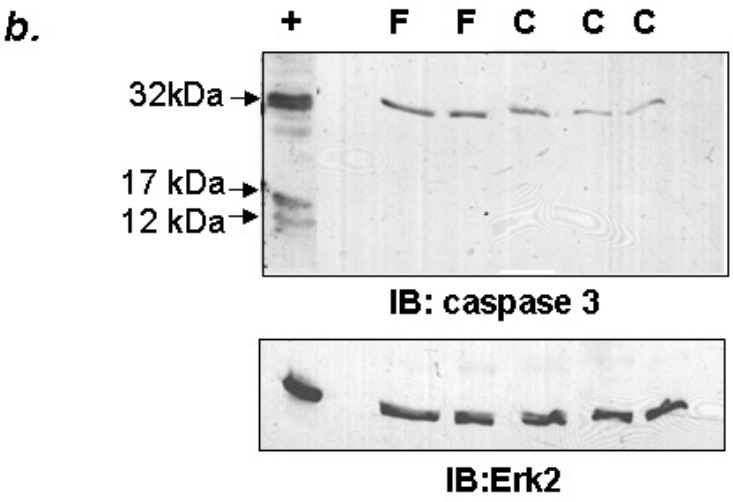
b.
+
F
F
C
C
C
32kDa
17 kDa
12 kDa
IB: caspase 3
IB:Erk2

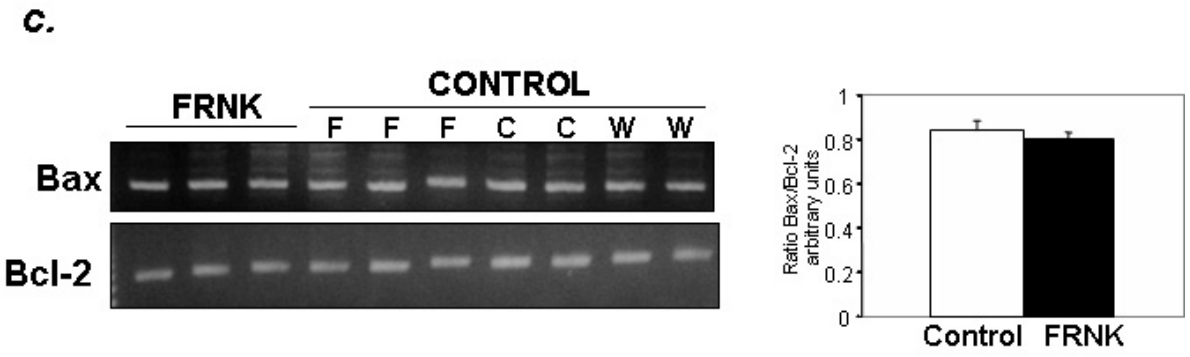
c.
FRNK
CONTROL
F
F
F
C
C
W
W
Bax
Bcl-2
Ratio Bax/Bcl-2 arbitrary units
1
0.8
0.6
0.4
0.2
0
Control
FRNK

Figure 4.7. Decreased FAK Activity Inhibits Cellular Proliferation. ***a,*** Quantification of ventricular BrdU incorporation in E13.5 control and FRNK embryos. *p,<0.05. ***b,*** Quantitative RT-PCR analysis of RNA from E13.5 hearts examined for expression of c-Fos. Data is represented as fold over control β-actin expression. *p,<0.05.

a.

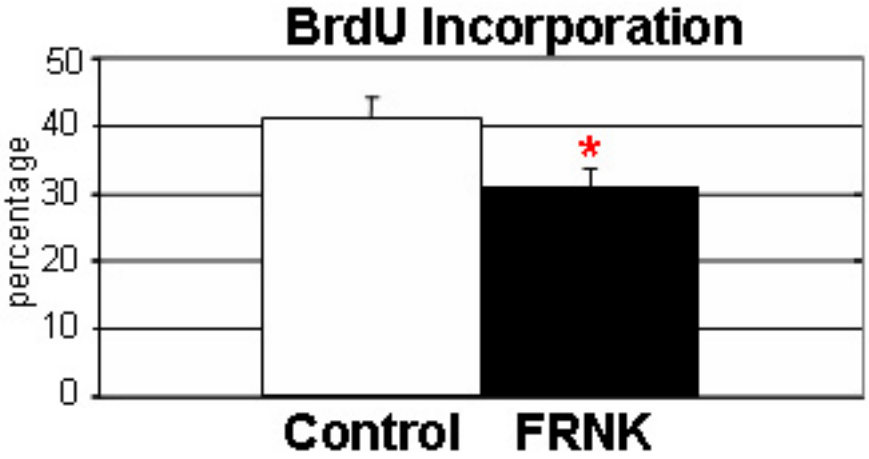
BrdU Incorporation
50
40
30
20
10
0
percentage
*
Control
FRNK

b.

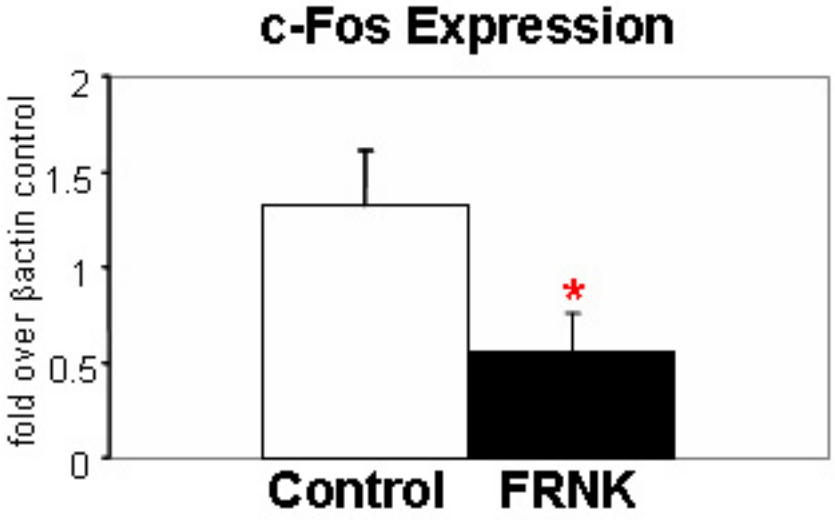
c-Fos Expression
2
1.5
1
0.5
0
fold over βactin control
*
Control
FRNK

Figure 4.8. Generation of SuperFAK Rescue Mice. ***a****,* Breeding strategy to create SuperFAK rescue mouse. First cross involves breeding the SuperFAK mouse with the Nkx2.5-Cre mouse. Progeny that are positive for Cre and the SuperFAK transgene are then bred with the $Cx1^{frnk}$ mouse. ***b,*** Gross morphological comparison of control ($CX1^{frnk}$) and SuperFAK rescue (SFR) hearts at day 2 postnatal (top panel). Paraffin embedded sections of control and SFR hearts were stained with hematoxylin and eosin (bottom panel).

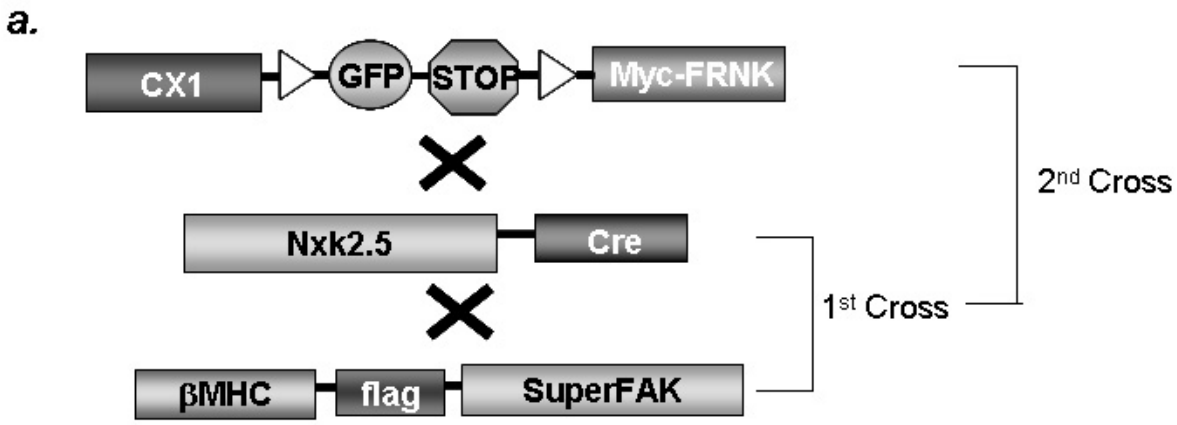
a.
CX1
GFP
STOP
Myc-FRNK
Nxk2.5
Cre
βMHC
flag
SuperFAK
1st Cross
2nd Cross

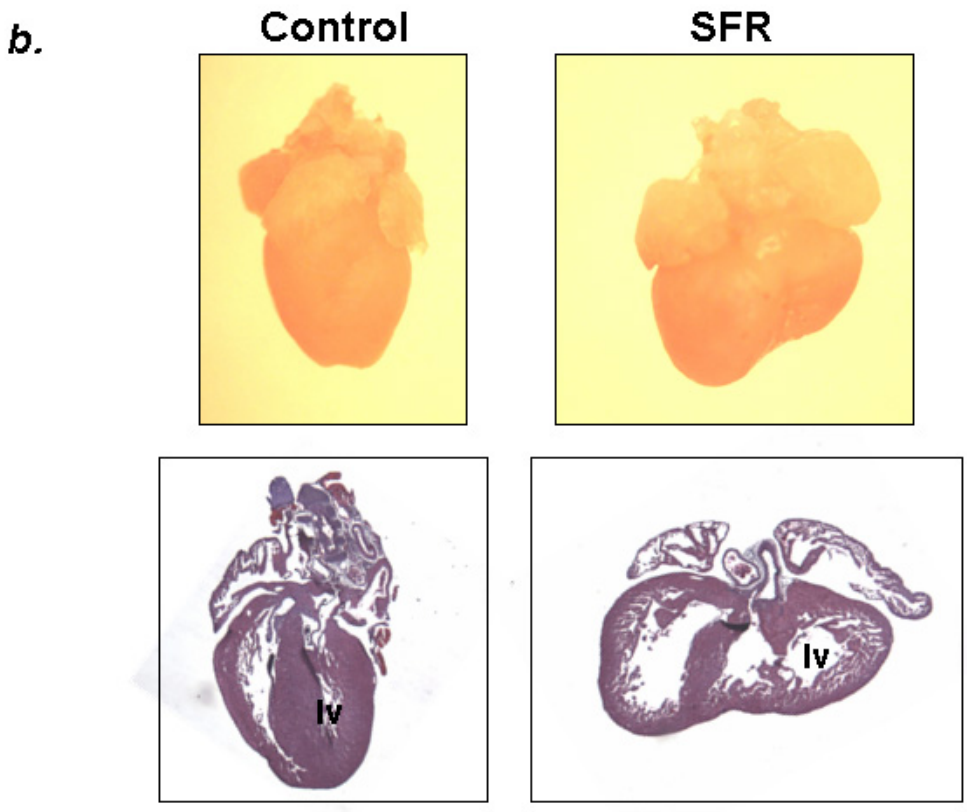
b.
Control
SFR
lv
lv

Figure 4.9. SuperFAK Alleviates Proliferation and Ventricular Septation Defect. High powered images show histological analysis of hematoxylin and eosin stained control ($CX1^{frnk}$) and SuperFAK rescued left ventricles.

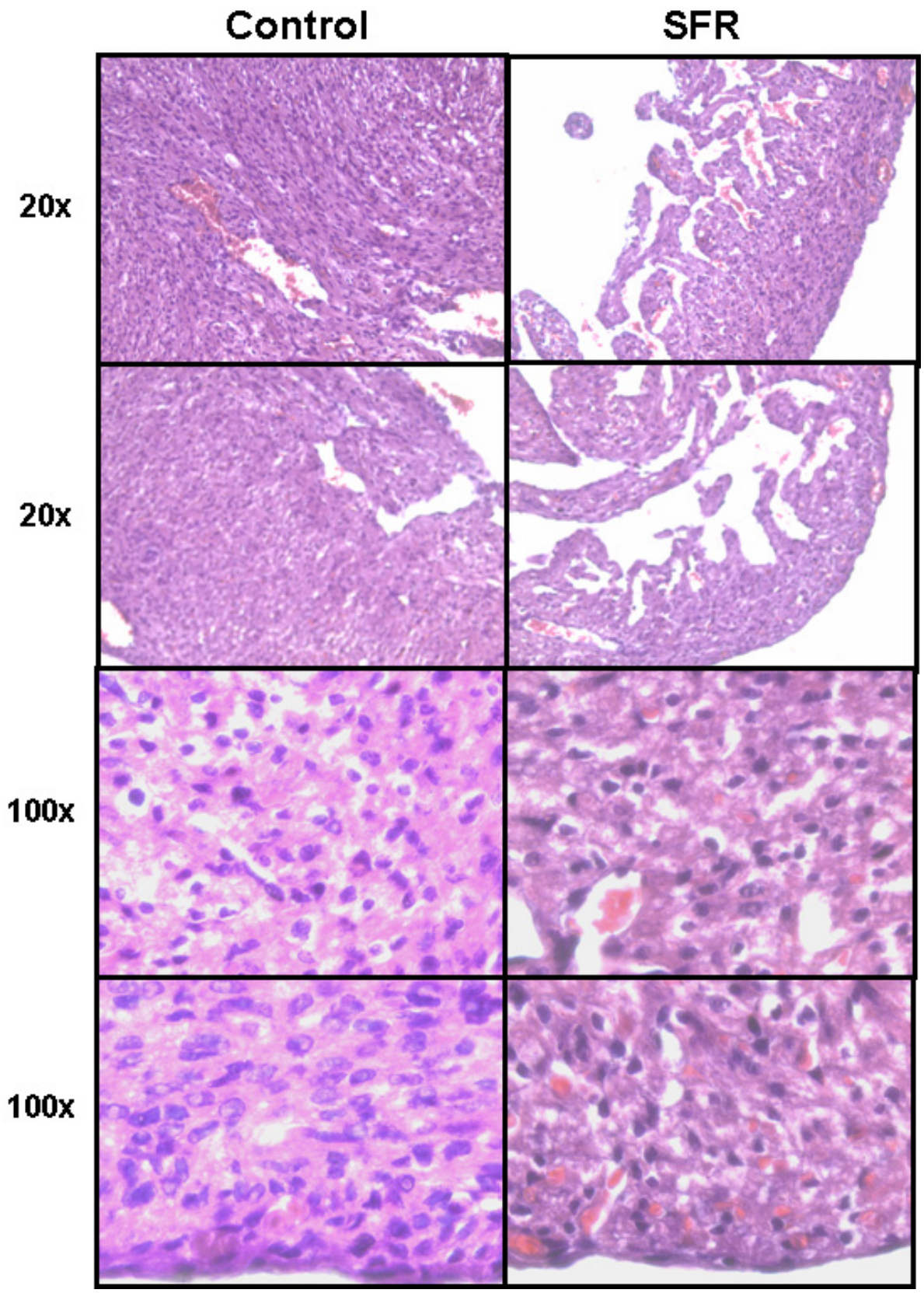
Control
SFR
20x
20x
100x
100x

Chapter V

OVERALL DISSCUSSION AND FUTURE DIRECTION

Germline deletion of FAK results in early embryonic lethality, making it difficult to study the specific role for FAK in cardiac development and disease. We have overcome this hurdle by creating various mouse lines which express FAK, or its dominant negative FRNK, in a tissue specific manner. We used these mice to explore the role of FAK in heart development, anabolic growth, and cardiac disease. Collectively, the use of these conditional mouse models revealed that FAK activity and/or expression is required for cardiomyocyte proliferation during development, is dispensable for anabolic growth of the heart, and is necessary and sufficient for the induction of cardiac hypertrophy.

As noted above, germline deletion of FAK is embryonic lethal between E8.5 and E10. The mesodermal defect resulting from the loss of FAK protein suggests that FAK may be important in cardiac development. In addition FN, the major activator of FAK, as well as FAK binding partners including p130Cas and paxillin, have been implicated in heart development [61-63]. To show that FAK activates critical pathways required for normal development and function of the heart, we induced cardiac field-specific FRNK expression, and subsequent inhibition of FAK activity, in Nkx2.5-Cre expressing cells.

Expression of FRNK in Nxk2.5-Cre expressing cells resulted in a more dramatic phenotype than we observed following FAK depletion using the same Cre line. Indeed, the conditional expression of FRNK in the heart field caused embryonic lethality between E14-E15, while the FAK deleted model, (termed FAK^{nk}) mice died postnatally [32]. FRNK expression resulted in a significant reduction in cardiomyocyte proliferation, atrial and ventricular septal defects, and malformations of the bicuspid and tricuspid valves. However, FAK^{nk} mice demonstrated malformations in the outflow tract that manifested as a profound sub-aortic ventricular septal defect with overriding aorta or double outlet right ventricle that resulted in defective blood oxygenation and peri-natal lethality [32]. The malformations noted in the FAK^{nk} mice were due to impaired cardiomyocyte migration. The differential phenotypes between the FAK^{nk} mouse and the current FRNK overexpressing model are most easily explained by the precise timing of the ablation of FAK protein and activity in the two models. The Nxk2.5 promoter drives Cre recombinase expression in cardiac progenitors at E7.5 and has been reported to induce recombination as early as E9 in cardiomyocytes [189]. However, due to a combination of inaccessibility of FAK alleles and a long FAK half-life, FAK protein in the FAK^{nk} mouse was not reduced until E13.5, days after the onset of FRNK expression at E10.5. Thus, by the time FAK protein was depleted in the FAK^{nk} hearts, these hearts has already undergone a robust proliferation burst and compaction of the ventricles [32]. Collectively, our studies reveal that FAK activity regulates cardiomyocyte proliferation during mid-gestation whereas FAK controls cardiomyocyte migration in late gestation.

The use of the novel heart specific constitutively active FAK model, SuperFAK, allowed us to determine if the phenotype observed in the CX1^{frnk}Nkx2.5^{cre} hearts was a cardiomyocyte autonomous effect or due to decreased FAK activity in non-myocyte Nxk2.5-cre expressing cells. Initial data from the SuperFAK rescue mouse revealed that increased FAK activity in cardiomyocytes was able to alleviate the proliferation defect and ventricular septal defect in the CX1^{frnk}Nkx2.5^{cre} hearts. These initial data proved especially interesting since activation of FAK in otherwise slow dividing or non-dividing cells was able to initiate proliferation, the key to reversing heart disease.

Due to the small number of SuperFAK rescue mice analyzed at this time, a variety of experiments will need to be completed to fully characterize the observed phenotype. Additional mice at postnatal day 1 will be sacrificed and their hearts examined for general morphology as well as histological differences in ventricular wall thickness, myofibrillar organization, deposition of ECM fibrosis, and cell size. SuperFAK rescue mice will also be monitored at various postnatal time points to examine any morbidity and mortality that may occur following extended stress on the heart. Protein lysates will be isolated from embryonic day 14.5 as well as postnatal day 1 hearts to determine the ratio of active FAK to FRNK. In addition, a variety of downstream effectors of FAK may be altered, including ERK, PI3K and AKT due to their role in cardiomyocyte growth [85, 199]. Lastly, to examine cellular proliferation in the SuperFAK rescue mice, embryonic hearts will be assessed at E14.5 following maternal BrdU exposure. These data will help to identify the specific pathways that

are altered in these mice and will confirm whether increased FAK activity is able to improve cardiomyocyte proliferation.

Although FAK activity was required for proper cardiac development in both the CX1^{frnk}Mlc2v^{cre} and MFKO models, where FAK is deleted or inhibited postnatal, FAK was dispensable for basal myocyte function. Both models showed similar heart morphology, histology, and function compared to controls at baseline. Although FAK resides with cytoskeletal proteins in the Z-disk, it is not an integral part of the contractile apparatus and may function primarily as an effector for integrin signaling. In wildtype embryos, FAK expression gradually increases from E8.0 onward and is ubiquitously expressed, although expression is most predominant in the mesoderm at midgestation (E8.5) [26]. This expression remains high throughout development, and then decreases postnatally into adulthood (Figure 4.1). Because of its comparably low levels in the adult heart, FAK signaling may not play a pivotal role in heart structure or function of the heart during adulthood.

Although FAK activity was dispensable for anabolic growth in the CX1^{frnk}Mlc2v^{cre} mice, data from the MFKO mice suggest that FAK protein plays a role in heart growth during aging. The heart is exposed to higher levels of IGF-1 and growth factor during anabolic growth than it is in the aged heart, and diminished levels of these hormones combined with deletion of FAK from the myocardium, may result in the significantly smaller MFKO hearts seen at 14 months of age. In addition, it is possible that the inhibition or deletion of FAK results in an impaired growth response, but this difference is not apparent until 14 months of age. Lastly, the differential downstream signals governing FAK deletion versus decreased FAK

activity may manifest in an impaired growth response during aging. To further elucidate these differences, a group of MycFRNK mice will need to be examined at 14 months of age for decreased heart size and cell size relative to littermate controls.

Previous work by our group and others indicate that FAK is important for the hypertrophic response. We have described three novel mouse models (MFKO, CX1^{frnk}Mlc2v^{cre}, and SuperFAK) that collectively support the idea that FAK signaling is necessary and sufficient for the progression of cardiac hypertrophy. Following biomechanical or adrenergic stimuli, activation of FAK results in the activation of the ERK and JNK growth promoting MAP kinases and the cytoskeleton-regulating small GTPases Rac and Rho, some of the same molecules implicated in myocyte hypertrophy [131, 136]. We showed that inhibition of FAK activity and deletion of FAK inhibits the progression of hypertrophy *in vivo.* Data from the MFKO mice suggest that ERK activation may be the primary mechanism for the blunted hypertrophic response.

Conditional activation of FAK stimulated the progression of cardiac hypertrophy in the absence of biomechanical stress. Since ERK signaling mediates cell growth and given that the MEK1-ERK1 signaling precedes the induction of hypertrophic gene expression *in vivo*, it is possible that activated FAK enhances the ERK-1/2 signaling pathway in the SuperFAK hearts. In addition to further characterizing the hypertrophic response present in these mice, we plan to examine the altered signaling pathways downstream of FAK that contribute to the hypertrophic phenotype.

In conclusion, the examination of a role for cardiac FAK from mid-gestation to aged adult highlights the importance of FAK in development and disease. These studies assessed the different biological functions of FAK in the myocardium, illustrating the importance of FAK in promoting proliferation during cardiac development and in promoting myocyte hypertrophy in the adult heart. Therefore, targeting FAK activity may be a promising avenue for the treatment of heart disease.

REFERENCES

1. AHA, *Heart Disease and Stroke Statisics-2006 Update.* American Heart Association, 2006. Dallas, Texas.

2. Ross, R.S. and T.K. Borg, *Integrins and the myocardium.* Circ Res, 2001. **88**(11): p. 1112-9.

3. Hynes, R.O., *Integrins: versatility, modulation, and signaling in cell adhesion.* Cell, 1992. **69**(1): p. 11-25.

4. Tamkun, J.W., et al., *Structure of integrin, a glycoprotein involved in the transmembrane linkage between fibronectin and actin.* Cell, 1986. **46**(2): p. 271-82.

5. de Melker, A.A. and A. Sonnenberg, *Integrins: alternative splicing as a mechanism to regulate ligand binding and integrin signaling events.* Bioessays, 1999. **21**(6): p. 499-509.

6. Giancotti, F.G. and E. Ruoslahti, *Integrin signaling.* Science, 1999. **285**(5430): p. 1028-32.

7. Guan, J.L., *Role of focal adhesion kinase in integrin signaling.* Int J Biochem Cell Biol, 1997. **29**(8-9): p. 1085-96.

8. Zhidkova, N.I., A.M. Belkin, and R. Mayne, *Novel isoform of beta 1 integrin expressed in skeletal and cardiac muscle.* Biochem Biophys Res Commun, 1995. **214**(1): p. 279-85.

9. van der Flier, A., et al., *A novel beta 1 integrin isoform produced by alternative splicing: unique expression in cardiac and skeletal muscle.* FEBS Lett, 1995. **369**(2-3): p. 340-4.

10. Burridge, K., et al., *Focal adhesions: transmembrane junctions between the extracellular matrix and the cytoskeleton.* Annu Rev Cell Biol, 1988. **4**: p. 487-525.

11. Clark, E.A. and J.S. Brugge, *Integrins and signal transduction pathways: the road taken.* Science, 1995. **268**(5208): p. 233-9.

12. Schaller, M.D., *Biochemical signals and biological responses elicited by the focal adhesion kinase.* Biochim Biophys Acta, 2001. **1540**(1): p. 1-21.

13. Cohen, L.A. and J.L. Guan, *Mechanisms of focal adhesion kinase regulation.* Curr Cancer Drug Targets, 2005. **5**(8): p. 629-43.

14. Martin, K.H., S.A. Boerner, and J.T. Parsons, *Regulation of focal adhesion targeting and inhibitory functions of the FAK related protein FRNK using a novel estrogen receptor "switch".* Cell Motil Cytoskeleton, 2002. **51**(2): p. 76-88.

15. Hildebrand, J.D., M.D. Schaller, and J.T. Parsons, *Paxillin, a tyrosine phosphorylated focal adhesion-associated protein binds to the carboxyl terminal domain of focal adhesion kinase.* Mol Biol Cell, 1995. **6**(6): p. 637-47.

16. Schaller, M.D., et al., *Autophosphorylation of the focal adhesion kinase, pp125FAK, directs SH2-dependent binding of pp60src.* Mol Cell Biol, 1994. **14**(3): p. 1680-8.

17. Schaller, M.D., J.D. Hildebrand, and J.T. Parsons, *Complex formation with focal adhesion kinase: A mechanism to regulate activity and subcellular localization of Src kinases.* Mol Biol Cell, 1999. **10**(10): p. 3489-505.

18. Calalb, M.B., T.R. Polte, and S.K. Hanks, *Tyrosine phosphorylation of focal adhesion kinase at sites in the catalytic domain regulates kinase activity: a role for Src family kinases.* Mol Cell Biol, 1995. **15**(2): p. 954-63.

19. Schlaepfer, D.D., et al., *Integrin-mediated signal transduction linked to Ras pathway by GRB2 binding to focal adhesion kinase.* Nature, 1994. **372**(6508): p. 786-91.

20. Hildebrand, J.D., J.M. Taylor, and J.T. Parsons, *An SH3 domain-containing GTPase-activating protein for Rho and Cdc42 associates with focal adhesion kinase.* Mol Cell Biol, 1996. **16**(6): p. 3169-78.

21. Sieg, D.J., C.R. Hauck, and D.D. Schlaepfer, *Required role of focal adhesion kinase (FAK) for integrin-stimulated cell migration.* J Cell Sci, 1999. **112 (Pt 16)**: p. 2677-91.

22. Reiske, H.R., et al., *Requirement of phosphatidylinositol 3-kinase in focal adhesion kinase-promoted cell migration.* J Biol Chem, 1999. **274**(18): p. 12361-6.

23. Zhao, J., R. Pestell, and J.L. Guan, *Transcriptional activation of cyclin D1 promoter by FAK contributes to cell cycle progression.* Mol Biol Cell, 2001. **12**(12): p. 4066-77.

24. Sonoda, Y., et al., *Anti-apoptotic role of focal adhesion kinase (FAK). Induction of inhibitor-of-apoptosis proteins and apoptosis suppression by the overexpression of FAK in a human leukemic cell line, HL-60.* J Biol Chem, 2000. **275**(21): p. 16309-15.

25. Chan, P.C., et al., *Suppression of ultraviolet irradiation-induced apoptosis by overexpression of focal adhesion kinase in Madin-Darby canine kidney cells.* J Biol Chem, 1999. **274**(38): p. 26901-6.

26. Furuta, Y., et al., *Mesodermal defect in late phase of gastrulation by a targeted mutation of focal adhesion kinase, FAK.* Oncogene, 1995. **11**(10): p. 1989-95.

27. Ilic, D., et al., *Reduced cell motility and enhanced focal adhesion contact formation in cells from FAK-deficient mice.* Nature, 1995. **377**(6549): p. 539-44.

28. Hungerford, J.E., et al., *Inhibition of pp125FAK in cultured fibroblasts results in apoptosis.* J Cell Biol, 1996. **135**(5): p. 1383-90.

29. Beggs, H.E., et al., *FAK deficiency in cells contributing to the basal lamina results in cortical abnormalities resembling congenital muscular dystrophies.* Neuron, 2003. **40**(3): p. 501-14.

30. Shen, T.L., et al., *Conditional knockout of focal adhesion kinase in endothelial cells reveals its role in angiogenesis and vascular development in late embryogenesis.* J Cell Biol, 2005. **169**(6): p. 941-52.

31. Braren, R., et al., *Endothelial FAK is essential for vascular network stability, cell survival, and lamellipodial formation.* J Cell Biol, 2006. **172**(1): p. 151-62.

32. Hakim, Z.S., et al., *Conditional Deletion of Focal Adhesion Kinase Leads to Defects in Ventricular Septation and Outflow Tract Alignment.* Mol Cell Biol, 2007.

33. DiMichele, L.A., et al., *Myocyte-restricted focal adhesion kinase deletion attenuates pressure overload-induced hypertrophy.* Circ Res, 2006. **99**(6): p. 636-45.

34. Avraham, H., et al., *RAFTK/Pyk2-mediated cellular signalling.* Cell Signal, 2000. **12**(3): p. 123-33.

35. Xiong, W. and J.T. Parsons, *Induction of apoptosis after expression of PYK2, a tyrosine kinase structurally related to focal adhesion kinase.* J Cell Biol, 1997. **139**(2): p. 529-39.

36. Okigaki, M., et al., *Pyk2 regulates multiple signaling events crucial for macrophage morphology and migration.* Proc Natl Acad Sci U S A, 2003. **100**(19): p. 10740-5.

37. Taylor, J.M., et al., *Selective expression of an endogenous inhibitor of FAK regulates proliferation and migration of vascular smooth muscle cells.* Mol Cell Biol, 2001. **21**(5): p. 1565-72.

38. Taylor, J.M., J.D. Rovin, and J.T. Parsons, *A role for focal adhesion kinase in phenylephrine-induced hypertrophy of rat ventricular cardiomyocytes.* J Biol Chem, 2000. **275**(25): p. 19250-7.

39. Eble, D.M., et al., *Endothelin-induced cardiac myocyte hypertrophy: role for focal adhesion kinase.* Am J Physiol Heart Circ Physiol, 2000. **278**(5): p. H1695-707.

40. Allan, L.D., et al., *Familial recurrence of congenital heart disease in a prospective series of mothers referred for fetal echocardiography.* Am J Cardiol, 1986. **58**(3): p. 334-7.

41. Hoffman, J.I., *Incidence of congenital heart disease: I. Postnatal incidence.* Pediatr Cardiol, 1995. **16**(3): p. 103-13.

42. Hoffman, J.I., *Incidence of congenital heart disease: II. Prenatal incidence.* Pediatr Cardiol, 1995. **16**(4): p. 155-65.

43. Olson, E.N., *A decade of discoveries in cardiac biology.* Nat Med, 2004. **10**(5): p. 467-74.

44. Sedmera, D., et al., *Developmental patterning of the myocardium.* Anat Rec, 2000. **258**(4): p. 319-37.

45. Kelly, R.G., N.A. Brown, and M.E. Buckingham, *The arterial pole of the mouse heart forms from Fgf10-expressing cells in pharyngeal mesoderm.* Dev Cell, 2001. **1**(3): p. 435-40.

46. Cai, C.L., et al., *Isl1 identifies a cardiac progenitor population that proliferates prior to differentiation and contributes a majority of cells to the heart.* Dev Cell, 2003. **5**(6): p. 877-89.

47. Abu-Issa, R., K. Waldo, and M.L. Kirby, *Heart fields: one, two or more?* Dev Biol, 2004. **272**(2): p. 281-5.

48. Buckingham, M., S. Meilhac, and S. Zaffran, *Building the mammalian heart from two sources of myocardial cells.* Nat Rev Genet, 2005. **6**(11): p. 826-35.

49. Laugwitz, K.L., et al., *Postnatal isl1+ cardioblasts enter fully differentiated cardiomyocyte lineages.* Nature, 2005. **433**(7026): p. 647-53.

50. Schwartz, R.J. and E.N. Olson, *Building the heart piece by piece: modularity of cis-elements regulating Nkx2-5 transcription.* Development, 1999. **126**(19): p. 4187-92.

51. Harvey, R.P., *NK-2 homeobox genes and heart development.* Dev Biol, 1996. **178**(2): p. 203-16.

52. Molkentin, J.D., et al., *Requirement of the transcription factor GATA4 for heart tube formation and ventral morphogenesis.* Genes Dev, 1997. **11**(8): p. 1061-72.

53. Srivastava, D. and E.N. Olson, *A genetic blueprint for cardiac development.* Nature, 2000. **407**(6801): p. 221-6.

54. Li, X., et al., *Interactions between two cytoskeleton-associated tyrosine kinases: calcium-dependent tyrosine kinase and focal adhesion tyrosine kinase.* J Biol Chem, 1999. **274**(13): p. 8917-24.

55. Carmeliet, P., et al., *Abnormal blood vessel development and lethality in embryos lacking a single VEGF allele.* Nature, 1996. **380**(6573): p. 435-9.

56. Suri, C., et al., *Requisite role of angiopoietin-1, a ligand for the TIE2 receptor, during embryonic angiogenesis.* Cell, 1996. **87**(7): p. 1171-80.

57. Brown, C.B., et al., *Requirement of type III TGF-beta receptor for endocardial cell transformation in the heart.* Science, 1999. **283**(5410): p. 2080-2.

58. Ranger, A.M., et al., *The transcription factor NF-ATc is essential for cardiac valve formation.* Nature, 1998. **392**(6672): p. 186-90.

59. Galvin, K.M., et al., *A role for smad6 in development and homeostasis of the cardiovascular system.* Nat Genet, 2000. **24**(2): p. 171-4.

60. Valencik, M.L., et al., *A lethal perinatal cardiac phenotype resulting from altered integrin function in cardiomyocytes.* J Card Fail, 2002. **8**(4): p. 262-72.

61. George, E.L., et al., *Defects in mesoderm, neural tube and vascular development in mouse embryos lacking fibronectin.* Development, 1993. **119**(4): p. 1079-91.

62. Honda, H., et al., *Cardiovascular anomaly, impaired actin bundling and resistance to Src-induced transformation in mice lacking p130Cas.* Nat Genet, 1998. **19**(4): p. 361-5.

63. Hagel, M., et al., *The adaptor protein paxillin is essential for normal development in the mouse and is a critical transducer of fibronectin signaling.* Mol Cell Biol, 2002. **22**(3): p. 901-15.

64. AHA, *Heart and stroke statistical update-2003 update.* Dallas, 2003. American Heart Association.

65. Mann DL, *Mechanisms and models in heart failure: A combinatorial approach.* Circulation, 1999. **100**: p. 999-1008.

66. Francis GS, C.C., *Compensatory and maladaptive responses to cardiac dysfunction.* Curr Opin Cardiol, 1994. **9**(3): p. 280-8.

67. Izumo S, N.-G.B., Mahdavi V., *Protooncogene induction and reprogramming of cardiac gene expression produced by pressure overload.* Proc Natl Acad Sci, 1998. **85**(2): p. 339-43.

68. Samuel JL, B.A., Dufour S, Dubus I, Contard F, Koteliansky V, Farhadian F, Marotte F, Thiery JP, Rappaport L, *Accumulation of fetal fibronectin mRNAs during the development of rat cardiac hypertrophy induced by pressure overload.* J Clin Invest, 1991. **88**(5): p. 1737-46.

69. Morita, H., J. Seidman, and C.E. Seidman, *Genetic causes of human heart failure.* J Clin Invest, 2005. **115**(3): p. 518-26.

70. Richardson, P., et al., *Report of the 1995 World Health Organization/International Society and Federation of Cardiology Task Force on the Definition and Classification of cardiomyopathies.* Circulation, 1996. **93**(5): p. 841-2.

71. Lilly, L., *Pathophysiology of Heart Disease: A Collaborative Project of Medical Students and Faculty*. 2 ed. 1993.Lippincott Williams and Wilkins. 401.

72. Chen, J. and K.R. Chien, *Complexity in simplicity: monogenic disorders and complex cardiomyopathies.* J Clin Invest, 1999. **103**(11): p. 1483-5.

73. Marx, J., *Heart disease. How to subdue a swelling heart.* Science, 2003. **300**(5625): p. 1492-6.

74. Tardiff, J.C., *Sarcomeric proteins and familial hypertrophic cardiomyopathy: linking mutations in structural proteins to complex cardiovascular phenotypes.* Heart Fail Rev, 2005. **10**(3): p. 237-48.

75. Richard, P., et al., *Hypertrophic cardiomyopathy: distribution of disease genes, spectrum of mutations, and implications for a molecular diagnosis strategy.* Circulation, 2003. **107**(17): p. 2227-32.

76. Blair, E., et al., *Mutations of the light meromyosin domain of the beta-myosin heavy chain rod in hypertrophic cardiomyopathy.* Circ Res, 2002. **90**(3): p. 263-9.

77. Karkkainen, S. and K. Peuhkurinen, *Genetics of dilated cardiomyopathy.* Ann Med, 2007. **39**(2): p. 91-107.

78. Chang, A.N. and J.D. Potter, *Sarcomeric protein mutations in dilated cardiomyopathy.* Heart Fail Rev, 2005. **10**(3): p. 225-35.

79. Badorff, C., et al., *Enteroviral protease 2A directly cleaves dystrophin and is inhibited by a dystrophin-based substrate analogue.* J Biol Chem, 2000. **275**(15): p. 11191-7.

80. Olson, T.M., et al., *Metavinculin mutations alter actin interaction in dilated cardiomyopathy.* Circulation, 2002. **105**(4): p. 431-7.

81. Oudit, G.Y., et al., *The role of phosphoinositide-3 kinase and PTEN in cardiovascular physiology and disease.* J Mol Cell Cardiol, 2004. **37**(2): p. 449-71.

82. Brazil, D.P., Z.Z. Yang, and B.A. Hemmings, *Advances in protein kinase B signalling: AKTion on multiple fronts.* Trends Biochem Sci, 2004. **29**(5): p. 233-42.

83. Toker, A. and L.C. Cantley, *Signalling through the lipid products of phosphoinositide-3-OH kinase.* Nature, 1997. **387**(6634): p. 673-6.

84. Carpenter, C.L. and L.C. Cantley, *Phosphoinositide kinases.* Curr Opin Cell Biol, 1996. **8**(2): p. 153-8.

85. Shioi, T., et al., *The conserved phosphoinositide 3-kinase pathway determines heart size in mice.* Embo J, 2000. **19**(11): p. 2537-48.

86. Oudit, G.Y., et al., *Phosphoinositide 3-kinase gamma-deficient mice are protected from isoproterenol-induced heart failure.* Circulation, 2003. **108**(17): p. 2147-52.

87. Crackower, M.A., et al., *Regulation of myocardial contractility and cell size by distinct PI3K-PTEN signaling pathways.* Cell, 2002. **110**(6): p. 737-49.

88. McMullen, J.R., et al., *Phosphoinositide 3-kinase(p110alpha) plays a critical role for the induction of physiological, but not pathological, cardiac hypertrophy.* Proc Natl Acad Sci U S A, 2003. **100**(21): p. 12355-60.

89. Patrucco, E., et al., *PI3Kgamma modulates the cardiac response to chronic pressure overload by distinct kinase-dependent and -independent effects.* Cell, 2004. **118**(3): p. 375-87.

90. Cho, H., et al., *Akt1/PKBalpha is required for normal growth but dispensable for maintenance of glucose homeostasis in mice.* J Biol Chem, 2001. **276**(42): p. 38349-52.

91. Hay, N. and N. Sonenberg, *Upstream and downstream of mTOR.* Genes Dev, 2004. **18**(16): p. 1926-45.

92. Proud, C.G., *Ras, PI3-kinase and mTOR signaling in cardiac hypertrophy.* Cardiovasc Res, 2004. **63**(3): p. 403-13.

93. McMullen, J.R., et al., *The insulin-like growth factor 1 receptor induces physiological heart growth via the phosphoinositide 3-kinase(p110alpha) pathway.* J Biol Chem, 2004. **279**(6): p. 4782-93.

94. Hardt, S.E. and J. Sadoshima, *Glycogen synthase kinase-3beta: a novel regulator of cardiac hypertrophy and development.* Circ Res, 2002. **90**(10): p. 1055-63.

95. Morisco, C., et al., *The Akt-glycogen synthase kinase 3beta pathway regulates transcription of atrial natriuretic factor induced by beta-adrenergic receptor stimulation in cardiac myocytes.* J Biol Chem, 2000. **275**(19): p. 14466-75.

96. Antos, C.L., et al., *Activated glycogen synthase-3 beta suppresses cardiac hypertrophy in vivo.* Proc Natl Acad Sci U S A, 2002. **99**(2): p. 907-12.

97. D'Angelo, D.D., et al., *Transgenic Galphaq overexpression induces cardiac contractile failure in mice.* Proc Natl Acad Sci U S A, 1997. **94**(15): p. 8121-6.

98. Gu, X. and S.P. Bishop, *Increased protein kinase C and isozyme redistribution in pressure-overload cardiac hypertrophy in the rat.* Circ Res, 1994. **75**(5): p. 926-31.

99. Akhter SA, L.L., Rockman HA, Iaccarino G, Lefkowitz RJ, Koch WJ, *Targeting the receptor-Gq interface to inhibit in vivo pressure overload myocardial hypertrophy.* Science, 1998. **280**(24): p. 574-577.

100. Shubeita HE, M.P., Harris AN, Knowlton KU, Glembotski CC, Brown JH, Chien KR, *Endothelin induction of inositol phospholipid hydrolysis, sarcomere assembly, and cardiac gene expression in ventricular myocytes. A paracrine mechanism for myocardial cell hypertrophy.* J Cell Biol, 1990. **265**(33): p. 20555-62.

101. Sadoshima J, X.Y., Slayter HS, Izumo S., *Autocrine release of angiotensin II mediates stretch-induced hypertrophy of cardiac myocytes in vitro.* Cell, 1993. **75**(5): p. 977-84.

102. Waspe, L.E., C.P. Ordahl, and P.C. Simpson, *The cardiac beta-myosin heavy chain isogene is induced selectively in alpha 1-adrenergic receptor-stimulated hypertrophy of cultured rat heart myocytes.* J Clin Invest, 1990. **85**(4): p. 1206-14.

103. Rockman HA, W.S., Mao L, Ross J Jr., *ANG II receptor blockade prevents ventricular hypertrophy and ANF gene expression with pressure overload in mice.* Am J Physiol, 1994. **266**(6 Pt 2): p. H2468-75.

104. Milano CA, D.P., Rockman HA, Bond RA, Venable ME, Allen LF, Lefkowitz RJ., *Myocardial expression of a constitutively active alpha 1B-adrenergic receptor in transgenic mice induces cardiac hypertrophy.* Proc Natl Acad Sci, 1994. **91**(21): p. 10109-13.

105. Hein L, S.M., Barsh GS, Pratt RE, Kobilka BK, Dzau VJ., *Overexpression of angiotensin AT1 receptor transgene in the mouse myocardium produces a lethal phenotype associated with myocyte hyperplasia and heart block.* Proc Natl Acad Sci, 1997. **94**(10): p. 6391-6.

106. D'Angelo DD, S.Y., Lorenz JN, Boivin GP, Walsh RA, Liggett SB, Dorn GW 2nd., *Transgenic Galphaq overexpression induces cardiac contractile failure in mice.* Proc Natl Acad Sci, 1997. **94**(15): p. 8121-6.

107. Laser M, W.C., Jiang W, Cooper G IV, Menick DR, Zile MR, Kuppuswamy D, *Integrin activation and focal complex formation in cardiac hypertrophy.* J Biol Chem, 2000. **275**(45): p. 35627-35630.

108. Bendall JK, H.C., Ratajczak P, Samuel JL, *Extracellular matrix and cardiac remodeling.* Arch Mal Coeur Vaiss, 2002. **95**(12): p. 1226-9.

109. Adams, J.W., et al., *Enhanced Galphaq signaling: a common pathway mediates cardiac hypertrophy and apoptotic heart failure.* Proc Natl Acad Sci U S A, 1998. **95**(17): p. 10140-5.

110. Ross RS, P.C., Shai SY, Goldhaber JI, Fenczik C, Glembotski CC, Ginsberg MH, Loftus JC, *Beta1 integrins participate in the hypertrophic response of rat ventricular myocytes.* Circ Res, 1998. **82**(11): p. 1160-1172.

111. Valencik ML, M.J., *Cardiac expression of a gain-of-function alpha(5)-integrin results in perinatal lethality.* Am J Physiol Heart Circ Physiol, 2001. **280**(1): p. H361-7.

112. Sadoshima J, X.Y., Slayter HS, Izumo S, *Autocrine release of angiotensin II mediates stretch-induced hypertrophy of cardiac myocytes in vitro.* Cell, 1993. **75**(5): p. 977-84.

113. Wang Y, H.S., Sah VP, Ross J Jr, Brown JH, Han J, Chien KR, *Cardiac muscle cell hypertrophy and apoptosis induced by distinct members of the p38 mitogen-activated protein kinase family.* J Biol Chem, 1998. **273**(4): p. 2161-2168.

114. Yazaki Y, K.I., *Role of protein kinase system in the signal transduction of stretch-mediated myocyte growth.* Basic Res Cardiol, 1992. **87**(Suppl2): p. 11-8.

115. Aikawa R, K.I., Yamazaki T, Zou Y, Kudoh S, Zhu W, Kadowaki T, Yazaki Y, *Rho family small G proteins play critical roles in mechanical stress-induced hypertrophic responses in cardiac myocytes.* Circ Res, 1999. **84**(4): p. 458-66.

116. Taylor JM, R.J., Parsons JT, *A role for focal adhesion kinase in phenylephrine-induced hypertrophy of rat ventricular cardiomyocytes.* J Biol Chem, 2000. **275**(25): p. 19250-7.

117. Burridge K, C.-W.M., *Focal adhesions, contractility, and signaling.* Annu Rev Cell Dev Biol, 1996. **12**: p. 463-518.

118. Miyamoto, S., et al., *Integrins can collaborate with growth factors for phosphorylation of receptor tyrosine kinases and MAP kinase activation: roles of integrin aggregation and occupancy of receptors.* J Cell Biol, 1996. **135**(6 Pt 1): p. 1633-42.

119. Zachary I, S.-S.J., Rozengurt E., *Bombesin, vasopressin, and endothelin stimulation of tyrosine phosphorylation in Swiss 3T3 cells. Identification of a novel tyrosine kinase as a major substrate.* J Biol Chem, 1992. **267**(27): p. 19031-4.

120. Schaller MD, H.J., Shannon JD, Fox JW, Vines RR, Parsons JT, *Autophosphorylation of the focal adhesion kinase, pp125FAK, directs SH2-dependent binding of pp60src.* Mol Cell Biol, 1994. **14**(3): p. 1680-8.

121. Hoshijima, M., et al., *The low molecular weight GTPase Rho regulates myofibril formation and organization in neonatal rat ventricular myocytes. Involvement of Rho kinase.* J Biol Chem, 1998. **273**(13): p. 7725-30.

122. Aoki, H., J. Sadoshima, and S. Izumo, *Myosin light chain kinase mediates sarcomere organization during cardiac hypertrophy in vitro.* Nat Med, 2000. **6**(2): p. 183-8.

123. Sah, V.P., et al., *Cardiac-specific overexpression of RhoA results in sinus and atrioventricular nodal dysfunction and contractile failure.* J Clin Invest, 1999. **103**(12): p. 1627-34.

124. Thorburn, A., *Ras activity is required for phenylephrine-induced activation of mitogen-activated protein kinase in cardiac muscle cells.* Biochem Biophys Res Commun, 1994. **205**(2): p. 1417-22.

125. Rapacciuolo, A., et al., *Important role of endogenous norepinephrine and epinephrine in the development of in vivo pressure-overload cardiac hypertrophy.* J Am Coll Cardiol, 2001. **38**(3): p. 876-82.

126. Bueno, O.F. and J.D. Molkentin, *Involvement of extracellular signal-regulated kinases 1/2 in cardiac hypertrophy and cell death.* Circ Res, 2002. **91**(9): p. 776-81.

127. Zhang, S., et al., *The role of the Grb2-p38 MAPK signaling pathway in cardiac hypertrophy and fibrosis.* J Clin Invest, 2003. **111**(6): p. 833-41.

128. Frey, N. and E.N. Olson, *Cardiac hypertrophy: the good, the bad, and the ugly.* Annu Rev Physiol, 2003. **65**: p. 45-79.

129. Eble DM, S.J., Govindarajan G, Lou J, Byron KL, Samarel AM, *Endothelin-induced cardiac myocyte hypertrophy: role for focal adhesion kinase.* Am J Physiol Heart Circ Physiol, 2000. **278**(8): p. H1695-707.

130. Govindarajan G, E.D., Lucchesi PA, Samarel AM, *Focal adhesion kinase is involved in angiotensin II-mediated protein synthesis in cultured vascular smooth muscle cells.* Circ Res, 2000. **87**(8): p. 710-6.

131. Dorn, G.W., 2nd and T. Force, *Protein kinase cascades in the regulation of cardiac hypertrophy.* J Clin Invest, 2005. **115**(3): p. 527-37.

132. Brancaccio, M., et al., *Integrin signalling: The tug-of-war in heart hypertrophy.* Cardiovasc Res, 2006.

133. Valencik, M.L. and J.A. McDonald, *Cardiac expression of a gain-of-function alpha(5)-integrin results in perinatal lethality.* Am J Physiol Heart Circ Physiol, 2001. **280**(1): p. H361-7.

134. Shai, S.Y., et al., *Cardiac myocyte-specific excision of the beta1 integrin gene results in myocardial fibrosis and cardiac failure.* Circ Res, 2002. **90**(4): p. 458-64.

135. Knoll, R., et al., *The cardiac mechanical stretch sensor machinery involves a Z disc complex that is defective in a subset of human dilated cardiomyopathy.* Cell, 2002. **111**(7): p. 943-55.

136. Parsons, J.T., *Focal adhesion kinase: the first ten years.* J Cell Sci, 2003. **116**(Pt 8): p. 1409-16.

137. Furuta, Y., et al., *Mesodermal defect in late phase of gastrulation by a targeted mutation of focal adhesion kinase, FAK.* Oncogene, 1995. **11**(10): p. 1989-95.

138. Ilic, D., et al., *Reduced cell motility and enhanced focal adhesion contact formation in cells from FAK-deficient mice.* Nature, 1995. **377**(6549): p. 539-44.

139. Yang, J.T., et al., *Overlapping and independent functions of fibronectin receptor integrins in early mesodermal development.* Dev Biol, 1999. **215**(2): p. 264-77.

140. Torsoni, A.S., et al., *Focal adhesion kinase is activated and mediates the early hypertrophic response to stretch in cardiac myocytes.* Circ Res, 2003. **93**(2): p. 140-7.

141. Taylor, J.M., J.D. Rovin, and J.T. Parsons, *A role for focal adhesion kinase in phenylephrine-induced hypertrophy of rat ventricular cardiomyocytes.* J Biol Chem, 2000. **275**(25): p. 19250-7.

142. Sadoshima, J., et al., *Tyrosine kinase activation is an immediate and essential step in hypotonic cell swelling-induced ERK activation and c-fos gene expression in cardiac myocytes.* Embo J, 1996. **15**(20): p. 5535-46.

143. Kuppuswamy, D., et al., *Association of tyrosine-phosphorylated c-Src with the cytoskeleton of hypertrophying myocardium.* J Biol Chem, 1997. **272**(7): p. 4500-8.

144. Laser, M., et al., *Integrin activation and focal complex formation in cardiac hypertrophy.* J Biol Chem, 2000. **275**(45): p. 35624-30.

145. Franchini, K.G., et al., *Early activation of the multicomponent signaling complex associated with focal adhesion kinase induced by pressure overload in the rat heart.* Circ Res, 2000. **87**(7): p. 558-65.

146. Melendez, J., et al., *Activation of pyk2/related focal adhesion tyrosine kinase and focal adhesion kinase in cardiac remodeling.* J Biol Chem, 2002. **277**(47): p. 45203-10.

147. Yi, X.P., et al., *Subcellular redistribution of focal adhesion kinase and its related nonkinase in hypertrophic myocardium.* Hypertension, 2003. **41**(6): p. 1317-23.

148. Pham, C.G., et al., *Striated muscle-specific beta(1D)-integrin and FAK are involved in cardiac myocyte hypertrophic response pathway.* Am J Physiol Heart Circ Physiol, 2000. **279**(6): p. H2916-26.

149. Kovacic-Milivojevic, B., et al., *Focal adhesion kinase and p130Cas mediate both sarcomeric organization and activation of genes associated with cardiac myocyte hypertrophy.* Mol Biol Cell, 2001. **12**(8): p. 2290-307.

150. Peng, X., et al., *Inactivation of focal adhesion kinase in cardiomyocytes promotes eccentric cardiac hypertrophy and fibrosis in mice.* J Clin Invest, 2006. **116**(1): p. 217-27.

151. Chen, J., S.W. Kubalak, and K.R. Chien, *Ventricular muscle-restricted targeting of the RXRalpha gene reveals a non-cell-autonomous requirement in cardiac chamber morphogenesis.* Development, 1998. **125**(10): p. 1943-9.

152. Shiraishi, I., et al., *Nuclear targeting of Akt enhances kinase activity and survival of cardiomyocytes.* Circ Res, 2004. **94**(7): p. 884-91.

153. Pereira, F.A., et al., *The orphan nuclear receptor COUP-TFII is required for angiogenesis and heart development.* Genes Dev, 1999. **13**(8): p. 1037-49.

154. Turner, C.E., et al., *Angiotensin II stimulation of rapid paxillin tyrosine phosphorylation correlates with the formation of focal adhesions in rat aortic smooth muscle cells.* J Cell Sci, 1995. **108 (Pt 1)**: p. 333-42.

155. Sundberg, L.J., et al., *An endogenous inhibitor of focal adhesion kinase blocks Rac1/JNK but not Ras/ERK-dependent signaling in vascular smooth muscle cells.* J Biol Chem, 2003. **278**(32): p. 29783-91.

156. Klingbeil, C.K., et al., *Targeting Pyk2 to beta 1-integrin-containing focal contacts rescues fibronectin-stimulated signaling and haptotactic motility defects of focal adhesion kinase-null cells.* J Cell Biol, 2001. **152**(1): p. 97-110.

157. Sieg, D.J., et al., *Pyk2 and Src-family protein-tyrosine kinases compensate for the loss of FAK in fibronectin-stimulated signaling events but Pyk2 does not fully function to enhance FAK- cell migration.* Embo J, 1998. **17**(20): p. 5933-47.

158. Condorelli, G., et al., *Akt induces enhanced myocardial contractility and cell size in vivo in transgenic mice.* Proc Natl Acad Sci U S A, 2002. **99**(19): p. 12333-8.

159. Hirota, H., et al., *Loss of a gp130 cardiac muscle cell survival pathway is a critical event in the onset of heart failure during biomechanical stress.* Cell, 1999. **97**(2): p. 189-98.

160. Ilic, D., et al., *Extracellular matrix survival signals transduced by focal adhesion kinase suppress p53-mediated apoptosis.* J Cell Biol, 1998. **143**(2): p. 547-60.

161. Essayem, S., et al., *Hair cycle and wound healing in mice with a keratinocyte-restricted deletion of FAK.* Oncogene, 2006. **25**(7): p. 1081-9.

162. Caron, K.M., et al., *Cardiac hypertrophy and sudden death in mice with a genetically clamped renin transgene.* Proc Natl Acad Sci U S A, 2004. **101**(9): p. 3106-11.

163. Wang, Y., et al., *Cardiac muscle cell hypertrophy and apoptosis induced by distinct members of the p38 mitogen-activated protein kinase family.* J Biol Chem, 1998. **273**(4): p. 2161-8.

164. Bueno, O.F., et al., *The MEK1-ERK1/2 signaling pathway promotes compensated cardiac hypertrophy in transgenic mice.* Embo J, 2000. **19**(23): p. 6341-50.

165. Konhilas, J.P., et al., *Sex modifies exercise and cardiac adaptation in mice.* Am J Physiol Heart Circ Physiol, 2004. **287**(6): p. H2768-76.

166. Barrick, C.J., et al., *Cardiac response to pressure overload in 129S1/SvImJ and C57BL/6J mice: temporal- and background-dependent development of concentric left ventricular hypertrophy.* Am J Physiol Heart Circ Physiol, 2007. **292**(5): p. H2119-30.

167. Deschepper, C.F., et al., *Characterization of blood pressure and morphological traits in cardiovascular-related organs in 13 different inbred mouse strains.* J Appl Physiol, 2004. **97**(1): p. 369-76.

168. Chien, K.R., *To Cre or not to Cre: the next generation of mouse models of human cardiac diseases.* Circ Res, 2001. **88**(6): p. 546-9.

169. Sadoshima, J., et al., *The MEKK1-JNK pathway plays a protective role in pressure overload but does not mediate cardiac hypertrophy.* J Clin Invest, 2002. **110**(2): p. 271-9.

170. Minamino, T., et al., *MEKK1 is essential for cardiac hypertrophy and dysfunction induced by Gq.* Proc Natl Acad Sci U S A, 2002. **99**(6): p. 3866-71.

171. Fagard, R.H., *Impact of different sports and training on cardiac structure and function.* Cardiol Clin, 1997. **15**(3): p. 397-412.

172. Adams, T.D., et al., *Noninvasive evaluation of exercise training in college-age men.* Circulation, 1981. **64**(5): p. 958-65.

173. Panidis, I.P., et al., *Development and regression of left ventricular hypertrophy.* J Am Coll Cardiol, 1984. **3**(5): p. 1309-20.

174. Selvetella, G., et al., *Adaptive and maladaptive hypertrophic pathways: points of convergence and divergence.* Cardiovasc Res, 2004. **63**(3): p. 373-80.

175. Laser, M., et al., *Integrin activation and focal complex formation in cardiac hypertrophy.* J Biol Chem, 2000. **275**(45): p. 35624-30.

176. Gabarra-Niecko, V., P.J. Keely, and M.D. Schaller, *Characterization of an activated mutant of focal adhesion kinase: 'SuperFAK'.* Biochem J, 2002. **365**(Pt 3): p. 591-603.

177. Hu, P., et al., *Minimally invasive aortic banding in mice: effects of altered cardiomyocyte insulin signaling during pressure overload.* Am J Physiol Heart Circ Physiol, 2003. **285**(3): p. H1261-9.

178. Chen, J., et al., *Selective requirement of myosin light chain 2v in embryonic heart function.* J Biol Chem, 1998. **273**(2): p. 1252-6.

179. Rindt, H., et al., *In vivo analysis of the murine beta-myosin heavy chain gene promoter.* J Biol Chem, 1993. **268**(7): p. 5332-8.

180. Gilmore, A.P. and L.H. Romer, *Inhibition of focal adhesion kinase (FAK) signaling in focal adhesions decreases cell motility and proliferation.* Mol Biol Cell, 1996. **7**(8): p. 1209-24.

181. Zhao, J.H., H. Reiske, and J.L. Guan, *Regulation of the cell cycle by focal adhesion kinase.* J Cell Biol, 1998. **143**(7): p. 1997-2008.

182. Ilic, D., et al., *Focal adhesion kinase is required for blood vessel morphogenesis.* Circ Res, 2003. **92**(3): p. 300-7.

183. Brancaccio, M., et al., *Melusin, a muscle-specific integrin beta1-interacting protein, is required to prevent cardiac failure in response to chronic pressure overload.* Nat Med, 2003. **9**(1): p. 68-75.

184. Hescheler, J. and B.K. Fleischmann, *Integrins and cell structure: powerful determinants of heart development and heart function.* Cardiovasc Res, 2000. **47**(4): p. 645-7.

185. Schroeder, J.A., et al., *Form and function of developing heart valves: coordination by extracellular matrix and growth factor signaling.* J Mol Med, 2003. **81**(7): p. 392-403.

186. Mohun, T., R. Orford, and C. Shang, *The origins of cardiac tissue in the amphibian, Xenopus laevis.* Trends Cardiovasc Med, 2003. **13**(6): p. 244-8.

187. Lee, K.F., et al., *Requirement for neuregulin receptor erbB2 in neural and cardiac development.* Nature, 1995. **378**(6555): p. 394-8.

188. Molkentin, J.D., *Calcineurin-NFAT signaling regulates the cardiac hypertrophic response in coordination with the MAPKs.* Cardiovasc Res, 2004. **63**(3): p. 467-75.

189. Moses, K.A., et al., *Embryonic expression of an Nkx2-5/Cre gene using ROSA26 reporter mice.* Genesis, 2001. **31**(4): p. 176-80.

190. Cohen, G.M., *Caspases: the executioners of apoptosis.* Biochem J, 1997. **326 (Pt 1)**: p. 1-16.

191. Morkin, E., *Control of cardiac myosin heavy chain gene expression.* Microsc Res Tech, 2000. **50**(6): p. 522-31.

192. Viragh, S. and C.E. Challice, *Origin and differentiation of cardiac muscle cells in the mouse.* J Ultrastruct Res, 1973. **42**(1): p. 1-24.

193. Conway, S.J., et al., *What cardiovascular defect does my prenatal mouse mutant have, and why?* Genesis, 2003. **35**(1): p. 1-21.

194. Epstein, J.A. and C.A. Buck, *Transcriptional regulation of cardiac development: implications for congenital heart disease and DiGeorge syndrome.* Pediatr Res, 2000. **48**(6): p. 717-24.

195. Wenink, A.C., et al., *Development of myocardial fiber organization in the rat heart.* Anat Embryol (Berl), 1996. **193**(6): p. 559-67.

196. Vrancken Peeters, M.P., et al., *The development of the coronary vessels and their differentiation into arteries and veins in the embryonic quail heart.* Dev Dyn, 1997. **208**(3): p. 338-48.

197. Mima, T., et al., *Fibroblast growth factor receptor is required for in vivo cardiac myocyte proliferation at early embryonic stages of heart development.* Proc Natl Acad Sci U S A, 1995. **92**(2): p. 467-71.

198. Heidkamp, M.C., et al., *GFP-FRNK disrupts focal adhesions and induces anoikis in neonatal rat ventricular myocytes.* Circ Res, 2002. **90**(12): p. 1282-9.

199. Bueno, O.F., et al., *The dual-specificity phosphatase MKP-1 limits the cardiac hypertrophic response in vitro and in vivo.* Circ Res, 2001. **88**(1): p. 88-96.